This dissertation has been 64–13,340
microfilmed exactly as received

SABBAGHIAN, Mehdy, 1935–
THERMOVISCOELASTICITY WITH TIME AND STRESS DEPENDENT COEFFICIENT OF EXPANSION.

The University of Oklahoma, Ph.D., 1964
Engineering Mechanics

University Microfilms, Inc., Ann Arbor, Michigan

Downloaded from SHAREOK. Persistent Handle URL: https://hdl.handle.net/11244/1805

THE UNIVERSITY OF OKLAHOMA

GRADUATE COLLEGE

THERMOVISCOELASTICITY WITH TIME AND STRESS DEPENDENT COEFFICIENT OF EXPANSION

A DISSERTATION

SUBMITTED TO THE GRADUATE FACULTY

in partial fulfillment of the requirements for the

degree of

DOCTOR OF PHILOSOPHY

BY

MEHDY SABBAGHIAN

Norman, Oklahoma

1964

THERMOVISCOELASTICITY WITH TIME AND STRESS DEPENDENT COEFFICIENT OF EXPANSION

APPROVED BY

C. W. Bert

C. M. Sliepcevich

Arthur Bernhart

J. W. Rayleigh

Hung-Ta Ho

DISSERTATION COMMITTEE

ABSTRACT

In analyzing the dynamic stresses and deformations in viscoelastic bodies as in elastic ones, the problem is concerned with the solution of boundary-value problems in which the time has a dominant role. For thermal stresses as in classical elasticity the stress-strain relation will contain terms due to thermal expansions. A few methods for thermal stress analysis have been suggested and applied. In all the previous work, the coefficient of thermal expansion is considered either as invariant or as a temperature-dependent parameter.

The basic objective of this study was to investigate the stress and time dependency of the thermal expansion coefficient of a viscoelastic material. The analytical part of this investigation consisted of the theoretical development of the stress and time dependency of thermal expansion coefficient for a general viscoelastic material under the influence of three-dimensional stresses. To check the analysis, a series of creep experiments was conducted at three constant temperature levels and stress applied as a step function. In all of the experimental cases, it was found that the application of the developed theory gave a better creep prediction

than did use of the assumption that the thermal expansion coefficient remained constant.

In the course of experimental investigation, the creep behavior of polymethyl methacrylate was studied at different temperatures and a relation developed among the stress, strain, time and temperature.

ACKNOWLEDGMENTS

The author wishes to express his very large debt of gratitude to all who have contributed to this work, particularly:

The Aerospace and Mechanical Engineering Faculty and especially Dr. Charles W. Bert under whose direction this project was undertaken.

Dr. C. M. Sliepcevich who provided the idea for this undertaking.

Other members of the Doctoral Committee, Dr. H. W. Bergmann, Dr. H. T. Ho and Dr. C. E. Springer for their encouragement.

Dr. T. J. Love and Dr. D. G. Harden for their co-operation in connection with establishing the experimental setup.

Mr. Earl Finch from the Aerospace Laboratories work shop for his suggestions and assistance in preparing the equipment.

Special thanks are also due to National Iranian Oil Co. and Conch Methane Services for their financial support.

The author expresses appreciation to his wife, Ferdows, for her patience throughout the course of the research.

TABLE OF CONTENTS

	Page
ABSTRACT	iii
ACKNOWLEDGMENTS	v
LIST OF TABLES	vii
LIST OF ILLUSTRATIONS	ix
Chapter	
I. INTRODUCTION	1
II. BASIC THEORY	9
1. A Survey of the Literature	
2. Constitutive Relations	
3. Effect of Stress and Time on Thermal Coefficient of Expansion	
III. PLANNING OF EXPERIMENTS	34
1. Low Stress Level Experiments	
2. High Stress Level Experiments	
IV. MATERIAL, SPECIMENS, AND EXPERIMENTAL APPARATUS	38
1. Material	
2. Specimens	
3. Experimental Setup	
V. EXPERIMENTAL RESULTS	51
VI. ANALYSIS OF EXPERIMENTAL RESULTS	82
VII. CONCLUSIONS AND SUGGESTIONS FOR FURTHER RESEARCH	97
1. Conclusions	
2. Some suggestions for future research	
REFERENCES	102
APPENDIX A TABLES	107

LIST OF TABLES

Table		Page
1.	Creep Data at 90° F and 400 psi	110
2.	Creep Data at 90° F and 266 psi	111
3.	Creep Data at 90° F and 213 psi	112
4.	Creep Data at 105° F and 480 psi	113
5.	Creep Data at 105° F and 400 psi	114
6.	Creep Data at 105° F and 320 psi	115
7.	Creep Data at 105° F and 280 psi	116
8.	Creep Data at 120° F and 400 psi	117
9.	Creep Data at 120° F and 320 psi	118
10.	Creep Data at 120° F and 280 psi	119
11.	Creep Data at 135° F and 525 psi	120
12.	Creep Data at 135° F and 410 psi	121
13.	Creep Data at 135° F and 360 psi	122
14.	Creep Data at 135° F and 240 psi	123
15.	Creep Data at 150° F and 400 psi	124
16.	Creep Data at 150° F and 320 psi	125
17.	Creep Data at 150° F and 240 psi	126
18.	Creep Data at 150° F and 200 psi	127
19.	Creep Data at 165° F and 400 psi	128
20.	Creep Data at 165° F and 320 psi	129
21.	Creep Data at 165° F and 240 psi	130

Table		Page
22.	Creep Data at 165°F and 200 psi	131
23.	Creep Data at 180°F and 400 psi	132
24.	Creep Data at 180°F and 320 psi	133
25.	Creep Data at 180°F and 240 psi	134
26.	Creep Data at 180°F and 200 psi	135
27.	Creep Data at 195°F and 400 psi	136
28.	Creep Data at 195°F and 320 psi	137
29.	Creep Data at 195°F and 240 psi	138
30.	Creep Data at 195°F and 200 psi	139
31.	Creep Data at 210°F and 240 psi	140
32.	Creep Data at 210°F and 200 psi	141
33.	Creep Data at 210°F and 160 psi	142
34.	Creep Data at 225°F and 200 psi	143
35.	Creep Data at 225°F and 160 psi	144
36.	Variation of Creep Constants with Temperature . .	145
37.	Creep Data at 140°F and 5000 psi	146
38.	Creep Data at 160°F and 4000 psi	147
39.	Creep Data at 190°F and 2600 psi	148
40.	Free Thermal Expansion of Methyl Methacrylate . .	149
41.	Creep Data at 160°F and 2600 psi	150
42.	Creep Data at 140°F and 2600 psi	151

LIST OF ILLUSTRATIONS

Figure		Page
1.	Maxwell Model	15
2.	Kelvin or Voigt Model	15
3.	Maxwell-Kelvin Model	15
4.	Dimensions of the Specimens	40
5.	Model Assembly	42
6.	Installation of Dial Indicator	43
7.	Enlarged Curved Section	45
8.	Loading Frame	48
9.	Frames Mounted in Oven	49
10.	Log strain versus log time at 90°F	57
11.	Log strain versus log time at 105°F	58
12.	Log strain versus log time at 120°F	59
13.	Log strain versus log time at 135°F	60
14.	Log strain versus log time at 150°F	61
15.	Log strain versus log time at 165°F	62
16.	Log strain versus log time at 180°F	63
17.	Log strain versus log time at 195°F	64
18.	Log strain versus log time at 210°F	65
19.	Log strain versus log time at 225°F	66
20.	Evaluation of Constants a and b	67
21.	Evaluation of Constants c and d	68

Figure		Page
22.	Evaluation of Constants c and d	69
23.	Variation of a, c and n with temperature . . .	70
24.	Log_{10} a, log_{10} 100c and log_{10} n versus temperature	71
25.	Creep Curves at 90°F	72
26.	Creep Curves at 105°F	73
27.	Creep Curves at 120°F	74
28.	Creep Curves at 135°F	75
29.	Creep Curves at 150°F	76
30.	Creep Curves at 165°F	77
31.	Creep Curves at 180°F	78
32.	Creep Curves at 195°F	79
33.	Creep Curves at 210°F	80
34.	Creep Curves at 225°F	81
35.	Creep Curve at 140°F and 5000 psi	83
36.	Creep Curve at 160°F and 4000 psi	84
37.	Creep Curve at 190°F and 2600 psi	85
38.	Creep Curve at 160°F and 2600 psi	86
39.	Creep Curve at 140°F and 2600 psi	87
40.	Percentage Deviation from Experimental Data After Thirty Minutes at 2600 psi versus Temperature	88
41.	Variation of Thermal Expansion Coefficient with and without Stress	99

THERMOVISCOELASTICITY WITH TIME AND STRESS DEPENDENT COEFFICIENT OF EXPANSION

CHAPTER I

INTRODUCTION

The increasing use of various kinds of high polymers in machine parts and other products, as well as the use of solid propellents in rocket engines, has led many scientists and engineers to investigate stress, strain, deformation and their time dependence in viscoelastic materials. These materials in general have viscous properties as well as elastic properties, or simply the stress-strain relation in viscoelastic bodies is time dependent. The theory for simple linear viscoelastic materials is well developed, while the theory for nonlinear viscoelastic bodies is still in an early stage of development.

Thermoviscoelasticity has been considered in the past few years. It is concerned with the stress and strain condition in a viscoelastic body due to a temperature gradient in the body. Different methods of solution have been proposed for thermoviscoelastic problems.

In 1944 Alfrey (1)[1] considered an isotropic,

---

[1]Numbers in parentheses refer to References at end.

incompressible, linear, viscoelastic material and extended the theory of perfect elasticity for small strains to viscoelastic bodies. He classified the problem into two categories: (1) surface forces prescribed and (2) surface displacements prescribed. In the first case, where the surface forces were prescribed, he proved that the stresses in a viscoelastic body subjected to a surface force $f(x,t)$, where $f(x,t)$ is an analytic function of time for $t > 0$, is given by

$$\sigma_{ik}(x,t) = \bar{\sigma}_{ik}(x,t); \; i = 1,2,3.$$

In the above equation $\bar{\sigma}_{ik}(x,t)$ is the static stress of an incompressible perfectly elastic body subjected to a surface force $f_i(x,t)$. To find the displacements, Alfrey assumed that the force can be written as the product of two separate functions of the independent variables as

$$f(x,t) = f_i(x)\, g(t).$$

Then the stress would be

$$\sigma_{ik}(x,t) = \bar{\sigma}_{ik}(x)\, g(t)$$

Multiplication of the elastic displacements due to $\bar{\sigma}_{ik}(x)$ in the perfectly elastic body with unit shear modulus and the viscoelastic response due to a shear force of 2 $g(t)$ will give the displacements in the analogous viscoelastic medium. For problems of the second kind he proved that the same operation may be performed on displacements to get the stresses.

Tobolsky and Andrews (2) studied the general molecular theory of materials under stress. They stated that actual substances, especially rubberlike substances, exhibit a complicated behavior under mechanical stress. Gross (3) formulated a relation between creep and relaxation functions.

In 1949 Mindlin (4) derived a mathematical optical-stress-strain-time-temperature relation in which stress and strain birefringence coefficients are time and temperature dependent. Read (5) considered stress-strain relations for compressible viscoelastic materials and proved that if stress, birefringence, and their time derivatives are linearly related, then the standard photoelastic technique can be used to determine the directions and differences of principal stresses.

Tsien (6) in 1950 generalized Alfrey's analogy for isotropic compressible media to cases where body forces are present. Schwarzl and Staverman (7) treated the question of whether or not, in the study of linear viscoelastic materials, a change of temperature is exactly analogous to a shift of the logarithmic time scale. When it is, they termed this material thermorheologically simple.

Freudenthal (8) mathematically proved that at different rates of heating or cooling the stresses produced in the material would be quite different. Hilton (9) considered temperature-dependent viscoelastic materials of the Kelvin[2] type, presented the solution for a thick-walled cylinder, and

---

[2]See Chapter II, Section 2 for definition of a Kelvin material.

compared the results with the temperature independent viscoelastic materials.

In 1955 Lee (10) considered the quasi-static case of a viscoelastic body, in which loading is such that the inertial force due to displacement is negligible, and by using the Laplace transform he analyzed the problem of proportional and nonproportional loading. He compared this method with the other approaches of stress analysis in viscoelastic materials. In the procedure of the Laplace transform method introduced by Lee both the boundary conditions and the governing differential equations must be transformed and become time independent. This will restrict the problem to those boundary conditions which are transferable, or have zero initial conditions where the given surface traction and displacements vanish at $t < 0$. But there are cases where this condition does not exist, and it is not possible to make the boundary conditions independent of time. For such a condition Radok (11) introduced a functional equation in which the boundary conditions are not required to be transformed, and instead of applying Laplace transform to the elastic solution, the elastic coefficients may be replaced by operators. With this procedure Radok actually expanded the range of applicability of Lee's method. In many cases involving simple elastic constants, he found the functional equations become differential equations in time which may be integrated for given initial conditions.

Olszak and Perzyna (12) derived variational theorems for the various models of viscoelastic bodies. Yamamoto (13) extended the classical linear theory of viscoelasticity to three dimensions and discussed three-dimensional nonlinear theory also. Morland and Lee (14) considered a thermo-rheologically simple material, and by using a shift factor for the temperature effect solved the problem of stress distribution in a cylinder with constant internal pressure and a steady state nonuniform temperature distribution. They pointed out the effect of nonuniform temperature distribution on the material behavior and particularized their problem to Kelvin and Maxwell type materials.

In 1960 Segawa (15) stated that the spring and dashpot mechanical model is not valid for three dimensions and large deformation. He derived Maxwell-body formulas for three dimensions and large deformations and illustrated that Alfrey's formula is a special case of it. Tschoegl (16) developed a technique which allows the application of electric circuit theory to the solution of mechanical and rheological problems. Hilton and Russell (17) extended Alfrey's analogy to thermal-stress problems. Since in most of the cases the temperature distribution is a separable function of time and space, the material behavior is also a function of time and space. They proved that if the temperature is in the form of

$$T = \sum_{m} H^{m}(t)\ F^{m}(x)$$

then the stress produced due to this temperature distribution is in the form of

$$\sigma_{ij}(x,t) = \sum_{m} g_m(t)\ \sigma_{ij}^{m}\ (x)$$

where $\sigma_{ij}^{m}(x)$ is the stress distribution in an elastic material and $g_m(t)$ is a viscoelastic response which can be calculated separately. The product of these two will give the stress distribution in a viscoelastic material.

Muki and Sternberg (18) considered the quasi-static transient thermal-stress analysis of a linear viscoelastic solid and solved two particular problems. Tokuoka (19) used the generalized Novozhilov's (20) nonlinear theory of elasticity for large deformation and expressed the generalized equilibrium equation in the Lagrange representation and by applying Hamilton's principle obtained the general stress-strain relations for three-dimensional geometrically and physically nonlinear viscoelasticity. He also applied (21) Hamilton's principle to the viscoelastic deformation; and by physically appropriate assumptions he obtained the three dimensional stress-strain relations for Maxwell-type materials.[3]

Pister (22) used the integral-transform method and considered the viscoelastic plate on a viscoelastic foundation. Lee and Rogers (23) discussed the constitutive relation for

---

[3]Maxwell-type materials are defined in Chapter II, Section 2.

viscoelastic material in the form of integral equations which are more general than the operator form. Shinozuka (24) considered the problem of thermal stresses in a hollow cylinder with variable inside radius for the general linear viscoelastic material.[4] Brener and Onat (25) investigated the possibility of finding free energy F and entropy production Θ of a solid from the knowledge of relaxation modulus with a thermodynamics approach and using the following equation.

$$\sigma(t)\,\dot{\epsilon}(t) = \dot{F} + T_o\dot{\Theta}$$

where T_o is a reference temperature and the dots indicate the time rate of change of the quantities.

Sternberg (26) extended Lee's Laplace-transform method to the thermal-stress problem for a general linear viscoelastic material. He assumed an incompressible linear viscoelastic body with temperature independent behavior. This, of course, is a crude assumption since viscoelastic materials are highly sensitive to temperature.

Except only in a very few papers the authors considered temperature independent viscoelastic characteristics, and none of them considered the stress and time dependent thermal coefficient of expansion.

In the course of the present investigation, it is theoretically proved that the thermal expansion coefficient of a viscoelastic material is a function of stress and time as

---

[4] See Chapter II, Section 2 for the definition of a general linear viscoelastic material.

well as a function of temperature. A series of experiments is also conducted to prove this theory. Behavior of polymethyl methacrylate is investigated at different temperature levels and a general relation among the stress, strain, time and temperature is developed.

CHAPTER II

BASIC THEORY

1. A Survey of the Literature

To date, in most of the books and research papers in the field of thermal stresses, the thermal coefficient of expansion has been used either as a constant or a temperature dependent coefficient. In 1956 Rosenfield and Averbach (27) investigated the effect of uniaxial stress on the thermal coefficient of expansion for an isotropic elastic material. C. W. Bert (28) in 1963 developed expressions for the effect of general three-dimensional stresses on the coefficient of expansion of an orthotropic elastic material and applied the results in general thermoelasticity theory. He proved that the thermal coefficient of expansion for elastic bodies will be influenced by the stresses as well as by the temperature and derived that the stresses and the coefficient of expansion are related by the following equations:

$$\frac{\partial \alpha_i}{\partial \sigma_i} = \frac{\partial}{\partial T}\left(\frac{1}{E_i}\right) = -\frac{1}{E_i^2}\frac{\partial E_i}{\partial T} \qquad (2\text{-}1)$$

$$\frac{\partial \alpha_i}{\partial \sigma_j} = \frac{\partial}{\partial T}\left(-\frac{\nu_{ij}}{E_i}\right) = \left(\frac{E_i}{\nu_{ij}}\right)^{-2}\frac{\partial}{\partial T}\left(\frac{E_i}{\nu_{ij}}\right) \qquad (2\text{-}2)$$

Thus,

$$\alpha_i = \alpha_{oi} + \frac{1}{E_i}\left[C_{ii}\sigma_i - C_{ij}\nu_{ij}\sigma_j - C_{ik}\nu_{ik}\sigma_k\right] \qquad (2\text{-}3)$$

with

$$C_{ii} = -\frac{1}{E_i}\frac{\partial E_i}{\partial T} \qquad (2\text{-}4)$$

$$C_{ij} = \left(-\frac{E_i}{\nu_{ij}}\right)^{-1}\frac{\partial}{\partial T}\left(\frac{E_i}{\nu_{ij}}\right) \qquad (2\text{-}5)$$

where σ, E_i, ν_{ij}, α and α_{oi} are stress, modulus of elasticity, Poisson's ratio, thermal coefficient of expansion, and thermal coefficient of expansion at zero stress, respectively.

Although the theory of thermoviscoelasticity has been developed to some extent (29), there has been no theory showing the dependence of thermal expansion coefficient on stresses and time for a viscoelastic material. The purpose of this chapter is to derive theoretical relations showing the effect of stress and time on coefficient of expansion.

2. Constitutive Relations

The constitutive relations for a general three-dimensional linear viscoelastic body have been represented in different ways by many authors. The two most common ways are usually called the operator representation and the integral representation.

The operator representation was used by Lee (30) in the following form:

$$P_1\sigma_{ii} = Q_1\varepsilon_{ii}, \qquad P_2 S_{ij} = Q_2 e_{ij} \qquad (2\text{-}6)$$

where P_1, P_2, Q_1 and Q_2 are the differential operators defined as follows:

$$P_1 = \sum_{i=0}^{n} a_i \frac{\partial^i}{\partial t^i}$$

$$P_2 = \sum_{i=0}^{m} b_i \frac{\partial^i}{\partial t^i}$$

$$Q_1 = \sum_{i=0}^{k} c_i \frac{\partial^i}{\partial t^i}$$

$$Q_2 = \sum_{i=0}^{\ell} d_i \frac{\partial^i}{\partial t^i}$$

Here k, ℓ, m and n are not necessarily equal; the a_i, b_i, c_i and d_i are material constants which may be temperature or time dependent. With the above definitions it is obvious that as the number of terms in the summations increases the solution becomes more complicated. For a perfectly elastic material, the coefficients a_i, b_i, c_i and d_i are zero for $i > 1$.

In the integral representation used by Gross (3), in which he formulated the relations between creep and relaxation functions, the constitutive relations are:

$$\begin{aligned} S_{ij}(x,t) &= \int_0^t G_2(t-\tau) \frac{\partial}{\partial \tau} e_{ij}(x,\tau) d\tau, \\ \sigma_{kk}(x,t) &= \int_0^t G_1(t-\tau) \frac{\partial}{\partial \tau} \epsilon_{kk}(x,\tau) d\tau, \end{aligned} \qquad (2\text{-}7)$$

$$e_{ij}(x,t) = \int_0^t J_2(t-\tau)\frac{\partial}{\partial\tau} S_{ij}(x,\tau)d\tau,$$

$$\varepsilon_{kk}(x,t) = \int_0^t J_1(t-\tau)\frac{\partial}{\partial\tau} \sigma_{kk}(x,\tau)d\tau, \qquad (2\text{-}7)$$

where G_1 and G_2 are the relaxation modulus in shear and the bulk modulus, respectively; J_1 and J_2 are creep functions; σ_{kk} and ε_{kk} are the volumetric stress and strain respectively with the regular tensor notation with summation on repeated indices and S_{ij} and e_{ij} are the deviatoric stresses and strains with the following definitions;

$$S_{ij} = \sigma_{ij} - \frac{1}{3}\delta_{ij}\sigma_{kk},$$

$$e_{ij} = \varepsilon_{ij} - \frac{1}{3}\delta_{ij}\varepsilon_{kk},$$

where δ_{ij} denotes the Kronecker delta function. In the case of sinusoidal deformation, the relaxation modulus G and creep function J amy be separated into two parts, namely the storage modulus and the loss modulus (31) as follows:

$$G = G' + iG'',$$

$$J = J' + iJ'',$$

where i denotes $\sqrt{-1}$, G' and J' are storage relaxation mcdulus and creep function and correspond to the elastic energy stored in the body in a cycle; G" and J" are the loss relaxation modulus and creep function and correspond to the energy

dissipated in the viscoelastic body due to the internal friction in one cycle; G' is defined as the ratio of stress to the strain, in phase with each other in a sinusoidal deformation; G" is the ratio of stress to the strain, 90° out of phase with each other in a sinusoidal deformation; J' is the ratio of strain to the stress in phase with each other and J" is the ratio of strain to the stress 90° out of phase in a sinusoidal deformation. The ratio of G"/G' is called the loss tangent. Although J and G are related by $J = (1/G)$, their individual components are not reciprocally related (32).

The behavior of different linear viscoelastic materials can be represented by different combinations of mechanical elements, namely Hookean (linear) springs and Newtonian (linear) dashpots. In general linear viscoelastic materials under instantaneously applied stress have three distinct phases of straining, called

1. Instantaneous elastic response associated with the spring element.
2. Delayed elastic response associated with spring and dashpot in parallel.
3. Viscous flow associated with the dashpot.

The first response is purely elastic and recoverable immediately after removing the stress. The second part is also recoverable but at a delayed time. The third part is not recoverable.

To find the exact behavior of a general linear viscoelastic body, it would be necessary to use an infinite number

of terms in the differential operators P and Q; then, as mentioned before, the mathematical solution of the problem becomes more complicated. This is one reason why some authors choose to use integral equations in their analyses. This corresponds to employing an infinite number of elements in the mechanical models. Yamamoto (13) started his analysis from the elementary model of the classical linear theory of viscoelasticity and extended it to three dimensions and showed that for three-dimensional nonlinear theory the spring must be non-Hookean and the dashpot non-Newtonian.

The simple viscoelastic models are those known as Maxwell, Kelvin (or Voigt), and Maxwell-Kelvin bodies (29). Behavior of each of these three models corresponds to the mechanical models shown in Figures 1, 2, and 3, respectively, with the following mathematical relations:

a. For a Maxwell body

$$\dot{\epsilon} = \frac{\dot{\sigma}}{E_m} + \frac{\sigma}{\eta_m} \tag{2-8}$$

or

$$D\epsilon = \left(\frac{D}{E_m} + \frac{1}{\eta_m} \right) \sigma \ .$$

Thus,

$$\epsilon = \left(\frac{1}{E_m} + \frac{1}{\eta_m D} \right) \sigma \tag{2-9}$$

where $D = \frac{d}{dt}$.

b. For a Kelvin or Voigt body

$$\sigma = E_k \epsilon + \eta_k \dot{\epsilon} \tag{2-10}$$

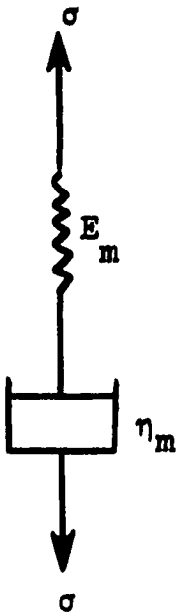

Maxwell Model
Figure 1

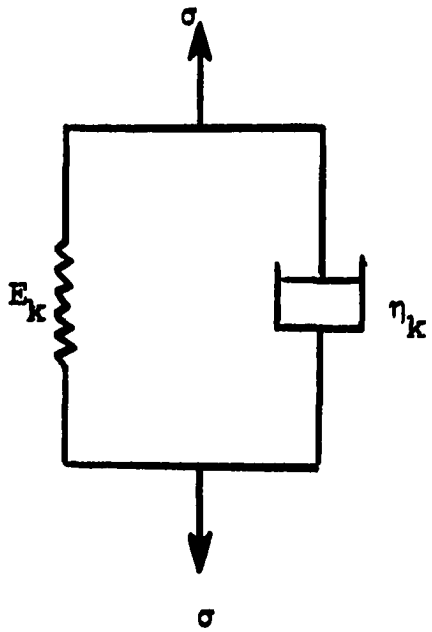

Kelvin or Voigt Model
Figure 2

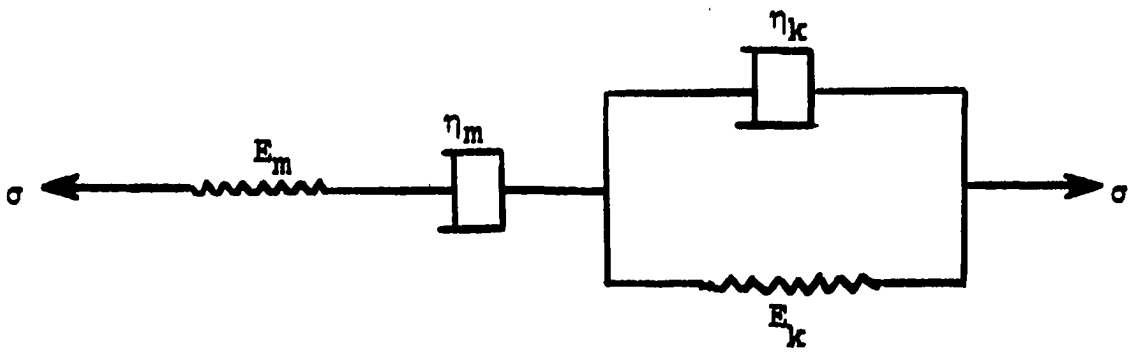

Maxwell-Kelvin Model
Figure 3

or

$$\sigma = (E_k + \eta_k D)\epsilon \ .$$

Then

$$\epsilon = \left(\frac{1}{E_k + \eta_k D} \right) \sigma \ . \qquad (2\text{-}11)$$

c. For a Maxwell-Kelvin body (General Linear Viscoelastic Material),

$$\epsilon = \epsilon_m + \epsilon_k \qquad (2\text{-}12)$$

where

$$\epsilon_m = \left(\frac{1}{E_m + \eta_m D} \right) \sigma$$

and

$$\epsilon_k = \left(\frac{1}{E_k + \eta_k D} \right) \sigma \ .$$

Thus,

$$\epsilon = \left[\frac{1}{E_m} + \frac{1}{\eta_k D} + \frac{1}{E_k + \eta_k D} \right] \qquad (2\text{-}13)$$

or

$$(a_0 + a_1 D + a_2 D^2)\sigma = (b_1 D + D^2)\epsilon \qquad (2\text{-}14)$$

Comparison of equations (2-13) and (2-14) results in the following relationships:

$$a_0 = \frac{E_k}{\eta_m \eta_k}$$

$$a_1 = \frac{1}{\eta_k} + \frac{E_k}{E_m \eta_k} + \frac{1}{\eta_m} \qquad (2\text{-}15)$$

$$a_2 = 1/E_m$$

$$b_1 = E_k/\eta_k$$

A material represented by a Kelvin model with a spring in series exhibits instantaneous and delayed elasticity but no viscous flow; this is sometimes referred to as the Standard Linear Solid (30).

3. Effect of Stress and Time on Thermal Coefficient of Expansion

In the previous section the constitutive relations for the various simple viscoelastic materials were described. In the present section are derived the mathematical relationships among time, stress and thermal coefficient of expansion for viscoelastic materials.

From the definition of expansion coefficient

$$\alpha_i = \frac{\partial \epsilon_i}{\partial T}$$

the following relations are obtained

$$\frac{\partial \alpha_i}{\partial \sigma_i} = \frac{\partial}{\partial \sigma_i} \frac{\partial \epsilon_i}{\partial T} \tag{2-16}$$

$$\frac{\partial \alpha_i}{\partial \sigma_j} = \frac{\partial}{\partial \sigma_j} \frac{\partial \epsilon_i}{\partial T} \tag{2-17}$$

Assuming that α_i is a continuous function of σ_i, σ_j and T, then it is possible to interchange the order of differentiation. Thus,

$$\frac{\partial \alpha_i}{\partial \sigma_i} = \frac{\partial}{\partial T}\left(\frac{\partial \epsilon_i}{\partial \sigma_i}\right)$$

$$\frac{\partial \alpha_i}{\partial \sigma_j} = \frac{\partial}{\partial T}\left(\frac{\partial \epsilon_i}{\partial \sigma_j}\right)$$

$$\frac{\partial \alpha_i}{\partial \sigma_k} = \frac{\partial}{\partial T}\left(\frac{\partial \epsilon_i}{\partial \sigma_k}\right) \qquad (2\text{-}18)$$

In an elastic body the relation among the stress, strain, volumetric and deviatoric stresses and strains are

$$\epsilon_{kk} = \frac{1}{3K}\sigma_{kk}$$

$$e_{ij} = \frac{1}{2G} S_{ij} \qquad (2\text{-}19)$$

$$e_{11} + \epsilon_{kk} = \epsilon_{11} = \frac{1}{3K}\left[\frac{\sigma_{11} + \sigma_{22} + \sigma_{33}}{3}\right] + \frac{1}{2G}\left[\frac{2\sigma_{11} - \sigma_{22} - \sigma_{33}}{3}\right]$$

$$\epsilon_{11} = \sigma_{11}\left[\frac{1}{9K} - \frac{1}{3G}\right] - \sigma_{22}\left[-\frac{1}{9K} + \frac{1}{6G}\right] - \sigma_{33}\left[\frac{1}{6G} - \frac{1}{9K}\right]$$

where G and K are shear and bulk modulus. For a viscoelastic material it is possible to derive expressions analogous to equations (2-19) as follows.

A. Using the constitutive equations (2-6)

$$\epsilon_{kk} = \frac{P_1}{Q_1}\sigma_{kk}$$

$$e_{11} = \frac{P_2}{Q_2} S_{11}$$

$$\epsilon_{kk} + e_{11} = \epsilon_{11} = \frac{P_1}{Q_1}\left[\frac{\sigma_{11} + \sigma_{22} + \sigma_{33}}{3}\right] + \frac{P_2}{Q_2}\left[\frac{\sigma_{11} - \sigma_{22} - \sigma_{33}}{3}\right]$$

or

$$\epsilon_{11} = \sigma_{11}\left[\frac{P_1}{3Q_1} + \frac{2P_2}{3Q_2}\right] - \sigma_{22}\left[\frac{P_2}{3Q_2} - \frac{P_1}{3Q_1}\right] - \sigma_{33}\left[\frac{P_2}{3Q_2} - \frac{P_1}{3Q_1}\right]$$

$$\epsilon_{11} = \frac{\sigma_{11}}{3}\left[\frac{2P_2}{Q_2} + \frac{P_1}{Q_1}\right] - \frac{\sigma_{22}}{3}\left[\frac{P_2}{Q_2} - \frac{P_1}{Q_1}\right] - \frac{\sigma_{33}}{3}\left[\frac{P_2}{Q_2} - \frac{P_1}{Q_1}\right] \tag{2-20}$$

Equations analogous to equation (2-20) can be obtained for ϵ_{22} and ϵ_{33} in a similar fashion. Equation (2-20) can be used to obtain expressions for $\frac{\partial \epsilon_{11}}{\partial \sigma_{11}}$, $\frac{\partial \epsilon_{11}}{\partial \sigma_{22}}$ and $\frac{\partial \epsilon_{11}}{\partial \sigma_{33}}$, with the following results:

$$\frac{\partial \epsilon_{11}}{\partial \sigma_{11}} = \frac{1}{3}\left[\frac{2P_2}{Q_2} + \frac{P_1}{Q_1}\right] \tag{2-21}$$

$$\frac{\partial \epsilon_{11}}{\partial \sigma_{22}} = -\frac{1}{3}\left[\frac{P_2}{Q_2} - \frac{P_1}{Q_1}\right] \tag{2-22}$$

$$\frac{\partial \epsilon_{11}}{\partial \sigma_{33}} = -\frac{1}{3}\left[\frac{P_2}{Q_2} - \frac{P_1}{Q_1}\right] \tag{2-23}$$

Substitution of equations (2-21), (2-22) and (2-23) into (2-18) results in

$$\frac{\partial \alpha_i}{\partial \sigma_{ii}} = \frac{1}{3}\frac{\partial}{\partial T}\left[\frac{2P_2}{Q_2} + \frac{P_1}{Q_1}\right]$$

$$\frac{\partial \alpha_i}{\partial \sigma_{jj}} = -\frac{1}{3}\frac{\partial}{\partial T}\left[\frac{P_2}{Q_2} - \frac{P_1}{Q_1}\right] \tag{2-24}$$

$$\frac{\partial \alpha_i}{\partial \sigma_{kk}} = -\frac{1}{3}\frac{\partial}{\partial T}\left[\frac{P_2}{Q_2} - \frac{P_1}{Q_1}\right] \tag{2-24}$$

After integration of equations (2-24); for the three-dimensional case, α becomes

$$\alpha = \alpha_{oi} + c_{ii}\sigma_{ii} + c_{ij}\sigma_{jj} + c_{ik}\sigma_{kk} \tag{2-25}$$

with

$$c_{ii} = \frac{1}{3}\frac{\partial}{\partial T}\left[\frac{2P_2}{Q_2} + \frac{P_1}{Q_1}\right]$$

$$c_{ij} = -\frac{1}{3}\frac{\partial}{\partial T}\left[\frac{P_2}{Q_2} - \frac{P_1}{Q_1}\right] \tag{2-26}$$

$$c_{ik} = -\frac{1}{3}\frac{\partial}{\partial T}\left[\frac{P_2}{Q_2} - \frac{P_1}{Q_1}\right]$$

for an isotropic material

$$c_{ik} = c_{ij} .$$

For the one-dimensional case, equations (2-21), (2-22) and (2-23) simplify as follows:

1. For the case of a Maxwell body, equation (2-8) defines the constitutive relation

$$\dot{\epsilon} = \frac{\dot{\sigma}}{E_m} + \frac{\sigma}{\eta_m} .$$

If the stress is a function of time

$$\sigma = f(t)$$

then t can be expressed in terms of σ

$$t = F(\sigma) \tag{2-27}$$

Differentiation of equation (2-27) gives

$$dt = \frac{\partial F(\sigma)}{\partial \sigma} d\sigma$$

or

$$\frac{\partial F(\sigma)}{\partial \sigma} = \frac{dt}{d\sigma} = \frac{1}{\dot{\sigma}} \tag{2-29}$$

Now substitution of equation (2-29) into (2-28) results in the following expression:

$$dt = \frac{1}{\dot{\sigma}} d\sigma \tag{2-30}$$

Integration of equation (2-8) with (2-30) gives

$$\epsilon = \frac{\sigma}{E_m} + \int_0^t \frac{\sigma}{\eta_m} dt$$

or

$$\epsilon = \frac{\sigma}{E_m} + \int \frac{\sigma}{\dot{\sigma}\eta_m} d\sigma \tag{2-31}$$

Now differentiating equation (2-28) with respect to σ gives the following expression:

$$\frac{\partial}{\partial \sigma} = \frac{1}{E_m} + \frac{\partial}{\partial \sigma}\left[\int \frac{\sigma}{\dot{\sigma}\eta_m} d\sigma\right]$$

or

$$\frac{\partial \epsilon}{\partial \sigma} = \frac{1}{E_m} + \frac{\sigma}{\dot{\sigma}\eta_m} \tag{2-32}$$

Substitution of equation (2-32) into (2-17) gives

$$\frac{\partial \alpha}{\partial \sigma} = \frac{\partial}{\partial T}\frac{1}{E_m} + \frac{\partial}{\partial T}\frac{\sigma}{\dot{\sigma}\eta_m}$$

or

$$\frac{\partial \alpha}{\partial \sigma} = -\frac{1}{E_m^2}\frac{\partial E_m}{\partial T} - \frac{\sigma}{\dot{\sigma}^2\eta_m}\frac{\partial \eta_m}{\partial T} \qquad (2\text{-}33)$$

After integration the expression for α becomes

$$\alpha = \alpha_0 + \frac{\sigma}{E_m^2}\frac{\partial E_m}{\partial T} - \frac{\sigma^2}{2\dot{\sigma}^2\eta_m}\frac{\partial \eta_m}{\partial T} \qquad (2\text{-}34)$$

for the special case when stress is constant

$$\sigma = \sigma_0$$

the constitutive equation (2-8) becomes

$$\epsilon = \frac{\sigma_0}{E_m} + \frac{\sigma_0}{\eta_m}t \qquad (2\text{-}35)$$

Differentiation of equation (2-35) with respect to σ_0 results in

$$\frac{\partial \epsilon}{\partial \sigma_0} = \frac{1}{E_m} + \frac{t}{\eta_m} \qquad (2\text{-}36)$$

Substitution of (2-36) in (2-17) gives

$$\frac{\partial \alpha}{\partial \sigma_0} = \frac{\partial}{\partial T}\frac{\partial \epsilon}{\partial \sigma} = \frac{\partial}{\partial T}\left[\frac{1}{E_m} + \frac{t}{\eta_m}\right]$$

or

$$\frac{\partial \alpha}{\partial \sigma_0} = -\frac{1}{E_m^2}\frac{\partial E_m}{\partial T} - \frac{t}{\eta_m^2}\frac{\partial \eta_m}{\partial T} \qquad (2\text{-}37)$$

now integrating equation (2-37) with the condition

$$\alpha = \alpha_0 \text{ at } \sigma_0 = 0$$

$$\alpha = \alpha_0 + \left[- \frac{1}{E_m^2} \frac{\partial E_m}{\partial T} - \frac{t}{\eta_m^2} \frac{\partial \eta_m}{\partial T} \right] \tag{2-38}$$

A Maxwell body approaches a perfectly elastic body when $\eta_m \to \infty$. To compare the results with those previously obtained for perfectly elastic materials, $\eta_m = \infty$ is substituted into (2-34) and (2-38) then in both cases (σ = constant and $\sigma \neq$ constant) gives

$$\alpha = \alpha_0 + \frac{\sigma}{E_m^2} \frac{\partial E_m}{\partial T}$$

which is identical to the equation which has been derived for a perfectly elastic material.

2. For the case of a Kelvin body equation (2-11) defines the constitutive relation

$$\epsilon = \frac{\sigma}{E_k + \eta_k D}$$

Differentiating with respect to σ to get

$$\frac{\partial \epsilon}{\partial \sigma} = \frac{1}{E_k + \eta_k D} \tag{2-39}$$

Taking $\frac{\partial \epsilon}{\partial \sigma} = y$, then equation (2-39) becomes

$$y = \frac{1}{E_k + \eta_k D}$$

or

$$(E_k + \eta_k D)y = 1$$

$$\frac{dy}{dt} + \frac{E_k}{\eta_k} y = \frac{1}{\eta_k} \tag{2-40}$$

Equation (2-40) is a differential equation with the following solution

$$y = e^{-\int p\, dt} \int_0^t e^{\int p\, dt}\, q\, dt \tag{2-41}$$

Here

$$p = E_k/\eta_k$$

$$q = 1/\eta_k$$

Therefore

$$y = \frac{\partial \varepsilon}{\partial \sigma} = e^{\frac{-E_k}{\eta_k} t} \int_0^t e^{\frac{E_k}{\eta_k} t}\, \frac{1}{\eta_k}\, dt \ .$$

After integration the following expression is obtained

$$\frac{\partial \varepsilon}{\partial \sigma} = y = \frac{1}{E_k}\left[\, 1 - e^{\frac{-E_k}{\eta_k} t} \,\right] \tag{2-42}$$

Substitution of (2-42) into (2-17) yields

$$\frac{\partial \alpha}{\partial \sigma} = \frac{\partial}{\partial T}\left[\, \frac{1}{E_k} - \frac{1}{E_k} e^{\frac{-E_k}{\eta_k} t} \,\right] .$$

Integrating the above equation gives

$$\alpha = \alpha_0 + \left[\, \frac{\partial}{\partial T}\left(\frac{1}{E_k} - \frac{1}{E_k} e^{\frac{-E_k}{\eta_k} t} \right) \right] \sigma \tag{2-43}$$

A Kelvin body approaches a perfectly elastic material when $\eta_k \to 0$. Substitution of $\eta_k = 0$ in equation (2-43) results in

$$\alpha = \alpha_0 + \left[\frac{\partial}{\partial T} \left(\frac{1}{E_k} \right) \right] \sigma$$

$$\alpha = \alpha_0 - \frac{\sigma}{E_k^2} \frac{\partial E_k}{\partial T}$$

which again is the same as the one which has been derived for perfectly elastic materials.

3. For the case of a Maxwell-Kelvin body equation (2-14) defines the constitutive relations

$$(a_0 + a_1 D + a_2 D^2)\sigma = (b_1 D + D^2)\epsilon$$

To solve the above equation, Laplace transform is applied (33)

$$(p^2 + b_1 p)\, \bar{\epsilon}(p) = (a_2 p^2 + a_1 p + a_0)\, \bar{\sigma}(p) \qquad (2\text{-}44)$$

where p is transformed variable, $\bar{\epsilon}(p)$ and $\bar{\sigma}(p)$ are transformed strain and stress respectively

$$\bar{\epsilon}(p) = \frac{a_2 p^2 + a_1 p + a_0}{(p^2 + b_1 p)}\, \bar{\sigma}(p)$$

$$\epsilon(t) = \mathcal{L}^{-1} \left[\frac{a_2 p^2 + a_1 p + a_0}{(p^2 + b_1 p)}\, \bar{\sigma}(p) \right] \qquad (2\text{-}45)$$

After transforming equation (2-45) to the original variable (t), it is possible to differentiate with respect to $\sigma(t)$.

Considering a step function for $\sigma(t)$, then

$$\sigma = \sigma_0 \, u(t) \tag{2-46}$$

Substituting this into equation (2-14) yields

$$(b_1 D + D^2) \, \epsilon(t) = (a_0 + a_1 D + a_2 D^2) \sigma_0 \, u(t)$$

Now applying the Laplace transform gives

$$(p^2 + b_1 p) \, \bar{\epsilon}(p) = \frac{a_2 p^2 + a_1 p + a_0}{p} \sigma_0 \tag{2-47}$$

Solving for transformed strain in terms of transformed stress

$$\epsilon(p) = \frac{a_2 p^2 + a_1 p + a_0}{p^2 (p + b_1)} \tag{2-48}$$

To get the strain in terms of time and stress, equation (2-48) should be transformed back to the original system (t). To do this equation (2-48) can be written in the following form

$$\bar{\epsilon}(p) = \left[\frac{a_2}{p + b_1} + \frac{a_1}{p(p + b_1)} + \frac{a_0}{p^2 (p + b_1)} \right] \sigma_0 \tag{2-49}$$

The inverse Laplace transform of equation (2-49) is as follows:

$$\epsilon(t) = \left[a_2 e^{-b_1 t} + \frac{a_1}{b_1} (1 - e^{-b_1 t}) + \frac{a_0}{b_1^2} (e^{-b_1 t} + b_1 t - 1) \right] \sigma_0$$

Substitution of coefficients a_0, a_1, a_2 and b_1 from equations (2-15) results in

$$\epsilon(t) = \left[\left(\frac{1}{E_m} + \frac{1}{E_k} \right) + \frac{t}{\eta_m} - \frac{1}{E_k} e^{\frac{-E_k}{\eta_k} t} \right] \sigma_0 \tag{2-50}$$

Differentiation with respect to σ_0 gives

$$\frac{\partial \epsilon}{\partial \sigma_0} = \frac{1}{E_m} + \frac{1}{E_k} + \frac{t}{\eta_m} - \frac{1}{E_k} e^{\frac{-E_k}{\eta_k} t} \tag{2-51}$$

Now substitution of equation (2-51) into (2-18) results in

$$\frac{\partial \alpha}{\partial \sigma} = \frac{\partial}{\partial T}\left[\frac{1}{E_m} + \frac{1}{E_k} + \frac{t}{\eta_m} - \frac{1}{E_k} e^{\frac{-E_k}{\eta_k} t} \right]$$

or

$$\frac{\partial \alpha}{\partial \sigma} = - \frac{1}{E_m^2} \frac{\partial E_m}{\partial T} - \frac{1}{E_k^2} \frac{\partial E_k}{\partial T} - \frac{t}{\eta_m^2} \frac{\partial \eta_m}{\partial T} + \frac{1}{E_k^2} e^{\frac{-E_k}{\eta_k} t} \frac{\partial E_k}{\partial T}$$

$$+ \frac{t}{E_k} e^{\frac{-E_k}{\eta_k} t} \frac{\partial}{\partial T}\left(\frac{E_k}{\eta_k} \right) \tag{2-52}$$

Integration of equation (2-52) gives the expression for α

$$\alpha = \alpha_0 \frac{\sigma_0}{E_m^2} \frac{\partial E_m}{\partial T} - \frac{\sigma_0}{E_k^2} \frac{\partial E_k}{\partial T} - \frac{\sigma_0 t}{\eta_m^2} \frac{\partial \eta_m}{\partial T} + \frac{\sigma_0}{E_k^2} e^{\frac{-E_k}{\eta_k} t} \frac{\partial E_k}{\partial T}$$

$$+ \frac{t\sigma_0}{E_k} e^{\frac{-E_k}{\eta_k} t} \frac{\partial}{\partial T}\left(\frac{E_k}{\eta_k} \right) \tag{2-53}$$

A Maxwell-Kelvin body reduces to a perfectly elastic body by letting $\eta_m \to \infty$ and $\eta_k \to 0$ (14). Thus, substituting into equation (2-53)

$$\eta_m = \infty \text{ and } \eta_k = 0 ,$$

then finally α becomes

$$\alpha = \alpha_0 - \frac{\sigma_0}{E_m^2}\frac{\partial E_m}{\partial T} - \frac{\sigma_0}{E_k^2}\frac{\partial E_k}{\partial T} \tag{2-54}$$

Equation (2-54) is the same as the one obtained for a perfectly elastic material. In this case it corresponds to a model with two springs in series.

B. Using constitutive equations (2-7)

$$e_{ij} = \int_0^t J_2(t - \tau)\frac{\partial S_{ij}(x,\tau)}{\partial \tau}\, d\tau$$

$$\epsilon_{kk} = \int_0^t J_1(t - \tau)\frac{\partial \sigma_{kk}(x,\tau)}{\partial \tau}\, d\tau$$

Applying the Laplace transform to the above equations gives

$$\begin{aligned} \bar{e}_{ij}(p) &= p\,\bar{J}_2(p)\,\bar{S}_{ij}(p) \\ \bar{\epsilon}_{kk}(p) &= p\,\bar{J}_1(p)\,\bar{\sigma}_{kk}(p) \end{aligned} \tag{2-55}$$

where the barred symbols denote the transformed variables and p is the Laplace transform parameter. Now adding $\bar{e}_{11}(x)$ and $\bar{\epsilon}_{kk}(p)$ to get the following relation

$$\bar{e}_{11}(p) + \bar{\epsilon}_{kk}(p) = \frac{2\bar{\epsilon}_{11} - \bar{\epsilon}_{22} - \bar{\epsilon}_{33}}{3} + \frac{\bar{\epsilon}_{11} + \bar{\epsilon}_{22} + \bar{\epsilon}_{33}}{3} = \bar{\epsilon}_{11}(p)$$

$$\bar{e}_{11}(p) + \bar{\epsilon}_{kk}(p) = \bar{\epsilon}_{11}(p) = \frac{p\bar{J}_2}{3}\left[\, 2\bar{\sigma}_{11} - \bar{\sigma}_{22} - \bar{\sigma}_{33} \,\right] + \frac{p\bar{J}_1}{3}\left[\, \bar{\sigma}_{11} + \bar{\sigma}_{22} + \bar{\sigma}_{33} \,\right]$$

After simplification the above equation becomes

$$\epsilon_{11}(p) = \frac{p}{3}\bar{\sigma}_{11}(p)\left[\,2\bar{J}_2(p) + \bar{J}_1(p)\,\right] - \frac{p}{3}\bar{\sigma}_{22}\left[\,\bar{J}_2(p) - \bar{J}_1(p)\,\right]$$

$$- \frac{p}{3}\bar{\sigma}_{33}\left[\,\bar{J}_2(p) - \bar{J}_1(p)\,\right] \qquad (2\text{-}56)$$

Findley (34, 35, 36, 37) and Onaran and Findley (38) showed that $J(t)$ is also a function of σ. Thus,

$$\begin{aligned} J_1 &= J_1(p,\bar{\sigma}) \\ J_2 &= J_2(p,\bar{\sigma}) \end{aligned} \qquad (2\text{-}57)$$

Now differentiating equation (2-56) with respect to $\bar{\sigma}_{11}$, $\bar{\sigma}_{22}$ and $\bar{\sigma}_{33}$ and considering equations (2-57) yields

$$\frac{\partial\bar{\epsilon}_{11}(p)}{\partial\bar{\sigma}_{11}(p)} = \frac{p}{3}\left\{\,2\bar{J}_2(p,\bar{\sigma}) + \bar{J}_1(p,\bar{\sigma}) - (\bar{\sigma}_{22} + \bar{\sigma}_{33})\left[\,\frac{\partial\bar{J}_2}{\partial\bar{\sigma}_{11}} - \frac{\partial\bar{J}_1}{\partial\bar{\sigma}_{11}}\,\right]\right.$$

$$\left. + \bar{\sigma}_{11}(p)\left[\,2\,\frac{\partial\bar{J}_2}{\partial\bar{\sigma}_{11}} + \frac{\partial\bar{J}_1}{\partial\bar{\sigma}_{11}}\,\right]\right\} \qquad (2\text{-}58)$$

$$\frac{\partial\bar{\epsilon}_{11}(p)}{\partial\bar{\sigma}_{22}(p)} = -\frac{p}{3}\left\{\bar{J}_2(p,\bar{\sigma}) - \bar{J}_1(p,\bar{\sigma}) + (\bar{\sigma}_{22} + \bar{\sigma}_{33})\left[\,\frac{\partial\bar{J}_2}{\partial\bar{\sigma}_{22}} - \frac{\partial\bar{J}_1}{\partial\bar{\sigma}_{22}}\,\right]\right.$$

$$\left. - \bar{\sigma}_{11}\left[\,2\,\frac{\partial\bar{J}_2}{\partial\bar{\sigma}_{22}} + \frac{\partial\bar{J}_1}{\partial\bar{\sigma}_{22}}\,\right]\right\} \qquad (2\text{-}59)$$

$$\frac{\partial\bar{\epsilon}_{11}(p)}{\partial\bar{\sigma}_{33}(p)} = -\frac{p}{3}\left\{\bar{J}_2(p,\bar{\sigma}) - \bar{J}_1(p,\bar{\sigma}) + (\bar{\sigma}_{22} + \bar{\sigma}_{33})\left[\,\frac{\partial\bar{J}_2}{\partial\bar{\sigma}_{33}} - \frac{\partial\bar{J}_1}{\partial\bar{\sigma}_{33}}\,\right]\right.$$

$$- \bar{\sigma}_{11} \left[2 \frac{\partial \bar{J}_2}{\partial \bar{\sigma}_{22}} + \frac{\partial \bar{J}_1}{\partial \bar{\sigma}_{22}} \right] \Big\} \qquad (2\text{-}60)$$

Transformation of equations (2-58), (2-59) and (2-60) to the original variable t results in

$$\frac{\partial \varepsilon_{11}(t)}{\partial \sigma_{11}(t)} = \frac{1}{3} \frac{d}{dt} \left[2J_2(t,\sigma) + J_1(t,\sigma) \right] + \frac{1}{3} \frac{d}{dt} \int_0^t \sigma_{11}(t)\, \psi_1(t-\lambda)\, d\lambda$$

$$- \frac{1}{3} \frac{d}{dt} \int_0^t \left\{ \sigma_{22}(t) + \sigma_{33}(t) \right\} \varphi_1(t-\lambda)\, d\lambda \qquad (2\text{-}61)$$

$$\frac{\partial \varepsilon_{11}}{\partial \sigma_{22}} = - \frac{1}{3} \frac{d}{dt} \left[J_2(t,\sigma) - J_1(t,\sigma) + \int_0^t \left\{ \sigma_{22}(t) + \sigma_{33}(t) \right\} \varphi(t-\lambda)\, d\lambda \right.$$

$$\left. - \int_0^t \sigma_{11}(t)\, \psi_2(t-\lambda)\, d\lambda \right] \qquad (2\text{-}62)$$

$$\frac{\partial \varepsilon_{11}}{\partial \sigma_{33}} = - \frac{1}{3} \frac{d}{dt} \left[J_2(t,\sigma) - J_1(t,\sigma) + \int_0^t \left\{ \sigma_{22}(t) + \sigma_{33}(t) \right\} \varphi_3(t-\lambda)\, d\lambda \right.$$

$$\left. - \int_0^t \sigma_{11}(t)\, \psi_3(t-\lambda)\, d\lambda \right] \qquad (2\text{-}63)$$

where

$$\psi_1 = 2 \frac{\partial J_2}{\partial \sigma_{11}} + \frac{\partial J_1}{\partial \sigma_{11}} ,$$

$$\psi_2 = 2 \frac{\partial J_2}{\partial \sigma_{11}} + \frac{\partial J_1}{\partial \sigma_{22}} ,$$

$$\psi_3 = 2\frac{\partial J_2}{\partial \sigma_{33}} + \frac{\partial J_1}{\partial \sigma_{33}} ,$$

$$\varphi_1 = \frac{\partial J_2}{\partial \sigma_{11}} - \frac{\partial J_1}{\partial \sigma_{11}} ,$$

$$\varphi_2 = \frac{\partial J_2}{\partial \sigma_{22}} - \frac{\partial J_1}{\partial \sigma_{22}} ,$$

$$\varphi_3 = \frac{\partial J_2}{\partial \sigma_{33}} - \frac{\partial J_1}{\partial \sigma_{33}} .$$

Substitution of equations (2-61), (2-62) and (2-63) into (2-18) leads to:

$$\frac{\partial \alpha_i}{\partial \sigma_{ii}} = \frac{\partial}{\partial T}\left\{\frac{1}{3}\frac{d}{dt}\left[2J_2(t,\sigma) + J_1(t,\sigma) + \int_0^t \sigma_{11}(t)\,\psi_1(t-\lambda)d\lambda - \int_0^t \{\sigma_{22}(t) + \sigma_{33}(t)\}\,\varphi_1(t-\lambda)d\lambda\right]\right\} ,$$

$$\frac{\partial \alpha_i}{\partial \sigma_{JJ}} = \frac{\partial}{\partial T}\left\{-\frac{1}{3}\frac{d}{dt}\left[J_2(t,\sigma) - J_1(t,\sigma) + \int \{\sigma_{22}(t) + \sigma_{33}(t)\}\,\varphi_2(t-\lambda)d\lambda - \int_0^t \sigma_{11}(t)\,\psi_2(t-\lambda)d\lambda\right]\right\} ,$$

$$\frac{\partial \alpha_i}{\partial \sigma_{kk}} = \frac{\partial}{\partial T}\left\{-\frac{1}{3}\frac{d}{dt}\left[J_2(t,\sigma) - J_1(t,\sigma) + \int_0^t \{\sigma_{22}(t) + \sigma_{33}(t)\}\,\varphi(t-\lambda)d\lambda - \int_0^t \sigma_{11}(t)\,\psi(t-\lambda)d\lambda\right]\right\} ,$$

Integration of the above equations gives the α as follows

$$\alpha_i = \alpha_{oi} + \int c_{ii} d\sigma_i + \int c_{ij} d\sigma_j + \int c_{ik} d\sigma_k \qquad (2\text{-}64)$$

where c_{ii}, c_{ij} and c_{ik} are defined as

$$c_{ii} = \frac{\partial \alpha_i}{\partial \sigma_{ii}} , \qquad (2\text{-}65)$$

$$c_{ij} = \frac{\partial \alpha_i}{\partial \sigma_{jj}} , \qquad (2\text{-}66)$$

$$c_{ik} = \frac{\partial \alpha_i}{\partial \sigma_{kk}} . \qquad (2\text{-}67)$$

Similar relations can be obtained for α_j and α_k by the same procedure.

For the one-dimensional case, equations (2-62) and (2-63) will vanish and equation (2-61) becomes

$$\frac{\partial \epsilon(t)}{\partial \sigma(t)} = \frac{d}{dt} \left[J(t,\sigma) + \int_0^t \sigma_{11}(t) \, \psi \, (t - \lambda) d\lambda \right] \qquad (2\text{-}68)$$

where

$$\psi = \frac{\partial J}{\partial \sigma} \qquad (2\text{-}69)$$

For the case of a constant applied stress

$$\sigma = \sigma_0$$

equation (2-68) becomes

$$\frac{\partial \epsilon(t)}{\partial \sigma_0} = \frac{d}{dt} J(t,\sigma_0) + \sigma_0 \frac{\partial}{\partial \sigma_0} J(t,\sigma_0) \qquad (2\text{-}70)$$

substitute in equation (2-18) to get

$$\frac{\partial \alpha}{\partial \sigma_0} = \frac{\partial}{\partial T}\left[\frac{d}{dt} J(t,\sigma_0) + \sigma_0 \frac{\partial}{\partial \sigma_0} J(t,\sigma_0)\right] \qquad (2\text{-}71)$$

Integration of equation (2-71) gives the α as follows

$$\alpha = \alpha_0 + \int Z \, d\sigma \ , \qquad (2\text{-}72)$$

where

$$Z = \frac{\partial \alpha}{\partial \sigma_0} \qquad (2\text{-}73)$$

Equations (2-25), (2-38), (2-43), (2-53), (2-64) and (2-72) are the relations among thermal coefficient of expansion, time and stresses applied on different materials. As it can be seen from these equations in the regular viscoelastic materials for which E and η decrease with the increase of temperature, α increases with the stress and in the few materials which E and η increase with the temperature, α decreases with the stress.

Therefore, it has been shown that according to the theory developed here α is not a constant but a time, temperature and stress dependent factor.

By the same procedure it is possible to find the mathematical relations for any combinations of springs and dashpots.

CHAPTER III

PLANNING OF EXPERIMENTS

In the preceding chapter it was derived that, for the uniaxial state of stress, the relation for the stress dependency of thermal expansion coefficient would be

$$\frac{\partial \alpha}{\partial \sigma} = \frac{\partial}{\partial T}\left[\frac{d}{dt} J(t,\sigma_0) + \sigma_0 \frac{\partial}{\partial \sigma_0} J(t,\sigma_0)\right] .$$

To investigate the validity of the above equation, two stages of experiment were planned: (1) low-stress-level experiments and (2) high-stress-level experiments.

1. Low-Stress-Level Experiments

In order to have enough information to carry out the second stage of experiments, it is necessary to know the variations of creep constant J with time, temperature and stress explicitly. Several methods have been developed (35, 42) to represent the stress-strain relation with time-dependent creep modulus. In parallel there have been some experimental investigations on the creep properties of viscoelastic materials (41, 44). However, the experimental investigations were not concerned with the change of creep coefficient with temperature. In the constitutive equation

suggested by Findley (48)

$$\varepsilon = a \sinh \frac{\sigma}{b} + ct^n \sinh \frac{\sigma}{d} \qquad (3\text{-}1)$$

there are constants a, b, c, d and n. At least some of these constants are highly affected by the temperature changes according to Findley.

To find the variations of these coefficients with temperature, it was planned to conduct some creep experiments at different temperatures. Since it was expected, according to the theory derived in Chapter II, that the thermal expansion coefficient varies with the stress, the experiments were planned to be conducted at low stress levels at this stage, in order to minimize the error due to this effect. On the other hand, to avoid a transient state of temperature distribution and consequent inconsistency of the results, it was decided to keep the temperature constant at each level during the experiments. From the experimental information the coefficients of creep can be determined such that equation (3-1) fits the experimental data. The procedure for doing this is explained in Chapter V.

Since the creep at low stress levels is very small and any small error due to the reading or due to the non-uniform condition may cause a major deviation in the results, four sets of experiments with different stresses were planned to be carried at each temperature level in order to check the consistency of the fitted curves and to be able to compare

them statistically. It was also planned to repeat these experiments at different temperatures, so that curves could be plotted for a, b, c, d and n versus temperature. From this information it is possible to predict the creep at any temperature and any stress level for the material considered with the assumption of constant thermal expansion coefficient.

It is interesting to note that, although the temperatures were kept constant during each experiment, after obtaining the above information the creep can be predicted at any variable temperature simply by considering the coefficients as a function of temperature and integrating equation (3-1) over the range of temperature change.

2. High-Stress-Level Experiments

At this stage it was planned to apply stresses of the order of 3000-5000 psi in order to observe the effect of stress on thermal expansion coefficient as much as possible. Again at this stage the temperature is kept constant. For the specified temperature the values of the constants of equation (3-1) can be obtained from the curves previously explained in section 1. With these coefficients and the specified stress, the curve for the strain versus time may be plotted. This is the creep curve assuming the thermal expansion coefficient is constant.

Now from equations (2-71) and (2-72) the predicted additional strain due to the variation of the thermal expansion coefficient can be calculated and added to the basic

creep deformation calculated from equation (3-1). The calculated strains may be compared with the experimental data obtained for creep at high stress level. With this procedure it was planned to check the derived equations at three different temperatures and different stresses.

It should be realized that equation (2-72) has two terms, the first term α_0 has already been compensated by letting the experimental models expand and stabilize at each temperature without any stresses, and then applying the stress.

CHAPTER IV

MATERIAL, SPECIMENS, AND EXPERIMENTAL APPARATUS

1. Material

A methyl methacrylate copolymer plastic* was employed in these experiments. This material is a slightly cross-linked copolymer. To predict any trouble in evaluating the creep and other experimental data, several materials were considered. These included copolymers like "Lucite," "Plexiglas," and polyvinyl chloride (39, 40, 41). From a study of the technical data on these materials, "Lucite" was selected. It has good creep properties (42) and also is relatively insensitive to humidity change (0.2-0.4 per cent water absorption in 24 hours, A.S.T.M. test method D570). Furthermore, it has almost the same machining characteristics and thermal conductivity as polyvinyl chloride (3.6×10^{-4} calories per second per square centimeter per °C per centimeter thickness) but it can stay at higher temperature (43). Commercial Lucite contains little plasticizing agent and mechanical properties of this material are known to be strongly affected by temperature, thus permitting a wide range of investigation.

---

*"Lucite," manufactured by E.I. du Pont.

Unfortunately, all of the available experimental creep data on "Lucite" indicate that the creep tests were carried at only one temperature level. Therefore, as a part of the present investigation, the creep behavior of "Lucite" has been investigated at several temperature levels. This was necessary in order to find the variation of creep coefficient of the material versus temperature as discussed in Chapter III.

2. Specimens

Several models were made to be used at different sets of experiments; they were all made out of a 1/4-inch-thick flat sheet of "Lucite." The gage lengths of all of the models were 8 in. and they were made stronger at the ends as shown in Figure 4. In order to be able to use and statistically compare the results of the tests, it is required to cut the models from the materials having the same condition as much as possible. To fulfill this requirement, all of the models were cut from one piece of plastic. Furthermore to prevent any nonhomogeneity among the models due to the molding stresses in different directions, all of the models were cut along the same axis. The models were 1/4 inch x 3/8 inch in cross section. One 1/4-inch-diameter hole was prepared on the centerline of the model at each end to center the model and apply the tension. But since the bearing area at the holes was only

$$\text{bearing area} = 1/4'' \times 1/4'' = 1/16 \text{ sq.in.}$$

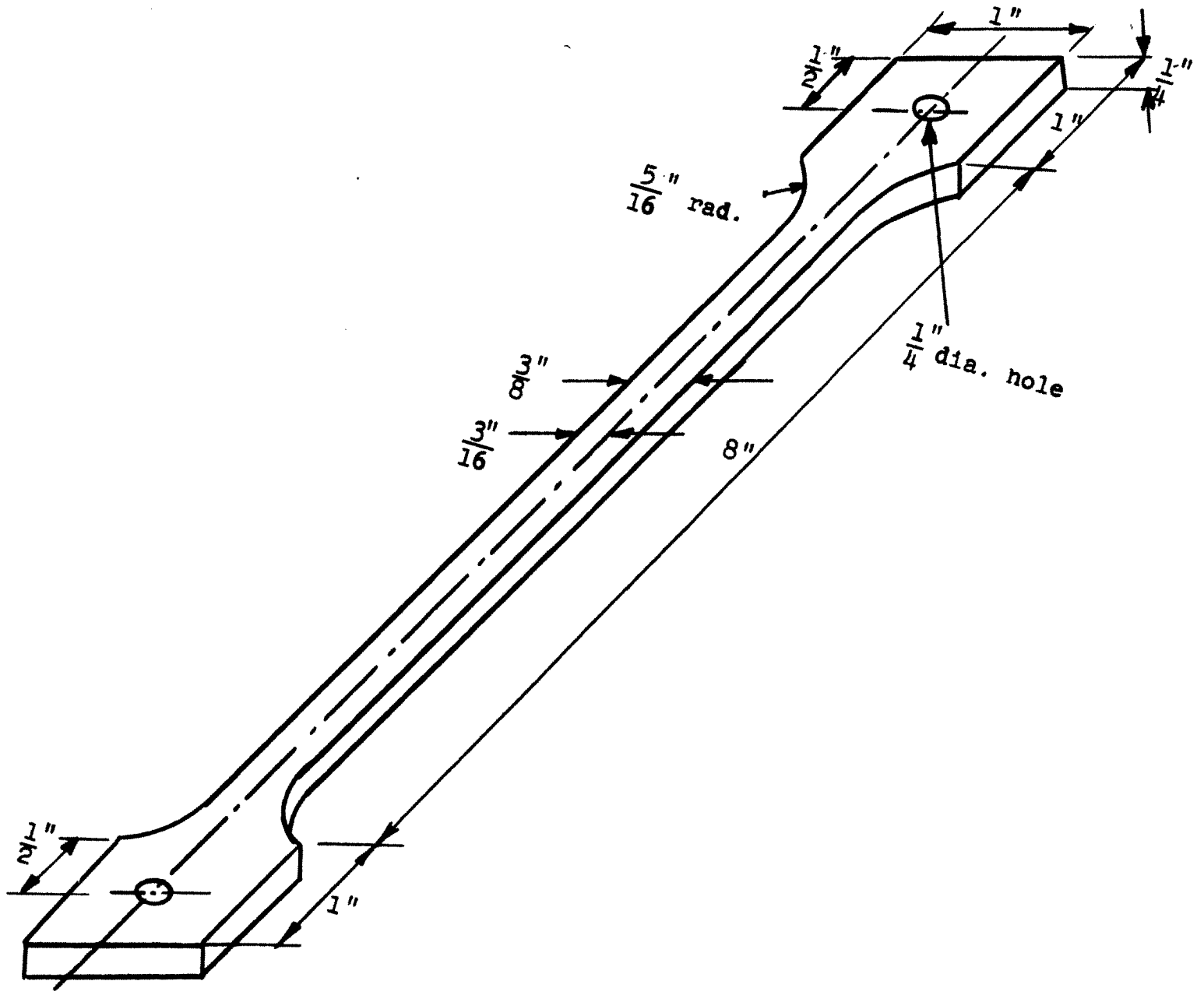

Figure 4. Dimensions of the Specimens

and in comparison with cross section of the model

cross sectional area = 3/8" x 1/4" = 3/32 sq.in.
at the gage length

was small, there was a chance for bearing failure due to compression force exerted by the steel pin and consequently misleading results. To prevent this situation, two clamps were prepared for each model as shown in Figure 5, to exert the tension load through the whole square area at the ends instead of using just the holes. Before tightening the clamps at each experiment, the model was centered by applying a small load and then the clamps were tightened. The dial gages used for the elongation measurements were numbered to read 1/10,000 in., but it was possible to estimate the fractions of 1/10 and therefore get measurement up to 1/100,000 in. The dial gages were installed in such a way to read directly the elongation of the gage length, as shown in the installation of the gage (Figure 6). To avoid friction between the clamps and loading frame, washers were used on each side of the specimen to increase the spacing between the two pieces of clamp.

As shown in Figure 4, the ends of the section called gage length have been smoothly enlarged to prevent failures at the grips. However, in the data reduction, it is assumed that the cross section is constant. The following calculations give an estimate of the percentage of error to be expected due to this assumption. These calculations are based

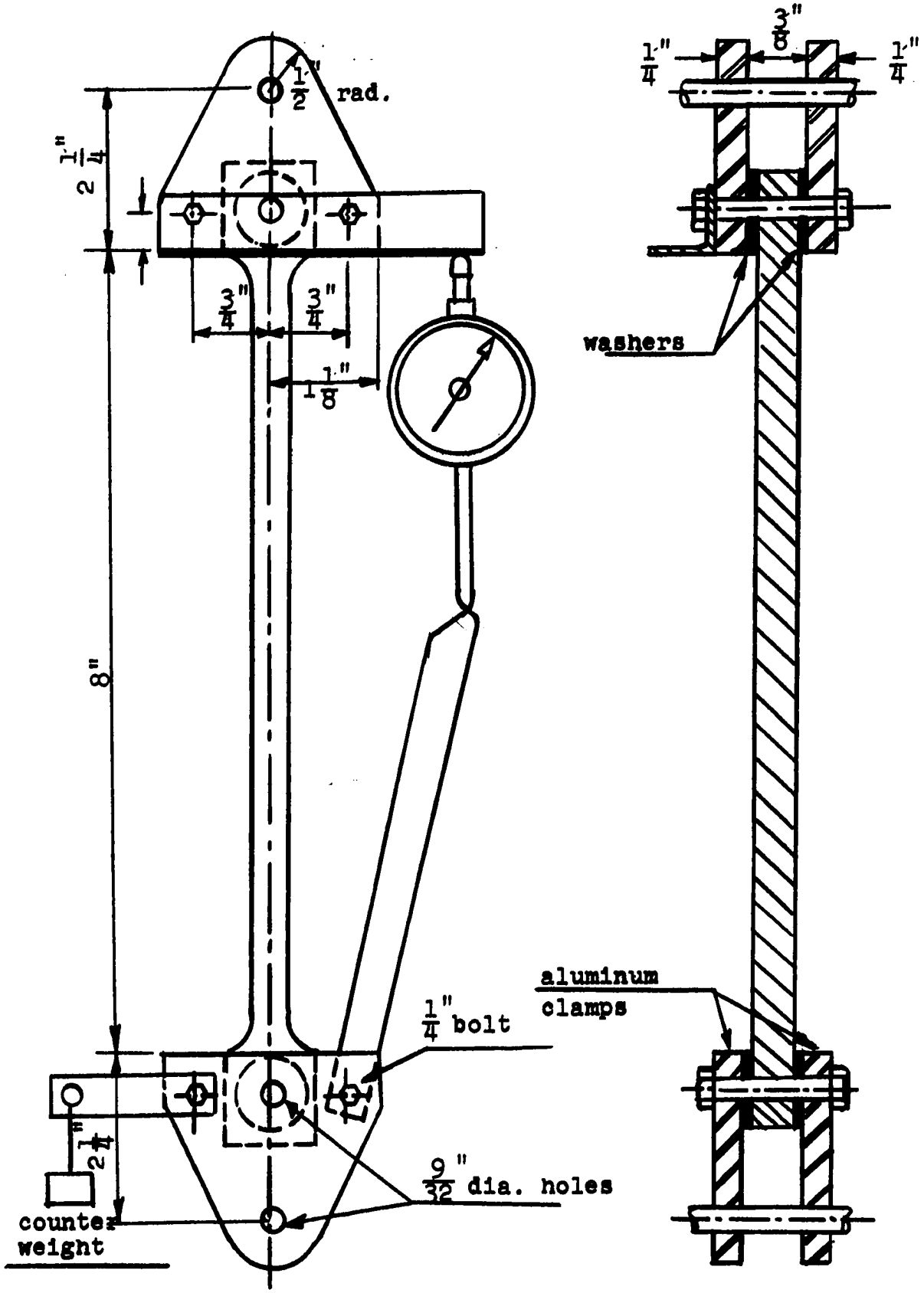

Figure 5. Model Assembly

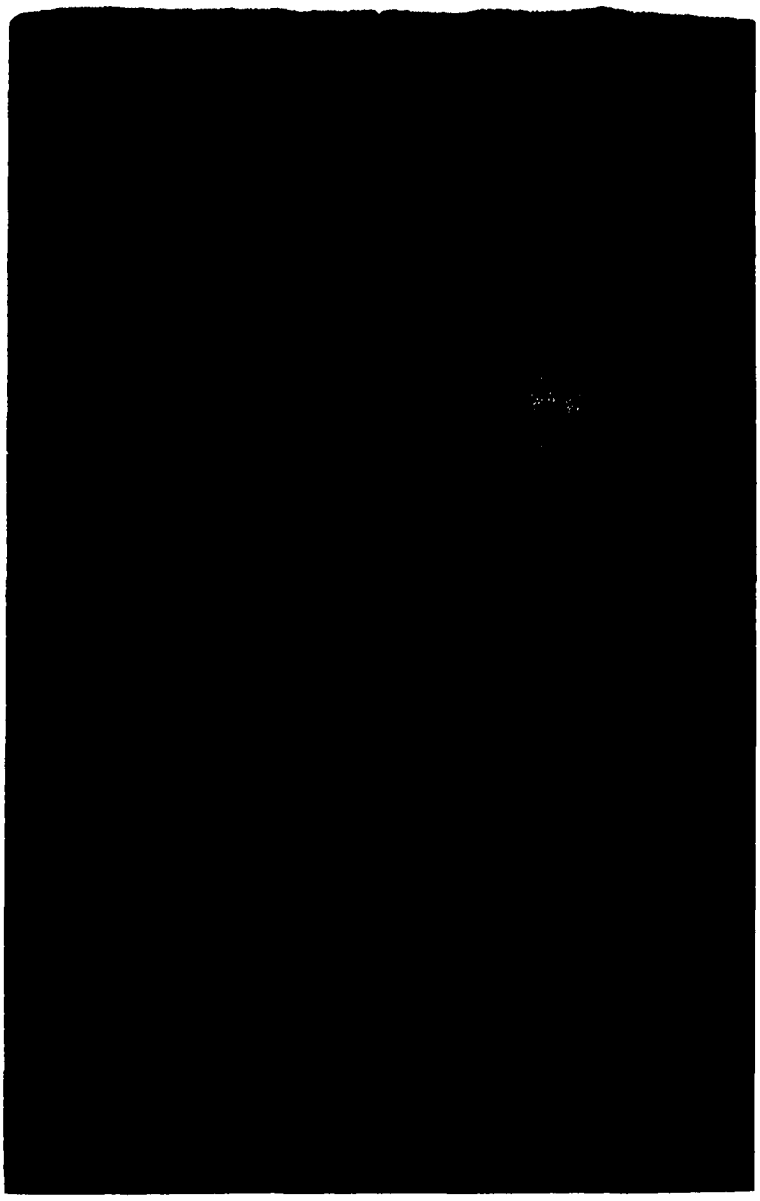

Figure 6. Installation of Dial Indicators

on elementary theory, in which stress-concentration effects are neglected.

Let F denote the applied load and E the Young's modulus. Then the strain is

$$\varepsilon = \frac{F}{1/4 \times 3/8 \times E}$$

$$\text{total elongation assuming constant cross section } \Delta\ell = \ell\varepsilon = \frac{8F}{1/4 \times 3/8 \times E} \text{ in.} \qquad (4\text{-}1)$$

$$\text{actual total elongation} = \Delta\ell' + \Delta\ell'' \qquad (4\text{-}2)$$

$$\Delta\ell' = \ell'\varepsilon = (8 - \tfrac{5}{8}) \frac{F/E}{1/4 \times 3/8} \quad \frac{7.375\ F/E}{1/4 \times 3/8} \text{ in.}$$

To find $\Delta\ell''$, the strain is calculated at an arbitrary point on the curved section and then integrated to give the elongation.

$$\text{stress at any point of the curved section} = \frac{F}{\frac{1}{4}(1 - \frac{5}{8}\cos\theta)} \text{ psi}$$

$$\text{strain} = \frac{F/E}{\frac{1}{4}(1 - \frac{5}{8}\cos\theta)}$$

Referring to Figure 7,

$$L = \frac{5}{16}\sin\theta$$

$$dL = \frac{5}{16}\cos\theta\, d\theta$$

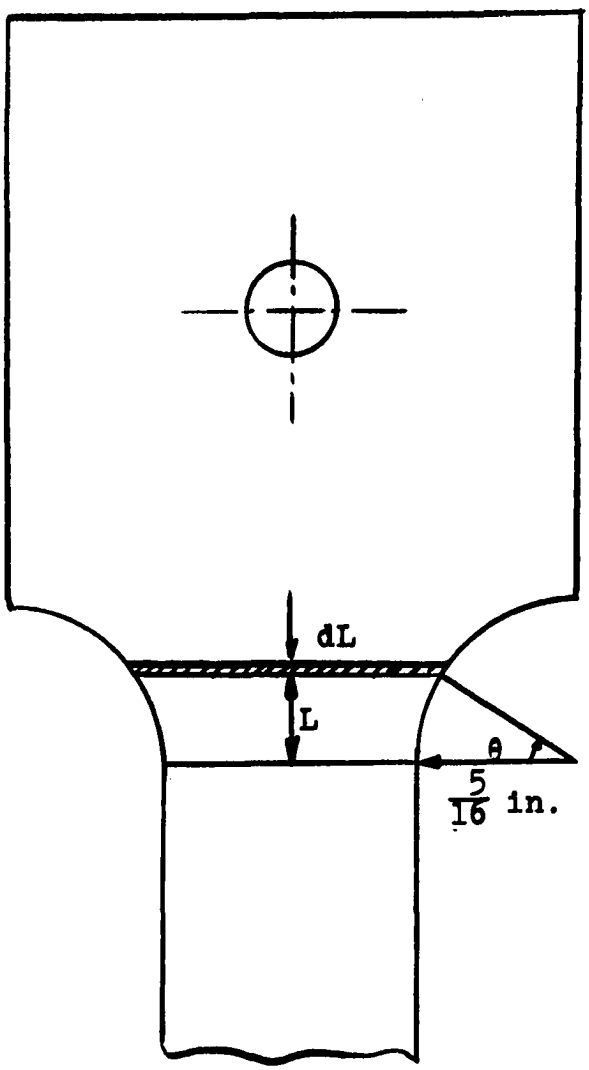

Figure 7

$$\text{elongation for small length } dL = \frac{\frac{5}{16}\,(F/E)\cos\theta}{\frac{1}{4}\,(1 - \frac{5}{8}\cos\theta)}\,d\theta$$

$$\text{total elongation for the curved sections at both ends} = \frac{5}{8}\int_0^{\frac{\pi}{2}} \frac{(F/E)\cos\theta}{\frac{1}{4}\,(1 - \frac{5}{8}\cos\theta)}\,d\theta$$

or

$$\Delta\ell'' = \frac{5(F/E)}{1/4}\int_0^{\frac{\pi}{2}} \frac{\cos\theta}{8 - 5\cos\theta}\,d\theta$$

$$\Delta\ell'' = \frac{5F/E}{1/4}\left[-\frac{\theta}{5} + \frac{16}{5\sqrt{39}}\tan^{-1}\left(\sqrt{\frac{13}{3}}\tan\frac{\theta}{2}\right)\right]_0^{\pi/2} \qquad (4\text{-}3)$$

After substitution of limits, equation (4-3) becomes

$$\Delta\ell = \frac{1.31\ F/E}{1/4}\ .$$

Thus:

$$\text{actual total elongation} = \Delta\ell' + \Delta\ell'' = \frac{7.375\ F/E}{1/4 \times 3/8} + \frac{1.31\ F/E}{1/4}\ \text{in.}$$

$$\text{and percentage of error} = \frac{\Delta\ell' + \Delta\ell'' - \Delta\ell}{\Delta\ell' + \Delta\ell''} \times 100$$

$$= \frac{\frac{7.375\ F/E}{1/4 \times 3/8} + \frac{1.31\ F/E}{1/4} - \frac{F/E}{1/4 \times 3/8}}{\frac{7.375\ F/E}{1/4 \times 3/8} + \frac{1.31\ F/E}{1/4}} \times 100$$

or

$$\text{percentage error} = \frac{35.7}{20.9} = 1.69\%$$

Therefore the error entering the calculations for the

above assumption would be less than 1.7%. Consideration of the stress-concentration effects by making an elasticity-theory analysis would be expected to result in an even smaller estimated error.

3. Experimental Setup

To carry out the experiments at each temperature level as nearly similarly as possible, four loading frames were designed with different loading ratios (Figure 8), so that tests under four different loads could be carried at the same temperature and humidity conditions. This avoids the possibility of different temperature and humidity fluctuations at different loadings but the same temperature level. The frames were prepared such that they could be used for any specimen length up to 12 inches.

All of the loading frames were completely enclosed in an oven specially designed and built for this purpose as shown in Figure 9. The heating system of the oven consisted of an electric heater which was mounted on the wall and was controlled by an automatic temperature controller. One electric fan was installed at the bottom under the loading frames, and the other one on the opposite wall where the heater was mounted. Since the viscoelastic materials are highly sensitive to vibrations, especially at higher temperatures, the fans were mounted on two separate stands in order to minimize the transfer of vibrations due to the fans through the structures. The fans were in continuous operation

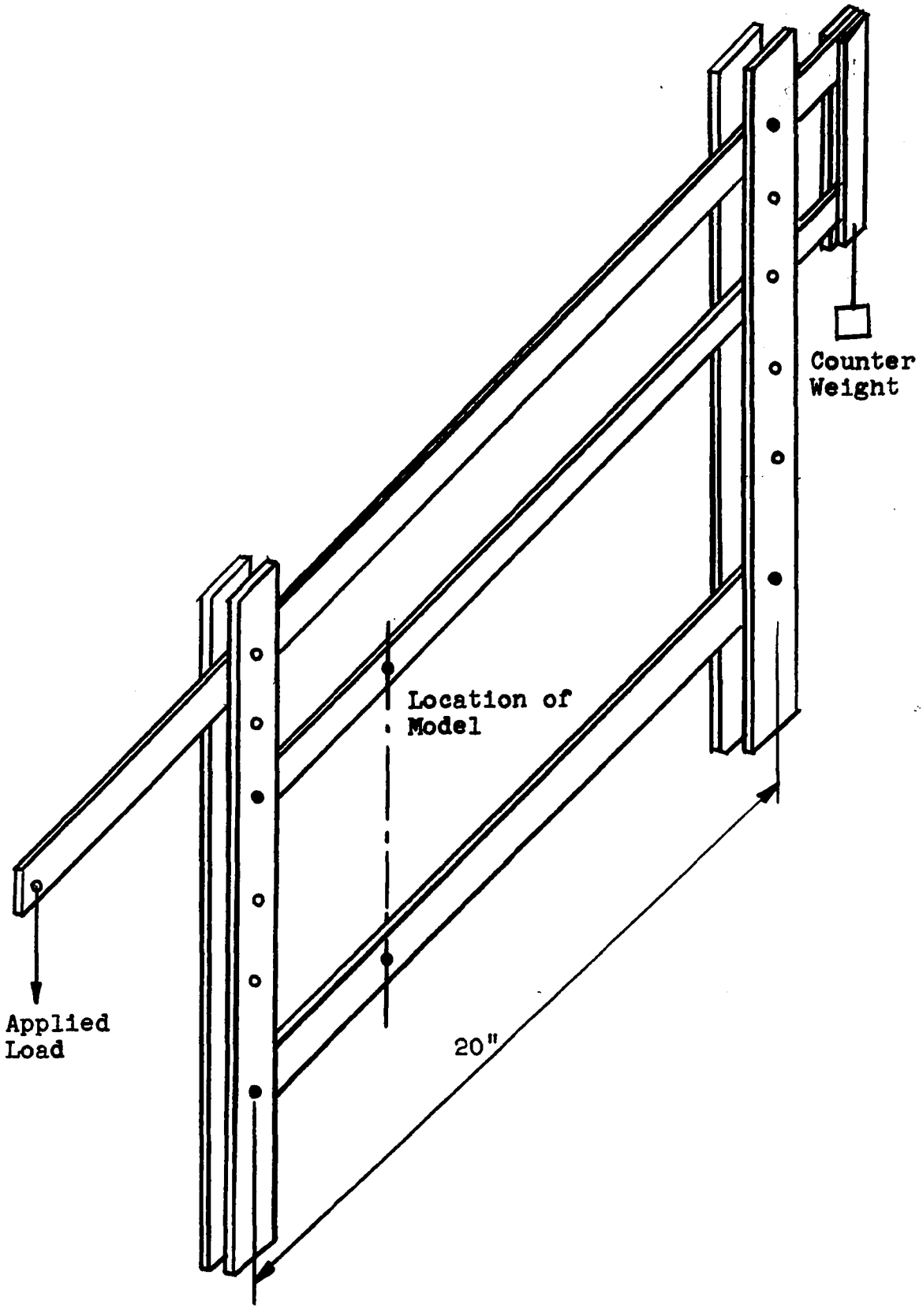

Figure 8. Loading Frame



Figure 9. Frames Mounted in Oven

while the oven was in use and the heater was in control. With this procedure the temperature was fairly well distributed, so that there was only about one degree Fahrenheit temperature difference between the front and back of the oven. The temperature was controlled within 1°F.

A glass door was prepared at the front, to be able to take all readings without opening the door and disturbing the temperature. In order to avoid the development of local hot spots on the specimens and to prevent temperature variations from one specimen to another due to direct radiation, a shield was used in front of the heater. Furthermore, the locations of specimens were so arranged that they were all almost the same distance from the heater.

CHAPTER V

EXPERIMENTAL RESULTS

In this chapter an effort has been made to express the creep behavior of the material by a mathematical expression.

As explained in Chapter III, experiments were conducted at low stress levels and at different temperatures to obtain the variations of the creep constants of the material with temperature. At low temperatures the experiments were conducted at periods of time up to 49 hours, but at higher temperatures a two-hour period was sufficient to get the necessary information. At the same time at higher temperatures the lower stresses were applied.

The results of creep experiments at different temperatures are tabulated in Tables 1 through 35, Appendix A, and the curves for the experimental strain versus time are plotted in Figures 25 through 34.

To find the creep coefficients, it is necessary to establish a constitutive relation among the stress, strain and time which fits the experimental data as closely as possible. Different kinds of equations have been suggested and applied by various investigators.

Marin (42) assumed a time-dependent stress-strain relation in the form of

$$\varepsilon = D\sigma^m + Bt\sigma^n \tag{5-1}$$

Where ε is the creep strain, t is the time, and σ is the stress level; D, B, m and n depend on the material.

Leaderman (45) suggested the following equation for creep in torsion

$$\varepsilon = A \log_{10} t + Bt + C \tag{5-2}$$

Where A, B and C are constants depending on material and stress.

Cottrel and Aytekin (46) used equation (5-3) for single crystal materials.

$$\varepsilon = \varepsilon_0 + At^{1/3} + Bt \tag{5-3}$$

Here A and B are constants of the material and ε_0 is the instantaneous strain.

Pao and Marin (47) also introduced the creep mathematical relations in the following form.

$$\varepsilon = A + B(1 - e^{-Ct}) + Dt \tag{5-4}$$

Where A, B, C and D are material constants and functions of stress.

Findley and Khosla (48) employed the creep equation in the form of

$$\varepsilon = \varepsilon_0 + mt^n \tag{5-5}$$

Where ϵ_0, m and n are material constants and ϵ_0 and m depend on stress as well. They showed that stress dependence of ϵ_0 and m can be expressed by a hyperbolic sine function such as

$$\epsilon_0 = a \sinh \frac{\sigma}{b} \tag{5-6}$$

$$m = c \sinh \frac{\sigma}{d} \tag{5-7}$$

which yields an equation for creep as follows:

$$\epsilon = a \sinh \frac{\sigma}{b} + ct^n \sinh \frac{\sigma}{d} \tag{5-8}$$

For the present investigation equation (5-8) has been employed also. In equation (5-8) the first term is independent of time with a and b material constants depending on temperature but independent of stress. The second term of equation (5-8) is time dependent, and constants c, n and d are again material constants independent of stress but temperature dependent.

To obtain the coefficients a, b, c, d and n from the experimental data, equation (5-5) can be rearranged as

$$\epsilon - \epsilon_0 = mt^n \tag{5-9}$$

Taking logarithm from both sides of equation (5-9) yields:

$$\log_{10} (\epsilon - \epsilon_0) = \log_{10} m + n \log_{10} t \tag{5-10}$$

Equation (5-10) is the equation of a straight line taking log $(\epsilon - \epsilon_0)$ as ordinate and log t as abscissa. The quantity n is the slope of the line and the value of m may be obtained

by letting t = 1 hour. The experimental curves corresponding to equation (5-10) are plotted in Figures 10 through 19. Having ϵ_0 and m for the different stresses and by the use of equations (5-6) and (5-7), the coefficients a, b, c and d can be obtained by trial such that the plot of ϵ_0 versus $\sinh \frac{\sigma}{b}$ and m versus $\sinh \frac{\sigma}{d}$ yield a straight line. This is done in Figures 20, 21 and 22 for different temperatures, where the values of a and c are the slopes of the lines. It was found that to get the straight lines for ϵ_0 versus $\sinh \frac{\sigma}{b}$ and m versus $\sinh \frac{\sigma}{d}$ the values of b and d are constant and independent of temperature

$$b = 40{,}000 \qquad d = 3{,}300,$$

but the values of a, c and n vary with temperature. The variation of these coefficients are tabulated in Table 36, Appendix A and are plotted in Figure 23.

In order to be able to differentiate the creep function J as necessary in equation (2-71), it is much more convenient and accurate to get mathematical expressions for variation of the constants with temperature. To do this, in Figure 24 $\log_{10} n$, $\log_{10} 100c$ and $\log_{10} a$ are plotted versus temperature. It is seen that the resulting curves are nearly straight lines. Now the mathematical expressions can be obtained very easily. Let

$$y_1 = -\log_{10} n = u_1 + v_1 T \qquad (5\text{-}11)$$

$$y_2 = -\log_{10} a = u_2 + v_2 T \qquad (5\text{-}12)$$

$$y_3 = -\log_{10} 100c = u_3 + v_3 T \qquad (5\text{-}13)$$

Where u_1, v_1, u_2, v_2, u_3 and v_3 may be obtained by choosing two arbitrary points on each line and putting their coordinates in equations (5-11), (5-12) and (5-13) and solving for the unknowns. In this way

$$u_1 = 1.800 \qquad v_1 = -\frac{50.6}{6500}$$

$$u_2 = 1.490 \qquad v_2 = -\frac{49}{8000}$$

$$u_3 = 1.935 \qquad v_3 = -\frac{68}{6500}$$

Substitution of these values in equations (5-11), (5-12) and (5-13) results in:

$$-\log_e n = -2.3 \log_{10} n = 2.3\left(1.800 - \frac{50.6}{8000} T\right),$$

$$-\log_e a = -2.3 \log_{10} n = 2.3\left(1.490 - \frac{49}{8000} T\right),$$

$$-\log_e 100c = -2.3 \log_{10} 100c = 2.3\left(1.935 - \frac{68}{6500}\right),$$

or

$$n = e^{(.0179T - 4.14)}, \qquad (5\text{-}14)$$

$$a = e^{(.0141T - 3.4)}, \qquad (5\text{-}15)$$

$$c = \frac{1}{100} e^{(.024T - 4.45)}. \qquad (5\text{-}16)$$

With equations (5-14), (5-15) and (5-16) the creep expression (equation 5-8) is completely defined in terms of stress, time, temperature and material behavior for Lucite as follows:

$$\varepsilon = e^{(.0141T - 3.4)} \sinh \frac{\sigma}{40,000}$$

$$+ \frac{1}{100} t^n e^{(.024T - 4.45)} \sinh \frac{\sigma}{3300} \qquad (5\text{-}17)$$

Where T is the temperature in degrees Fahrenheit and n is given by equation (5-14).

With the obtained coefficients a, b, c, d and n and equation (5-8) the theoretically predicted creep is calculated and plotted in Figures 25 through 34.

It should be mentioned here that although the experimental curves and the curves from equation (5-8) differ from one another and in the worst cases as much as 10 percent, but in comparison with the worst cases of (38) and (42) which have 8 percent and 30 percent deviation respectively, these curves seem to be in reasonable agreement.

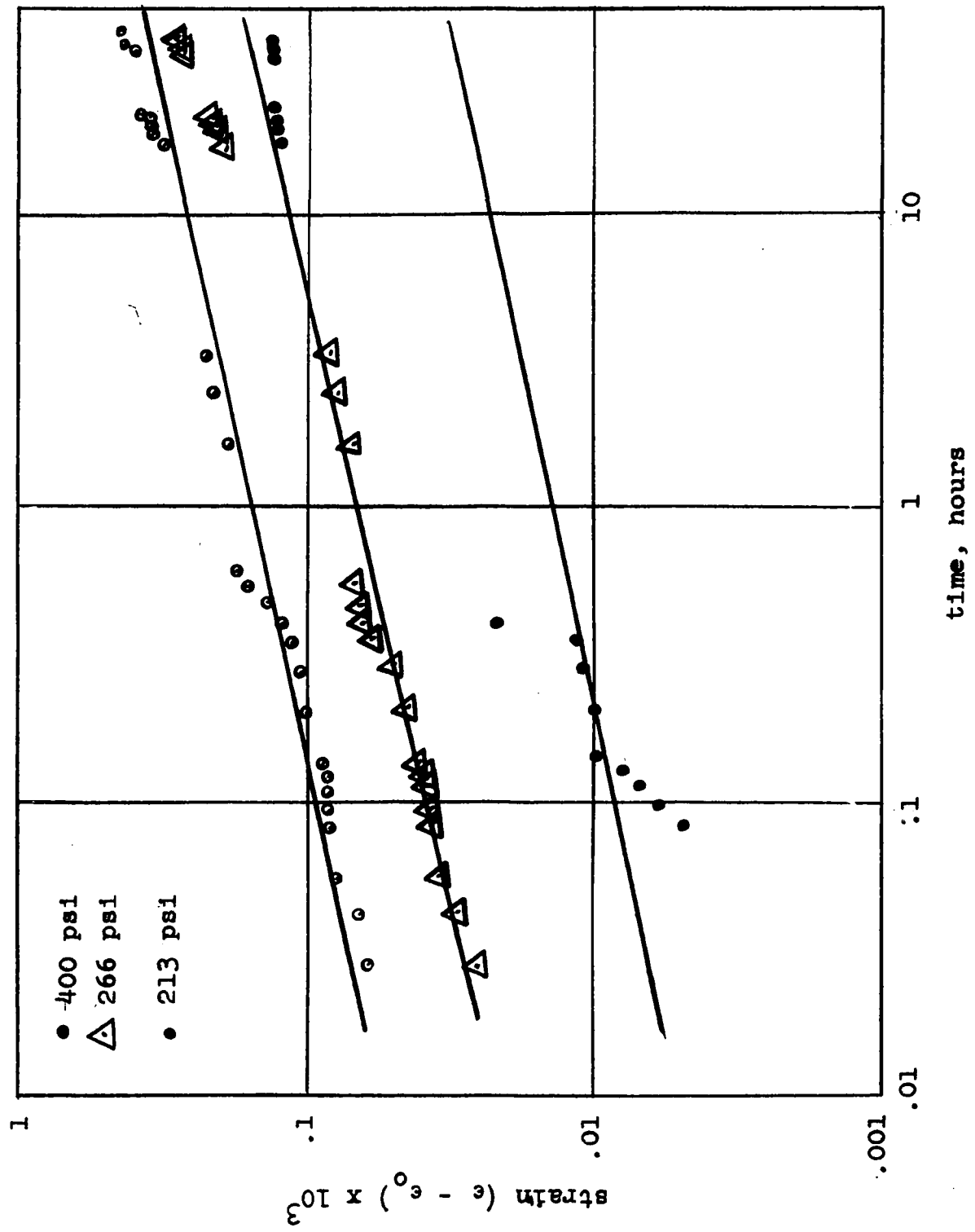

Figure 10. Log strain versus log time at 90°F

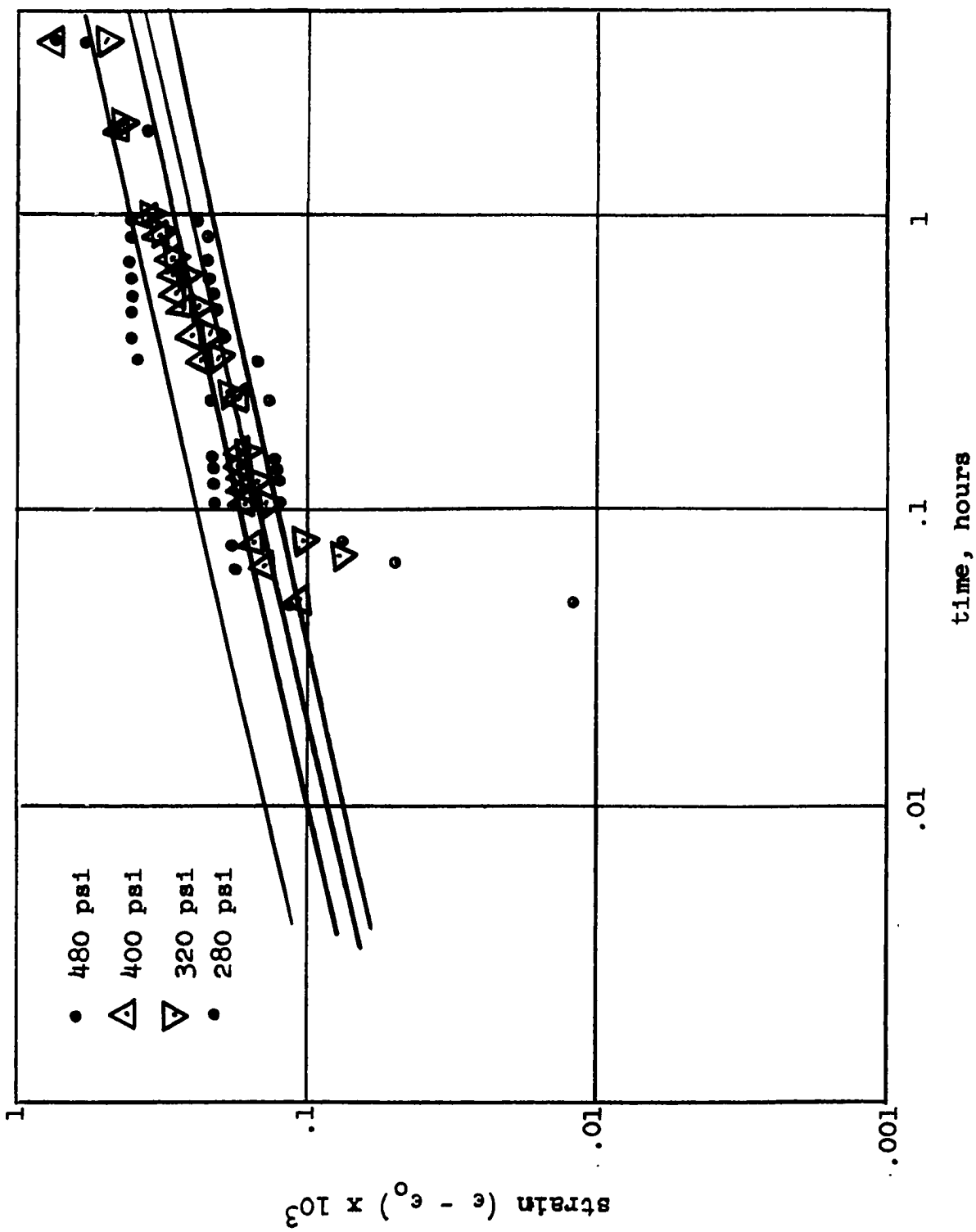

Figure 11. Log strain versus log time at 105°F

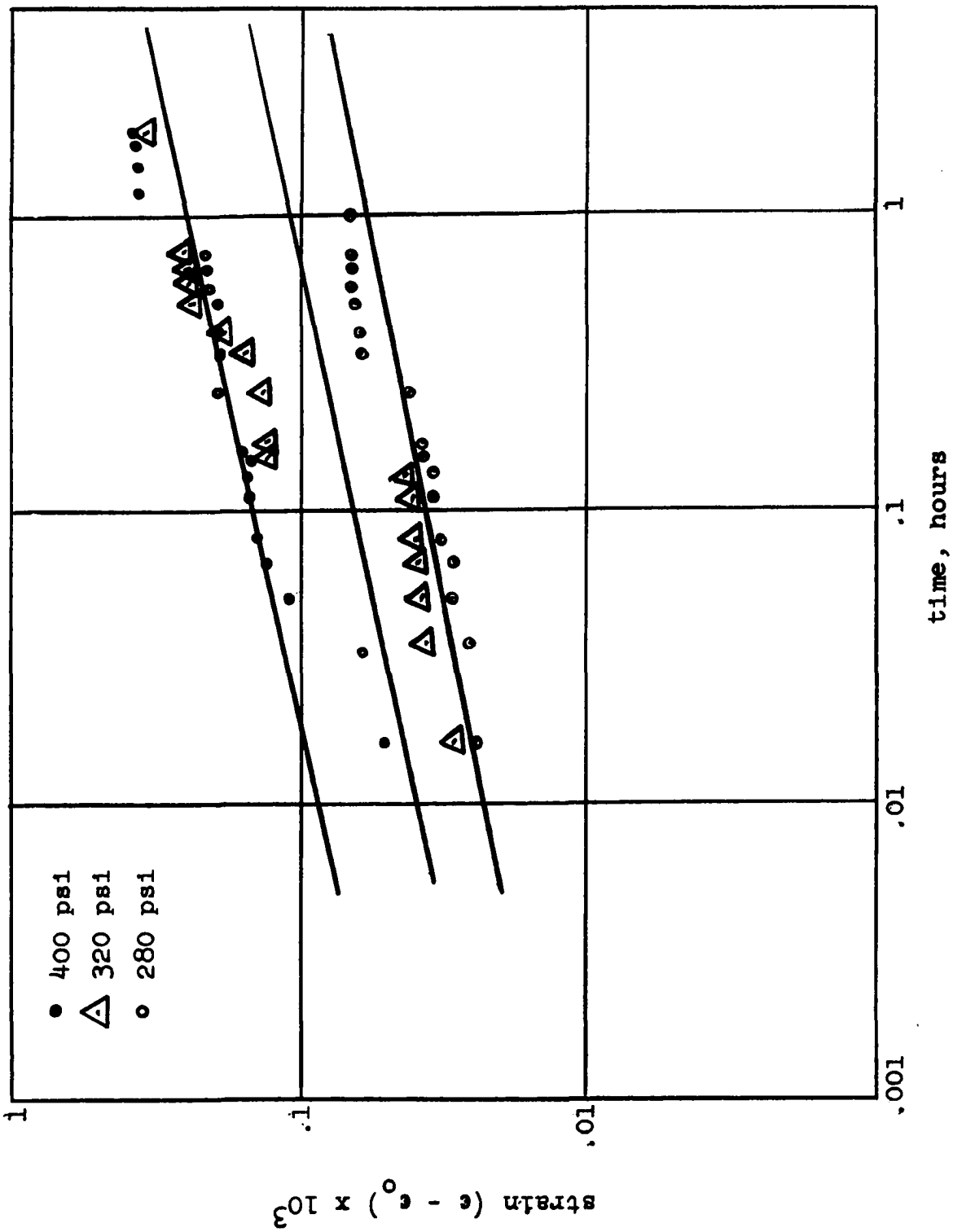

Figure 12. Log strain versus log time at 120°F

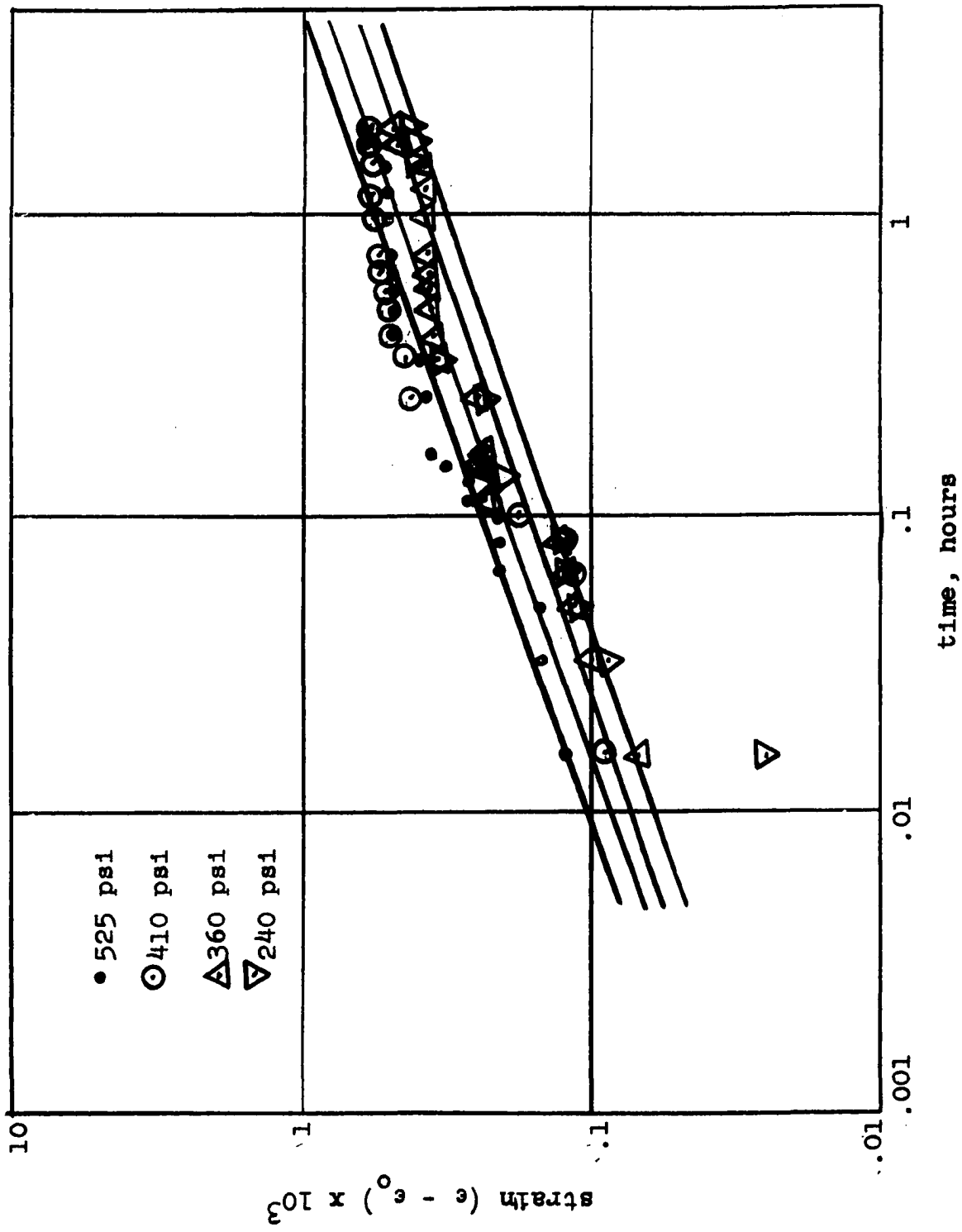

Figure 13. Log strain versus log time at 135°F

Figure 14. Log strain versus log time at 150°F

Figure 15. Log strain versus log time at 165°F

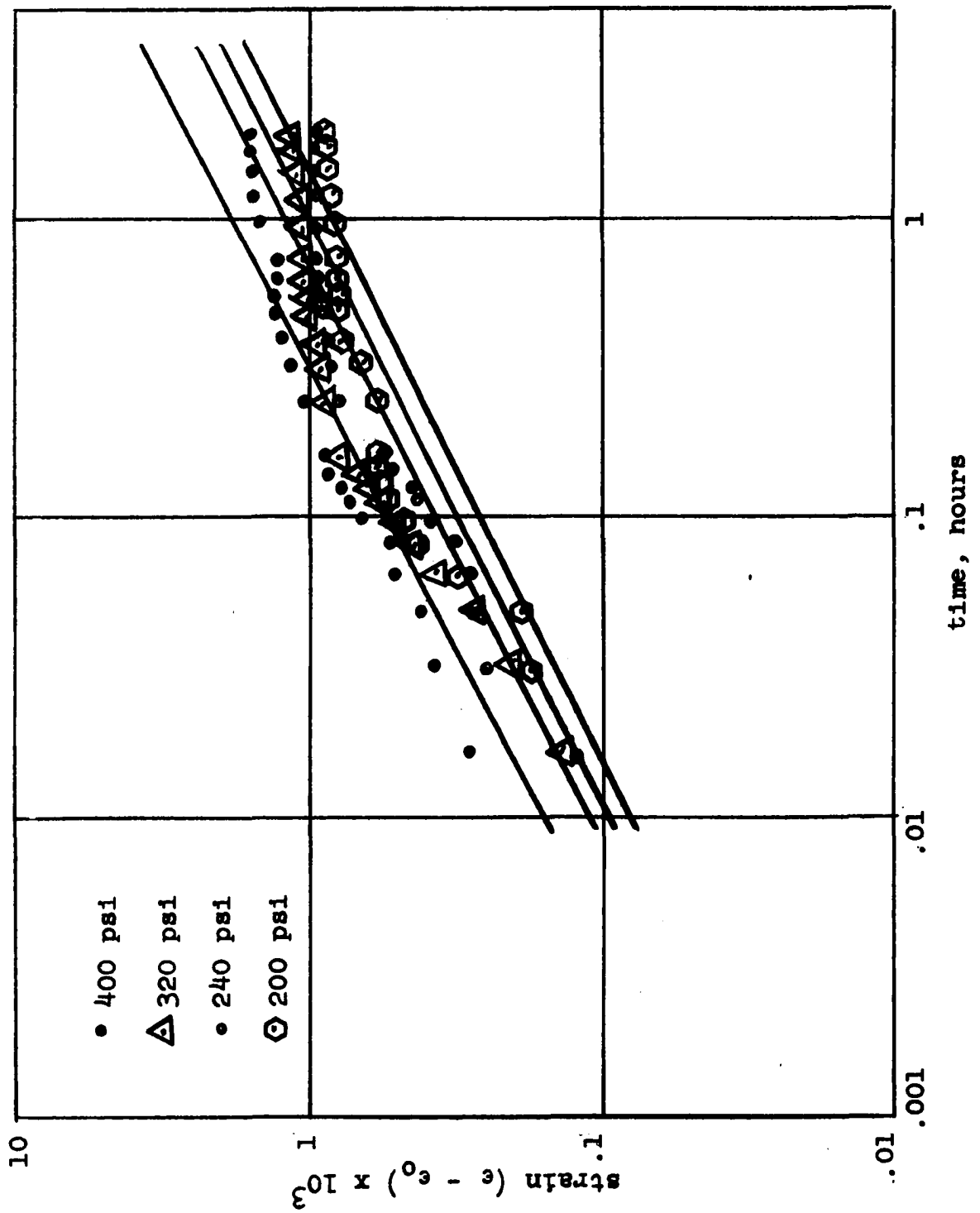

Figure 16. Log strain versus log time at 180°F

Figure 17. Log strain versus log time at 195°F

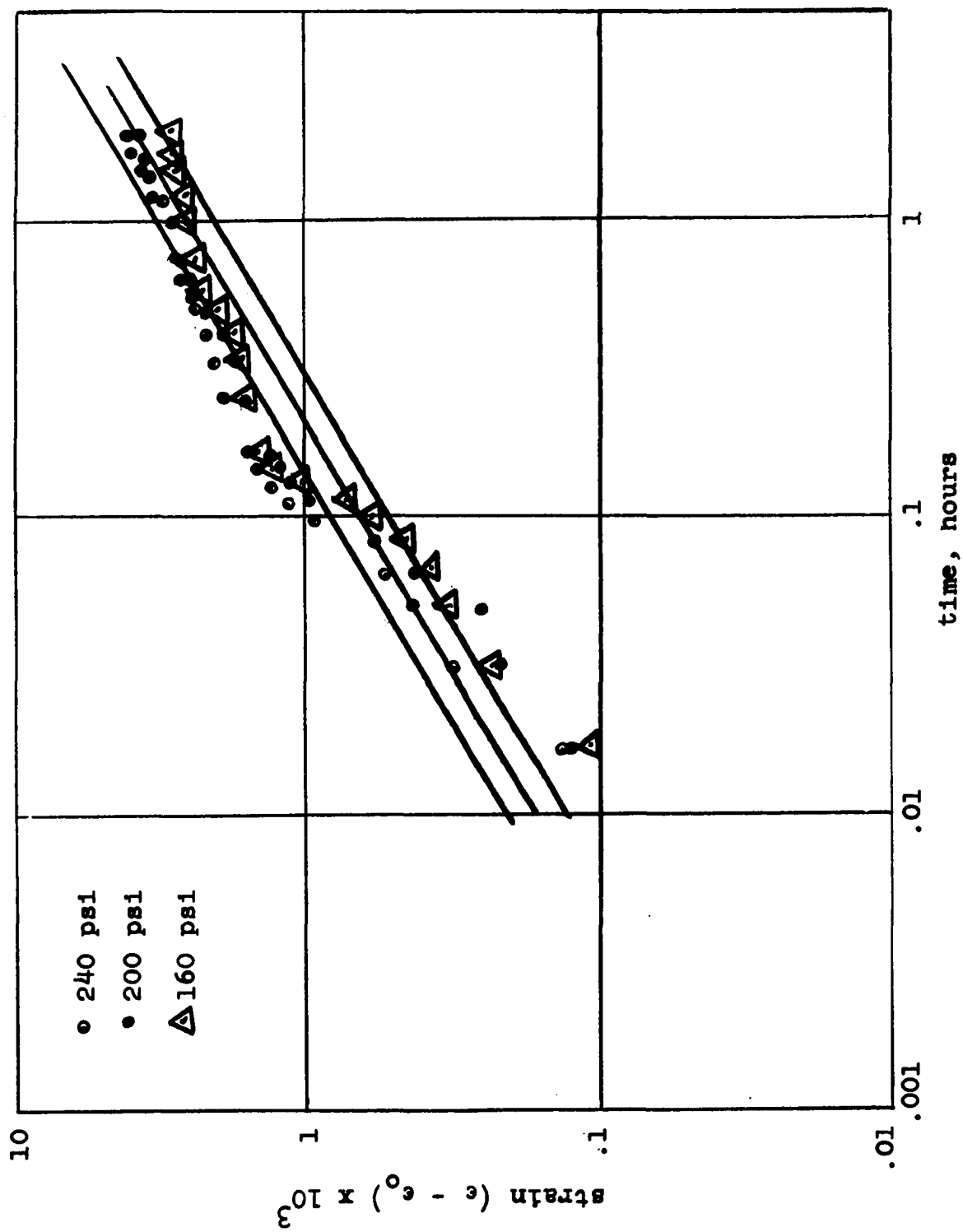

Figure 18. Log strain versus log time at 210°F

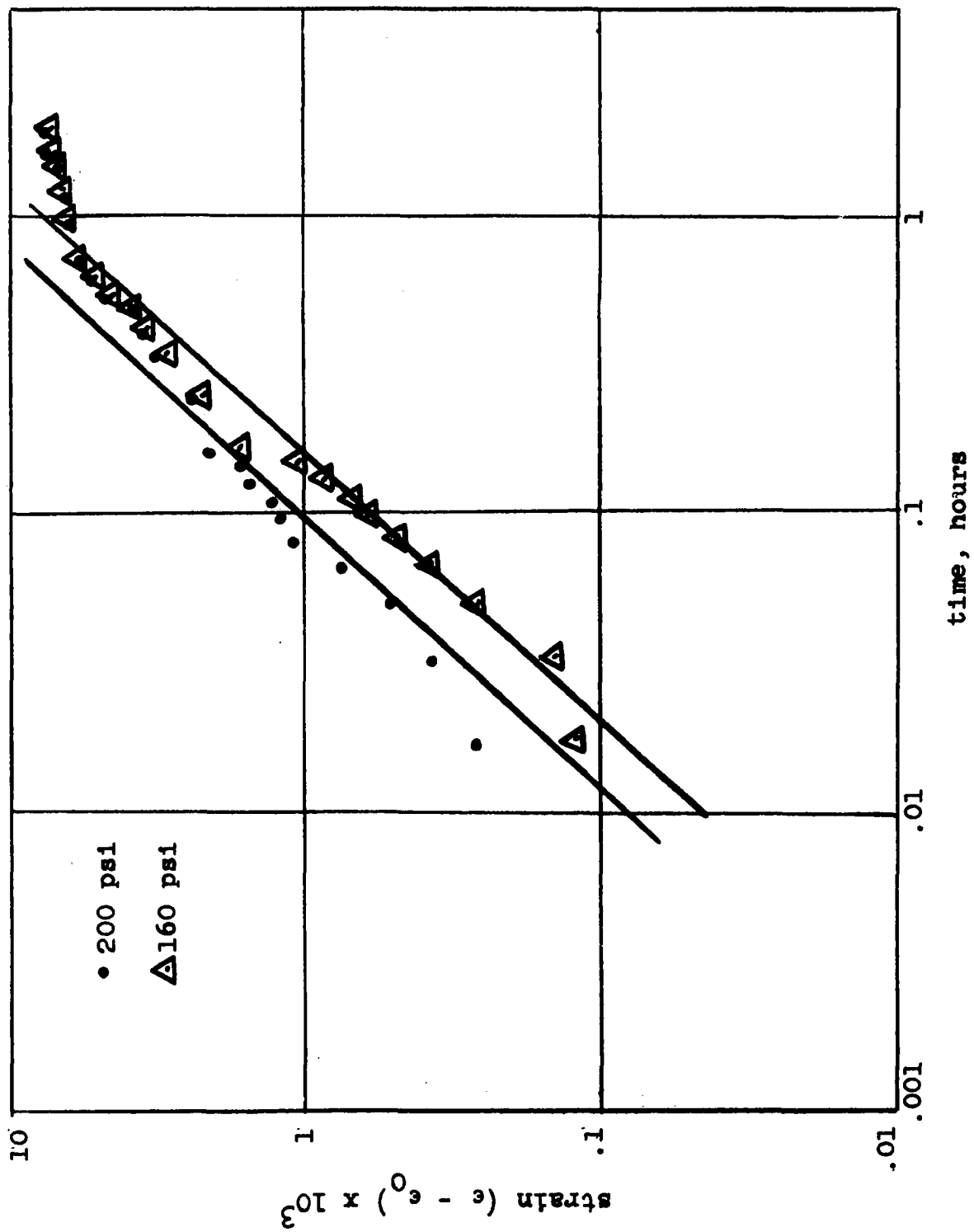

Figure 19. Log strain versus log time at 225°F

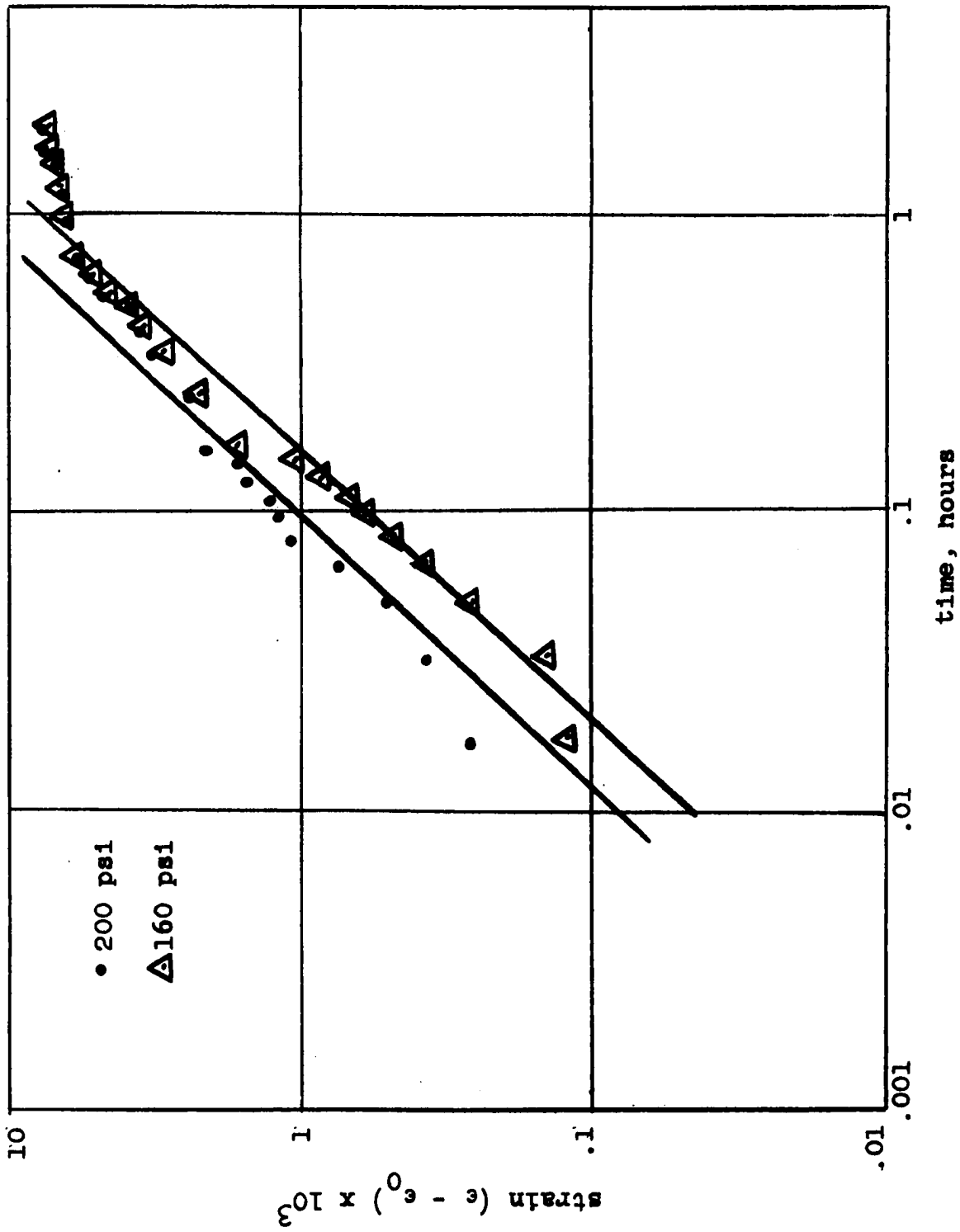

Figure 19. Log strain versus log time at 225°F

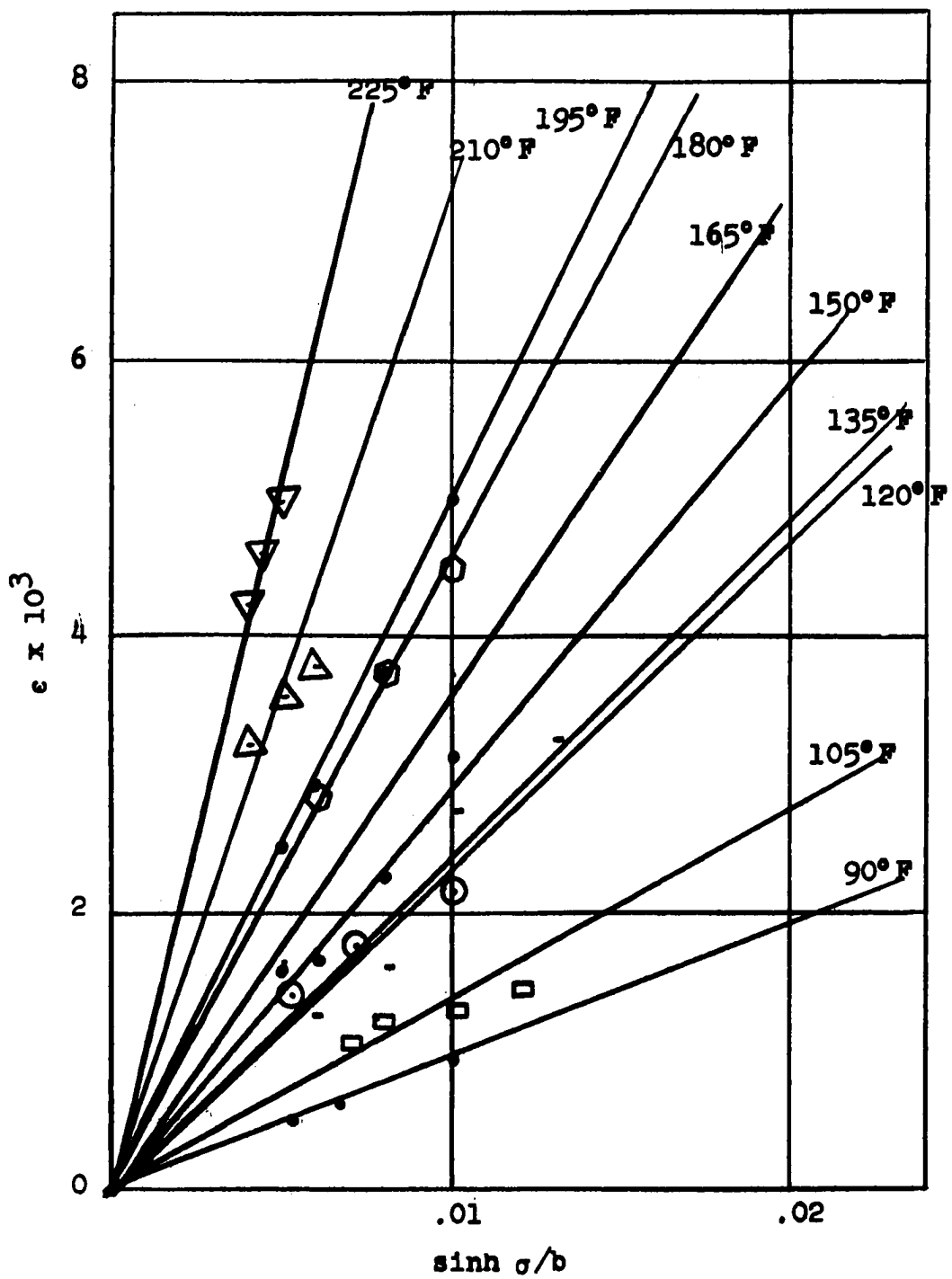

Figure 20. Evaluation of constants a and b

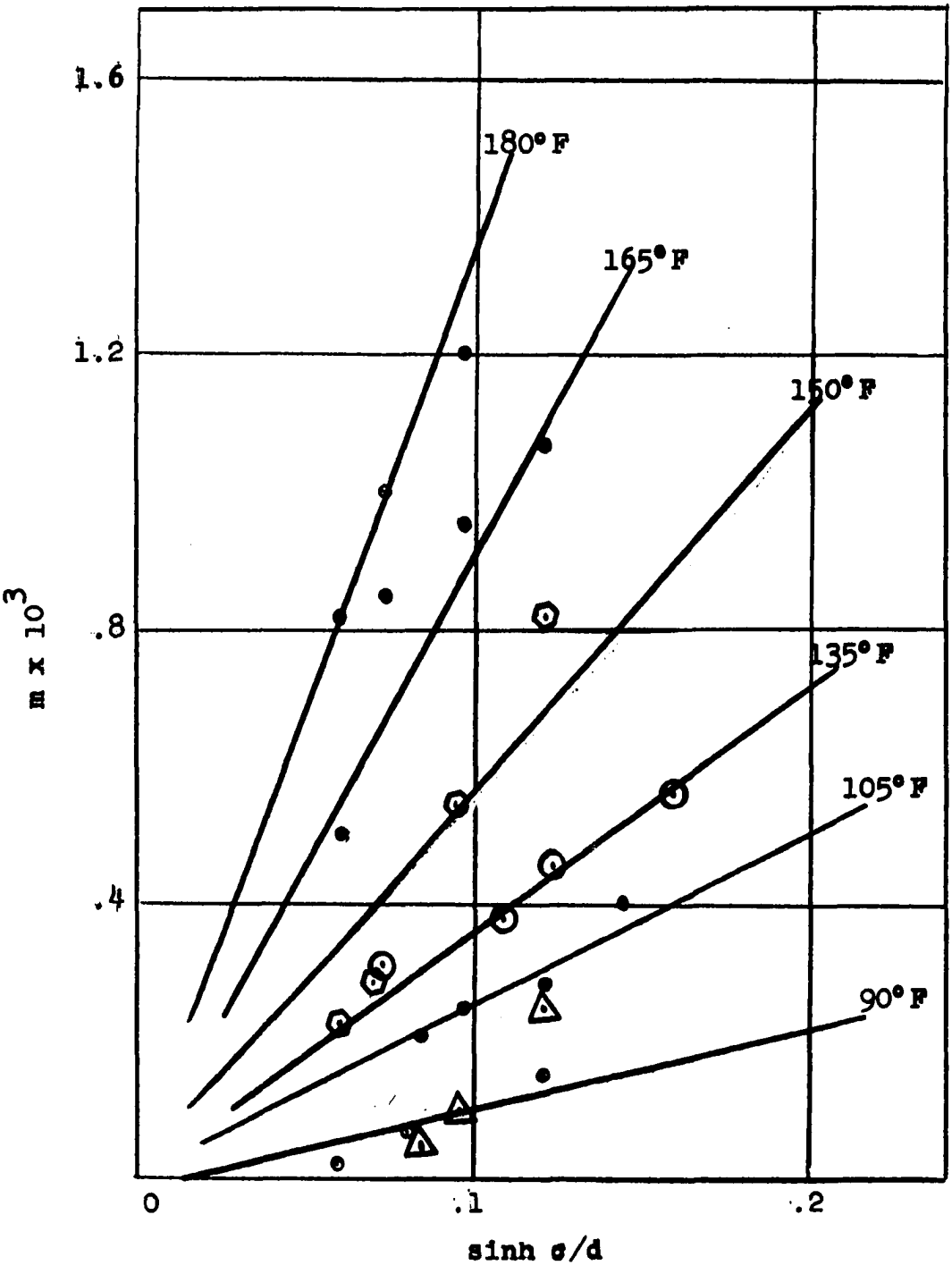

Figure 21. Evaluation of constants c and d

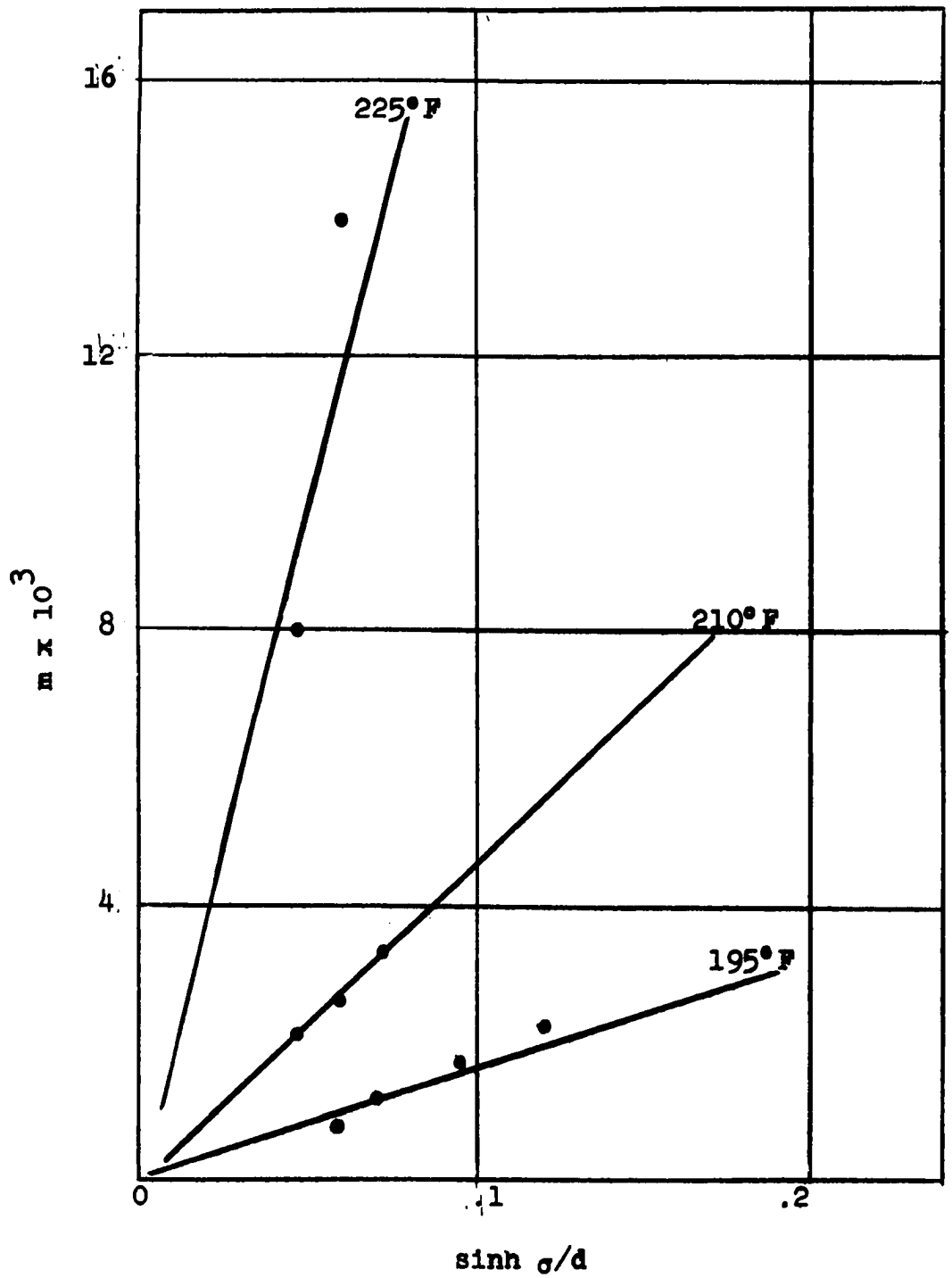

Figure 22. Evaluation of constants c and d

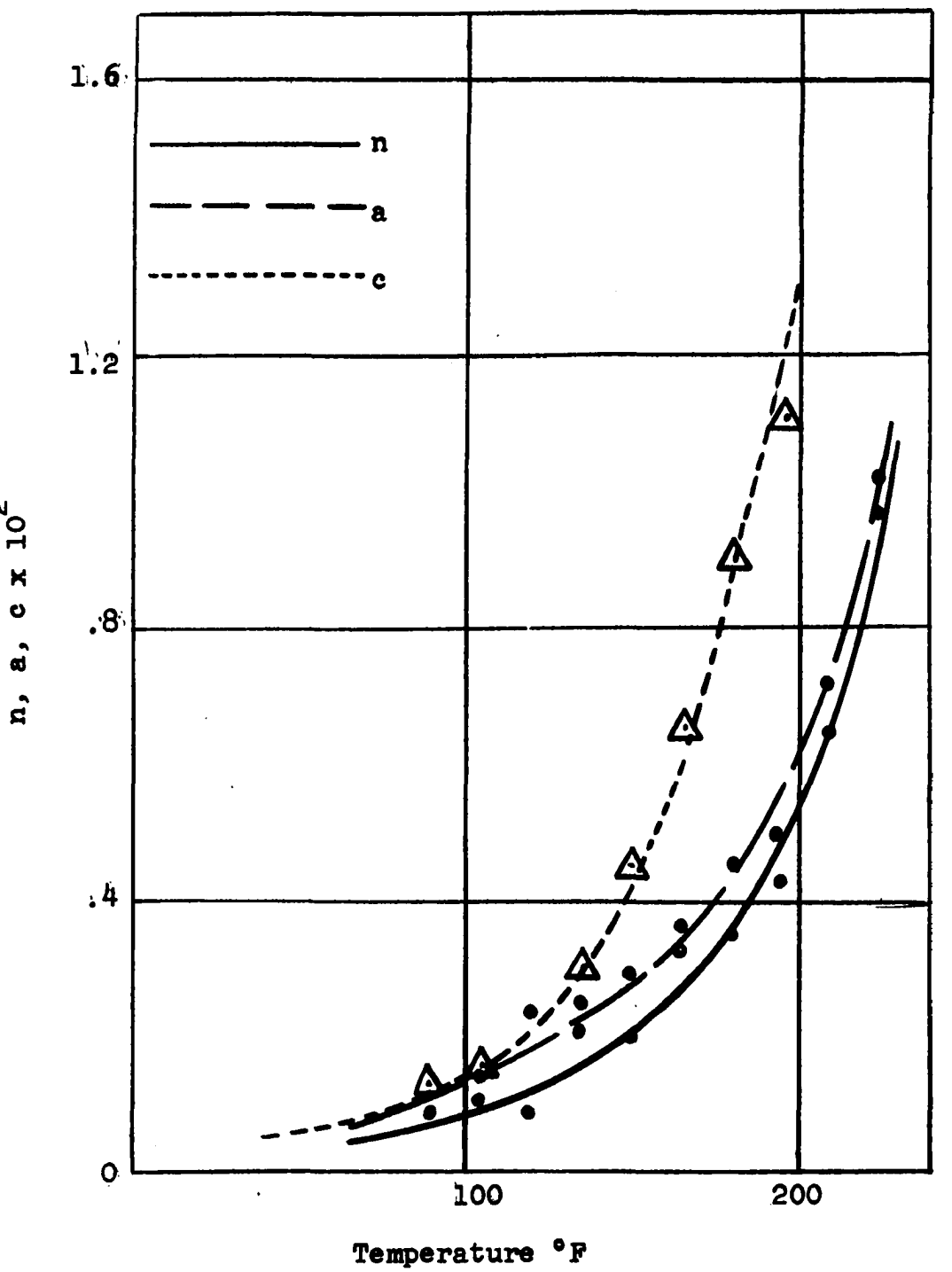

Figure 23. Variation of a, c and n with temperature

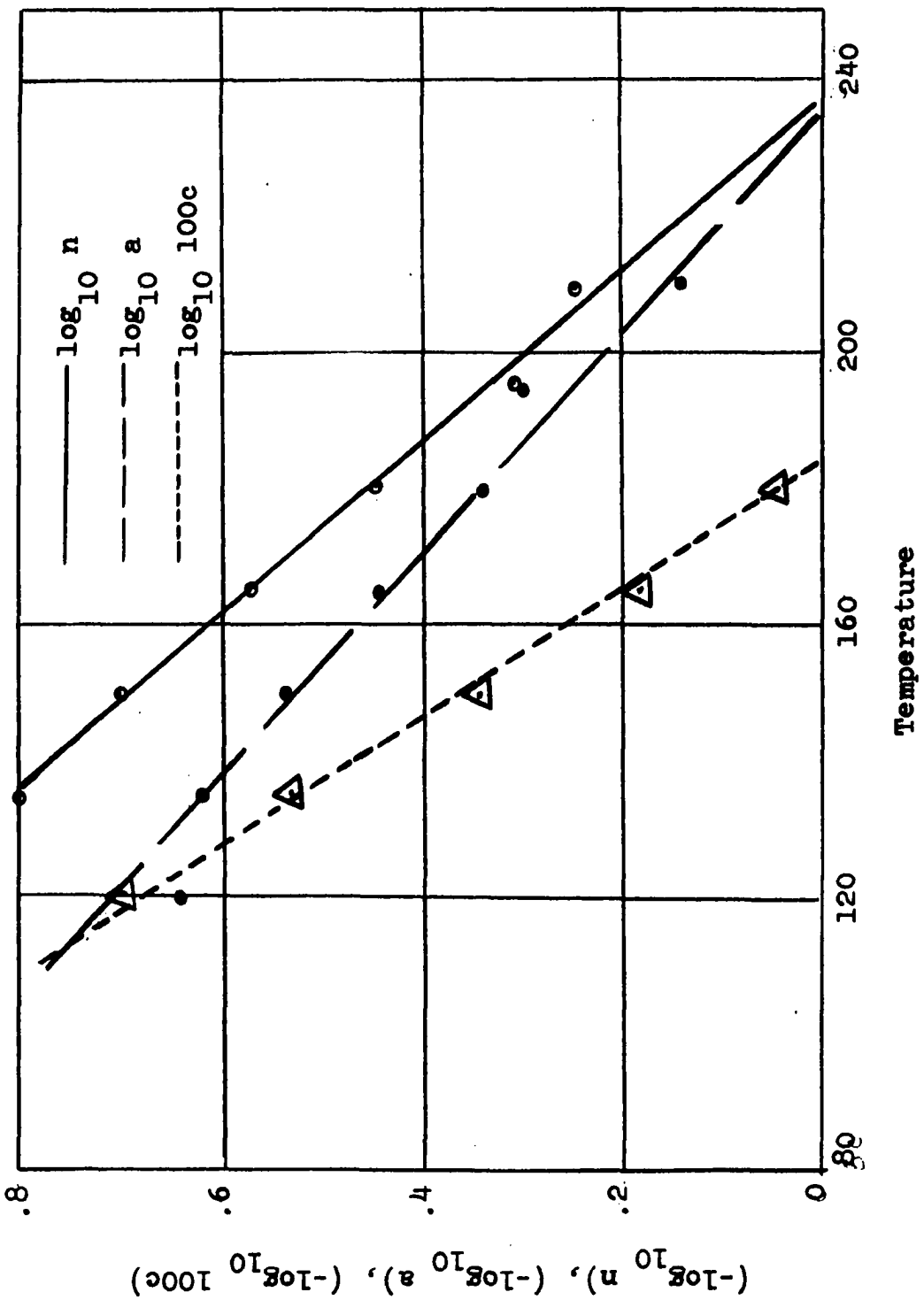

Figure 24. Log_{10} a, log_{10} c and log_{10} n versus temperature

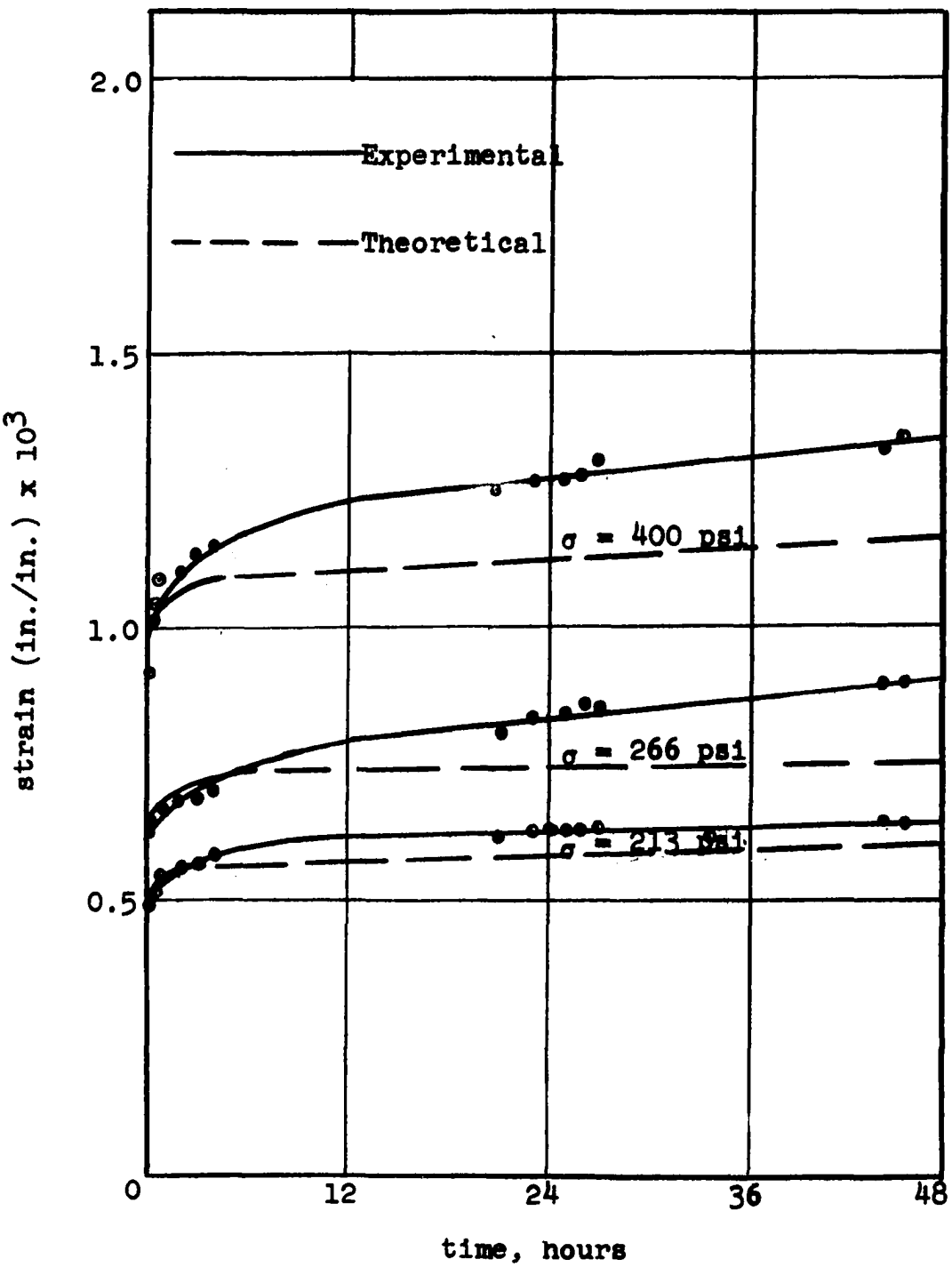

Figure 25. Creep curves at 90°F

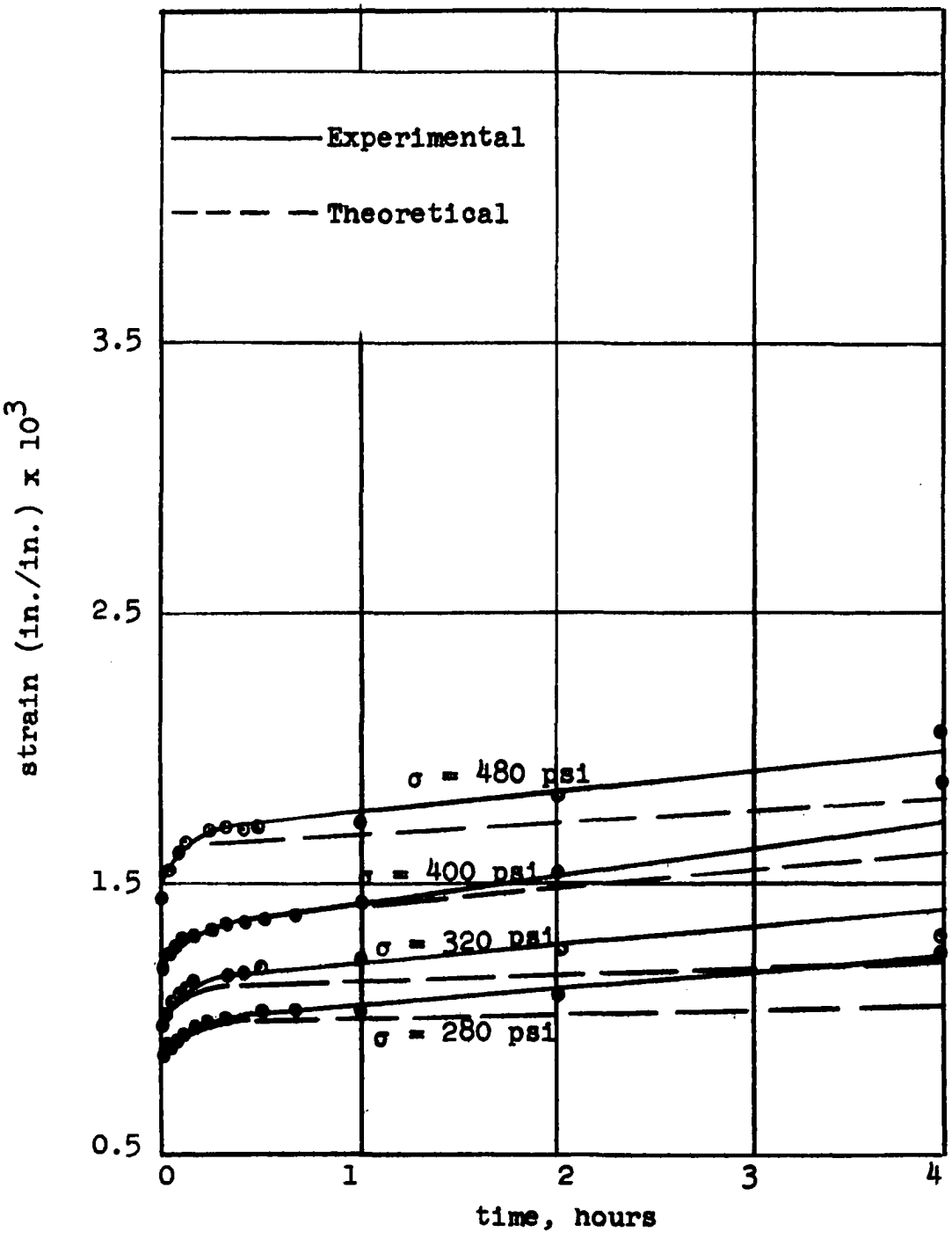

Figure 26. Creep curves at 105°F

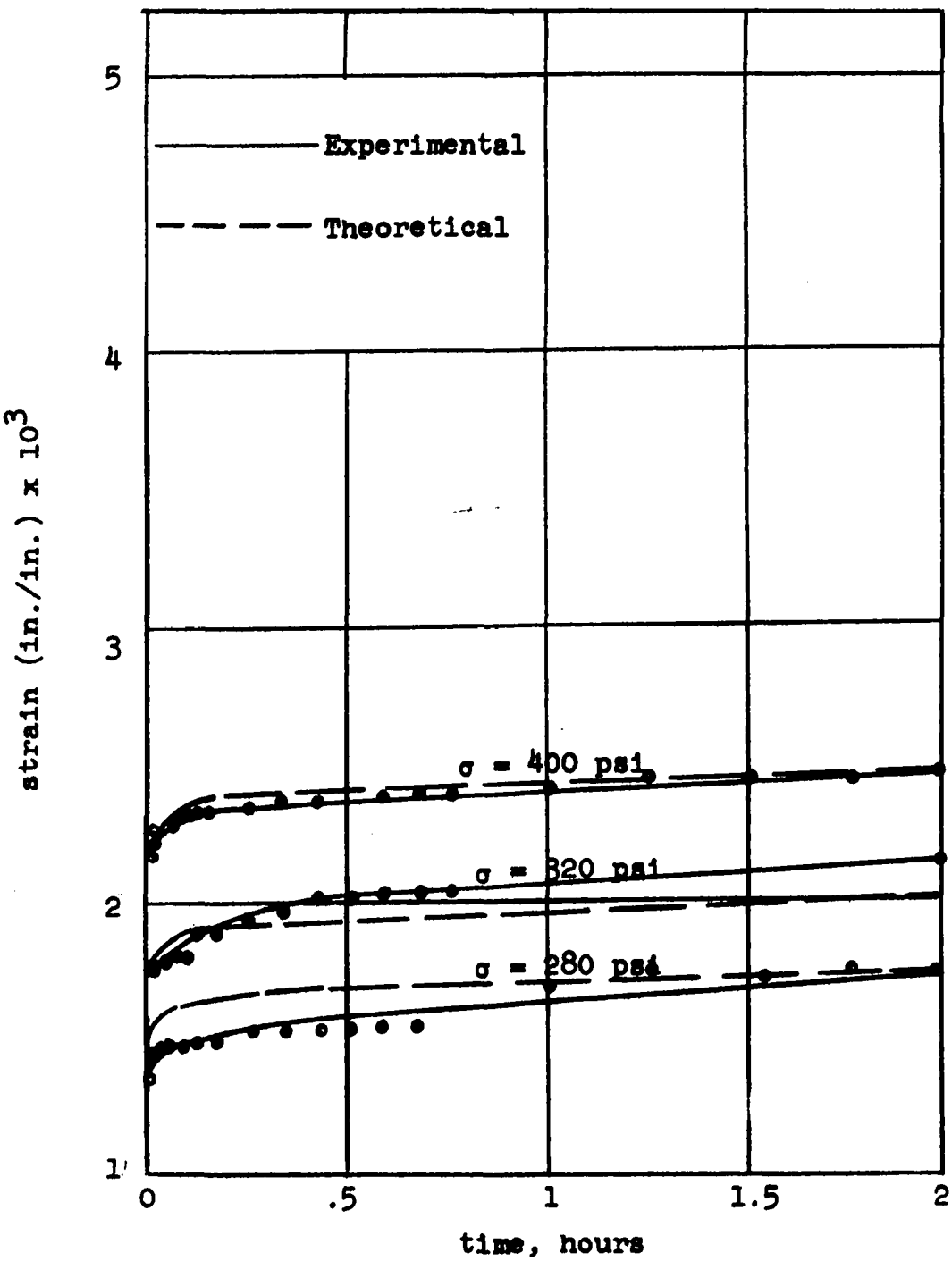

Figure 27. Creep curves at 120° F

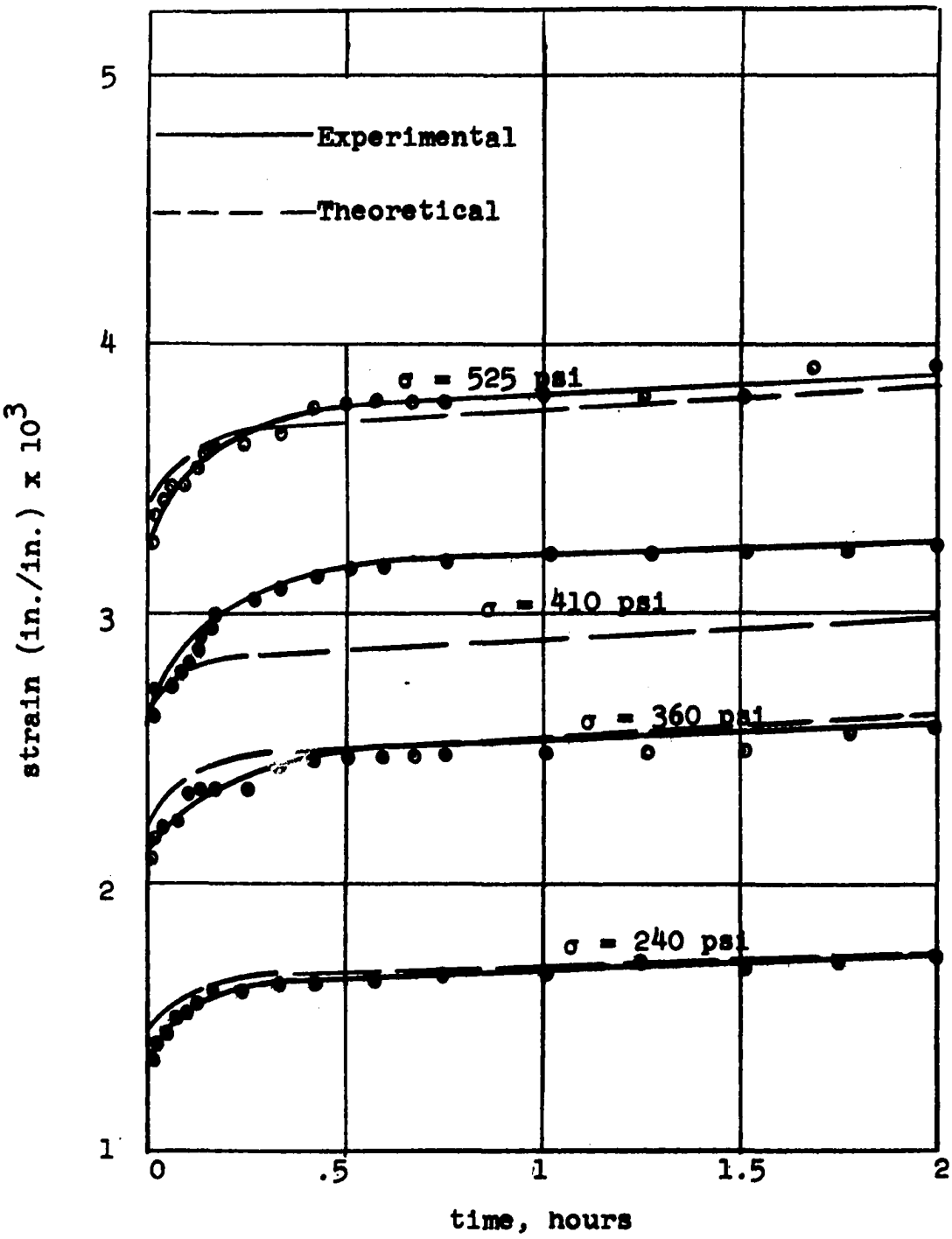

Figure 28. Creep curves at 135°F

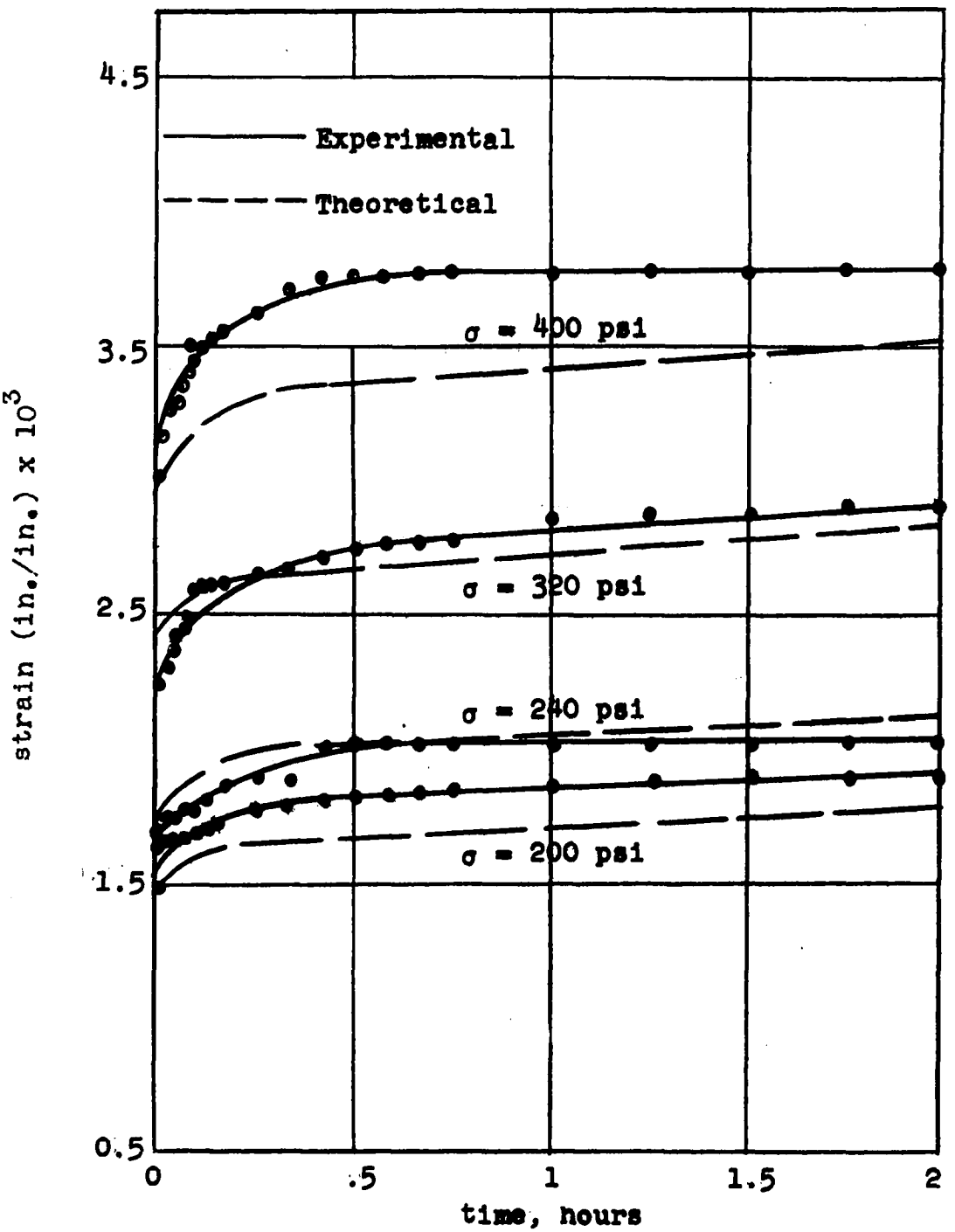

Figure 29. Creep curves at 150°F

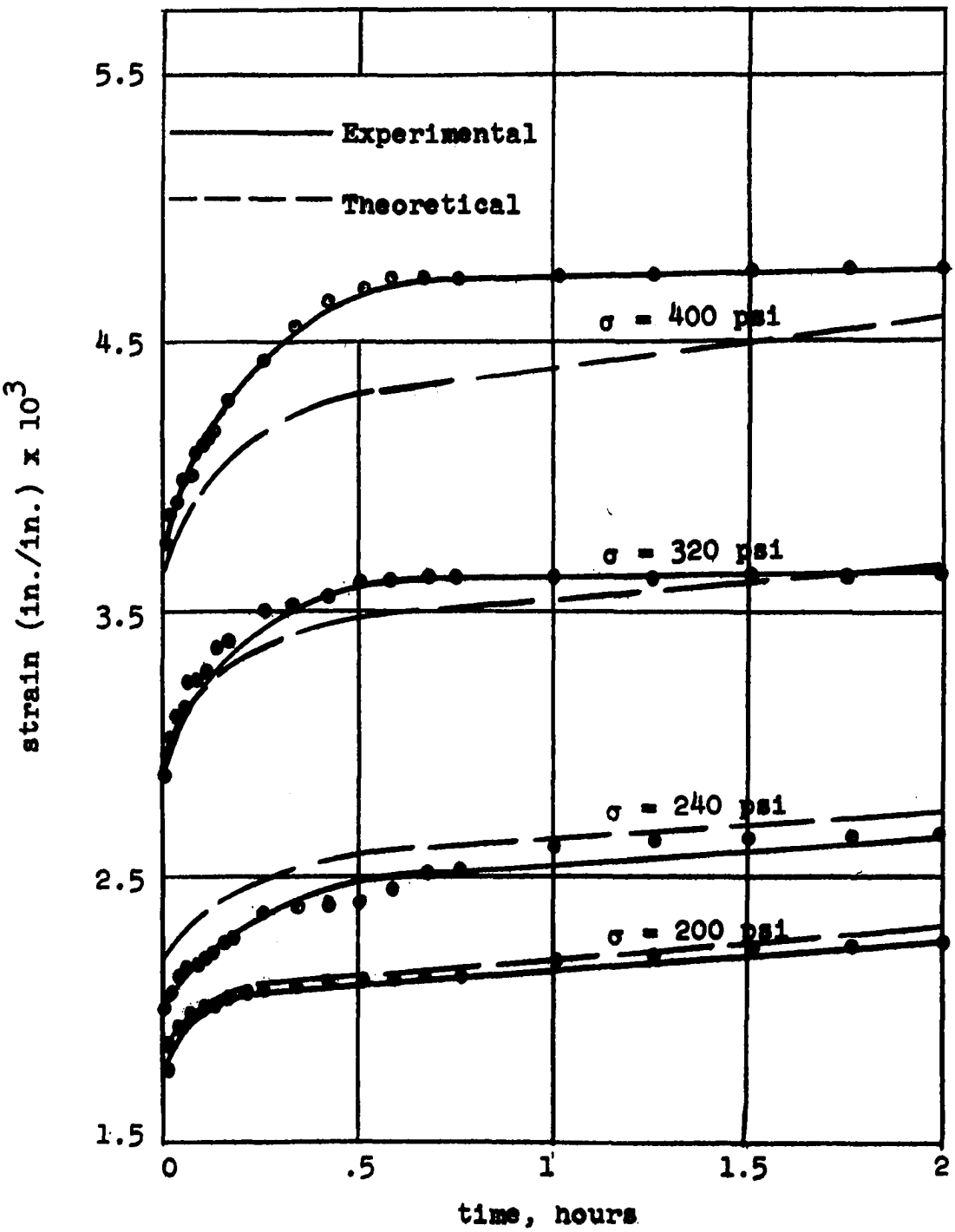

Figure 30. Creep curves at 165°F

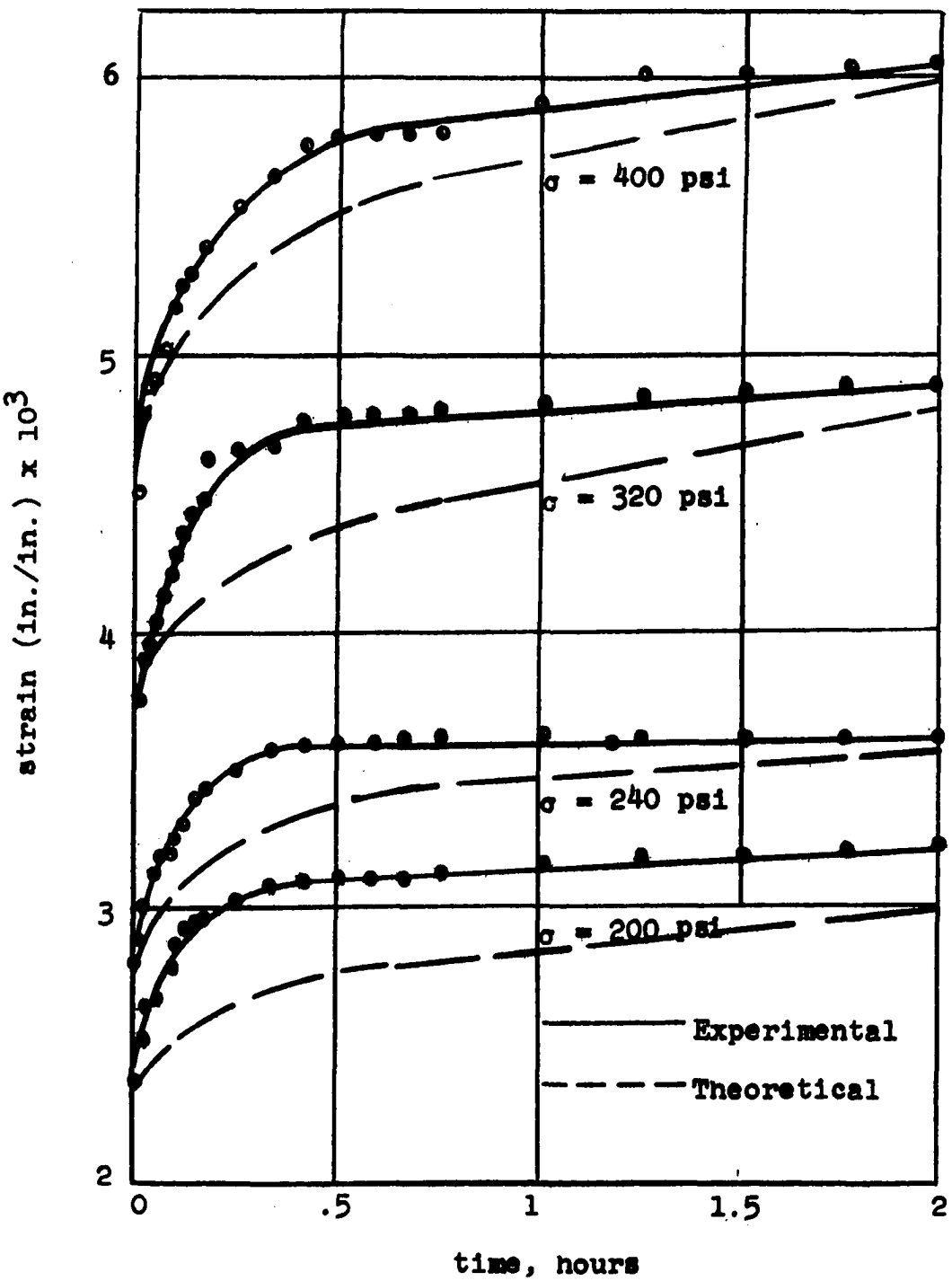

Figure 31. Creep curves at 180°F

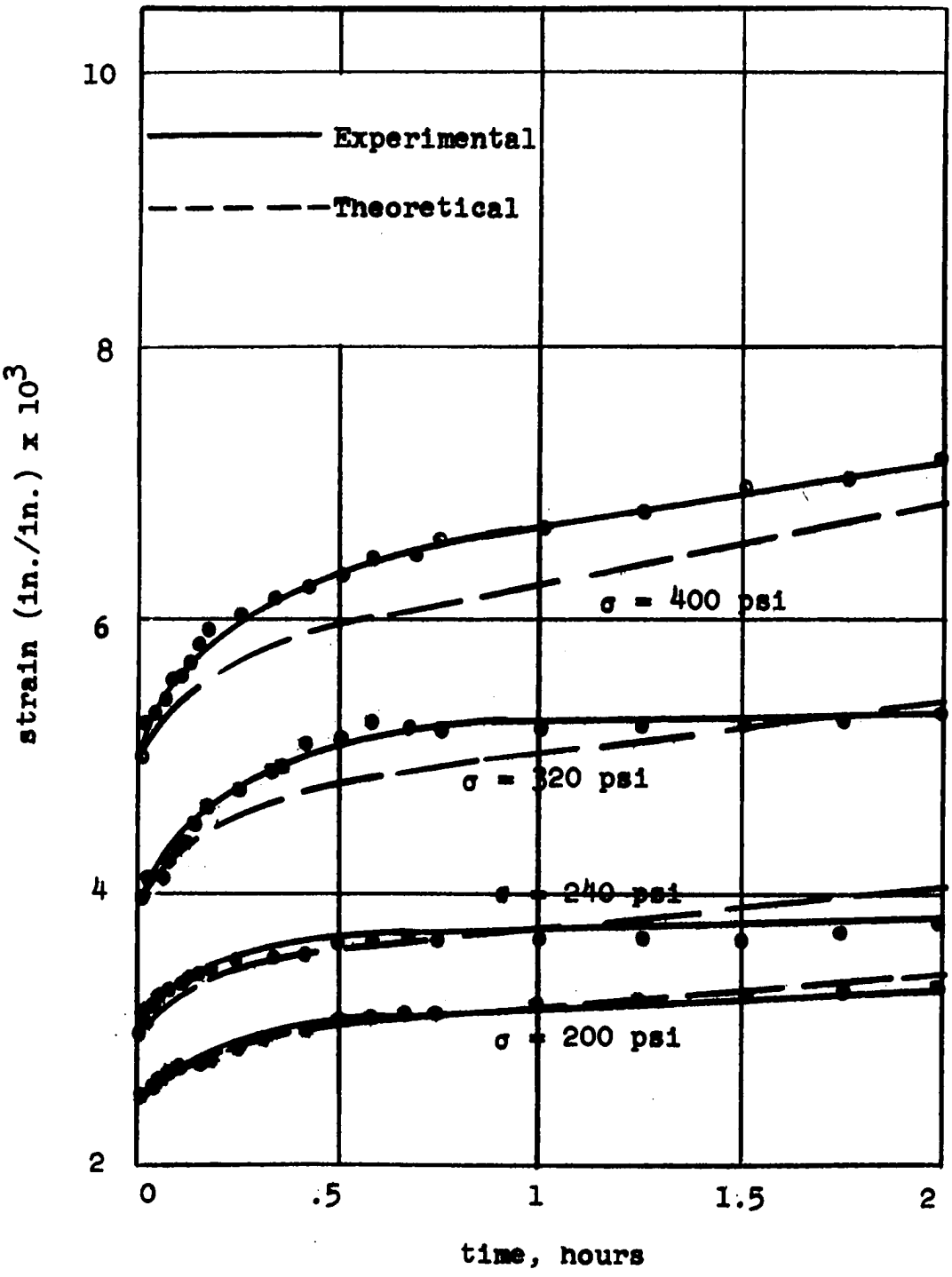

Figure 32. Creep curves at 195°F

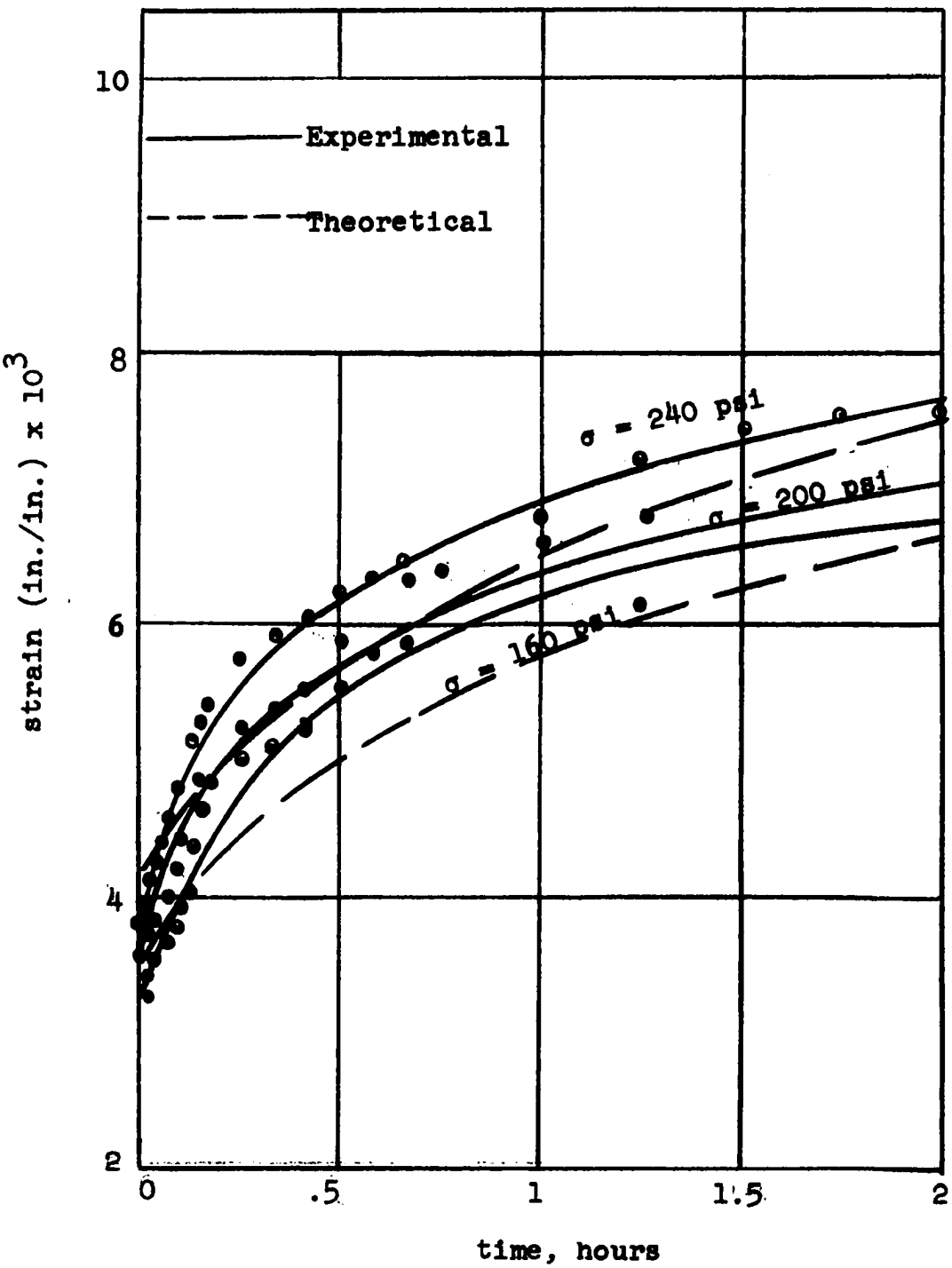

Figure 33. Creep curves at 210°F

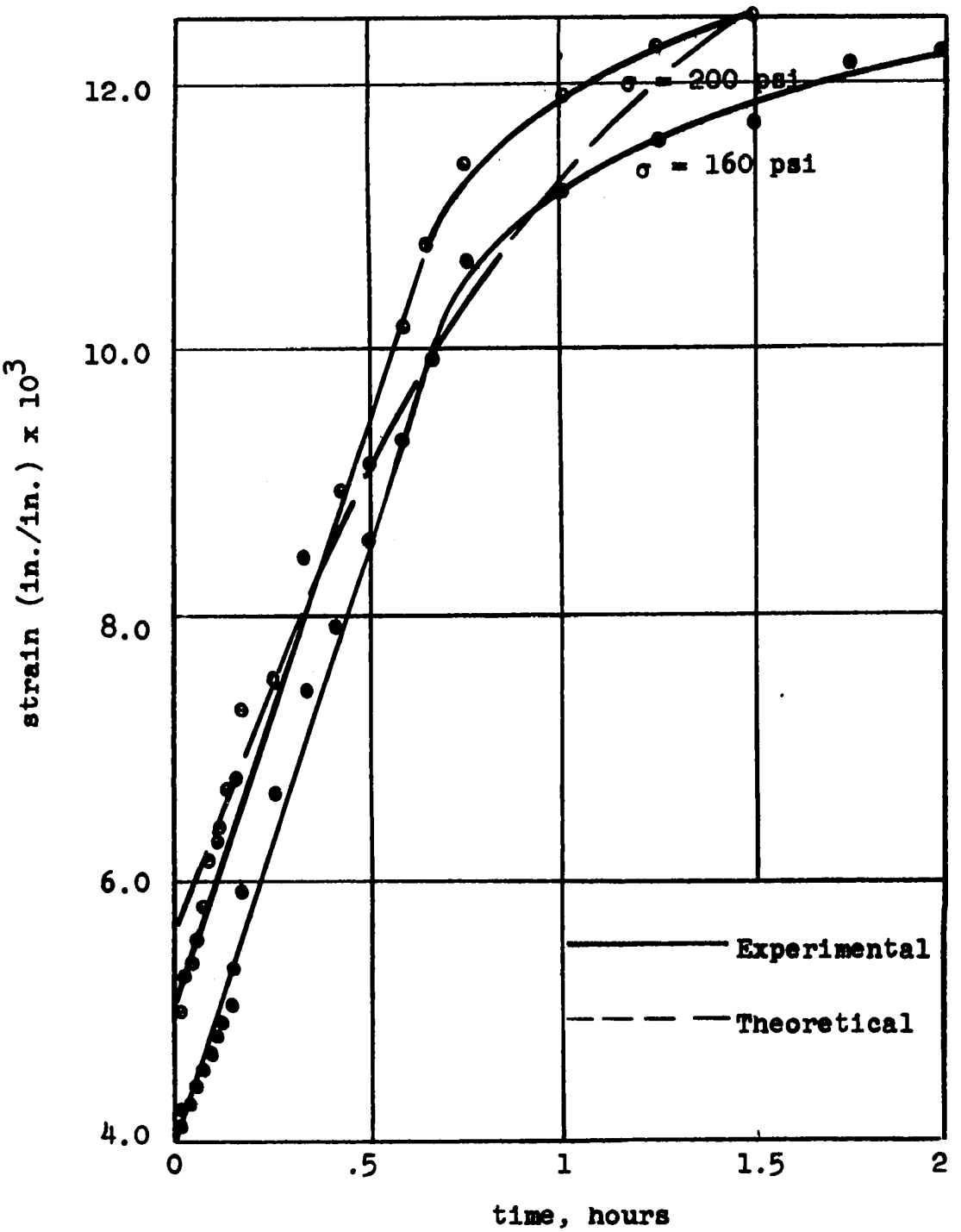

Figure 34. Creep curves at 225° F

CHAPTER VI

ANALYSIS OF EXPERIMENTAL RESULTS

As explained in Chapter III, experiments were carried out at high stress level in the range of 2600-5000 psi and at different temperatures. The creep data for the high-stress experiments are tabulated in Tables 37 through 41, Appendix A and experimental creep curves are plotted in Figures 35 through 39. The theoretical creep curves based on information obtained in Chapter V and equation (5-8) are also plotted in Figures 35 through 39. These curves correspond to the assumption that the thermal expansion coefficient is not a function of stress. But as it is clear the theoretical and experimental creep strains differed about 17 to 23 percent after a two-hour period, while in previous chapter where theoretical creep equations were fitted to the low-stress experimental data, the deviation was only about zero to 10 percent. This indicates that it would be a better prediction of creep if the additional strains due to the change of thermal expansion coefficient be added to the predicted creep which has been calculated from equation (5-8).

As mentioned in Chapter III, since the models are stabilized at any particular temperature and are expanded

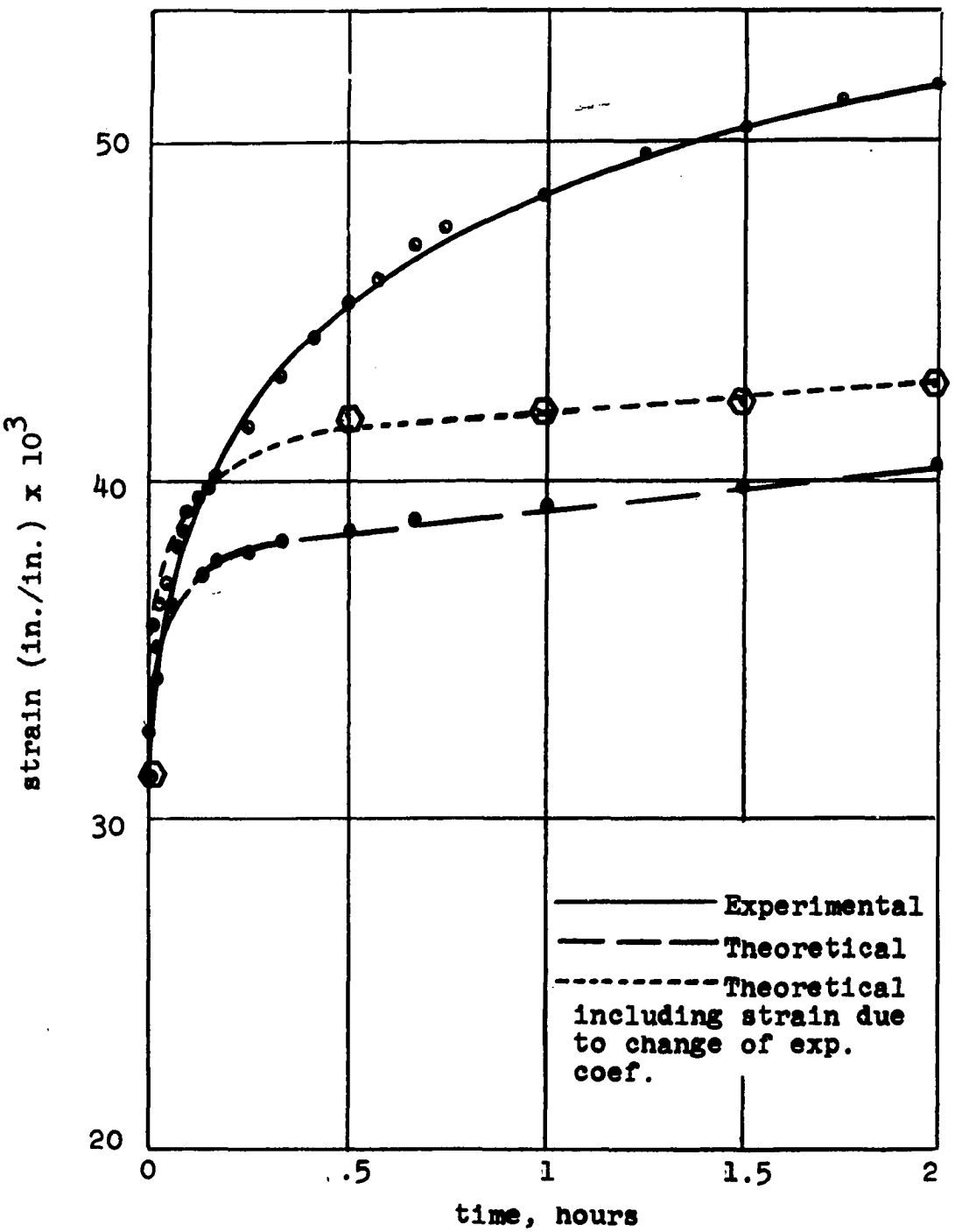

Figure 35. Creep curve at 140°F and 5000 psi

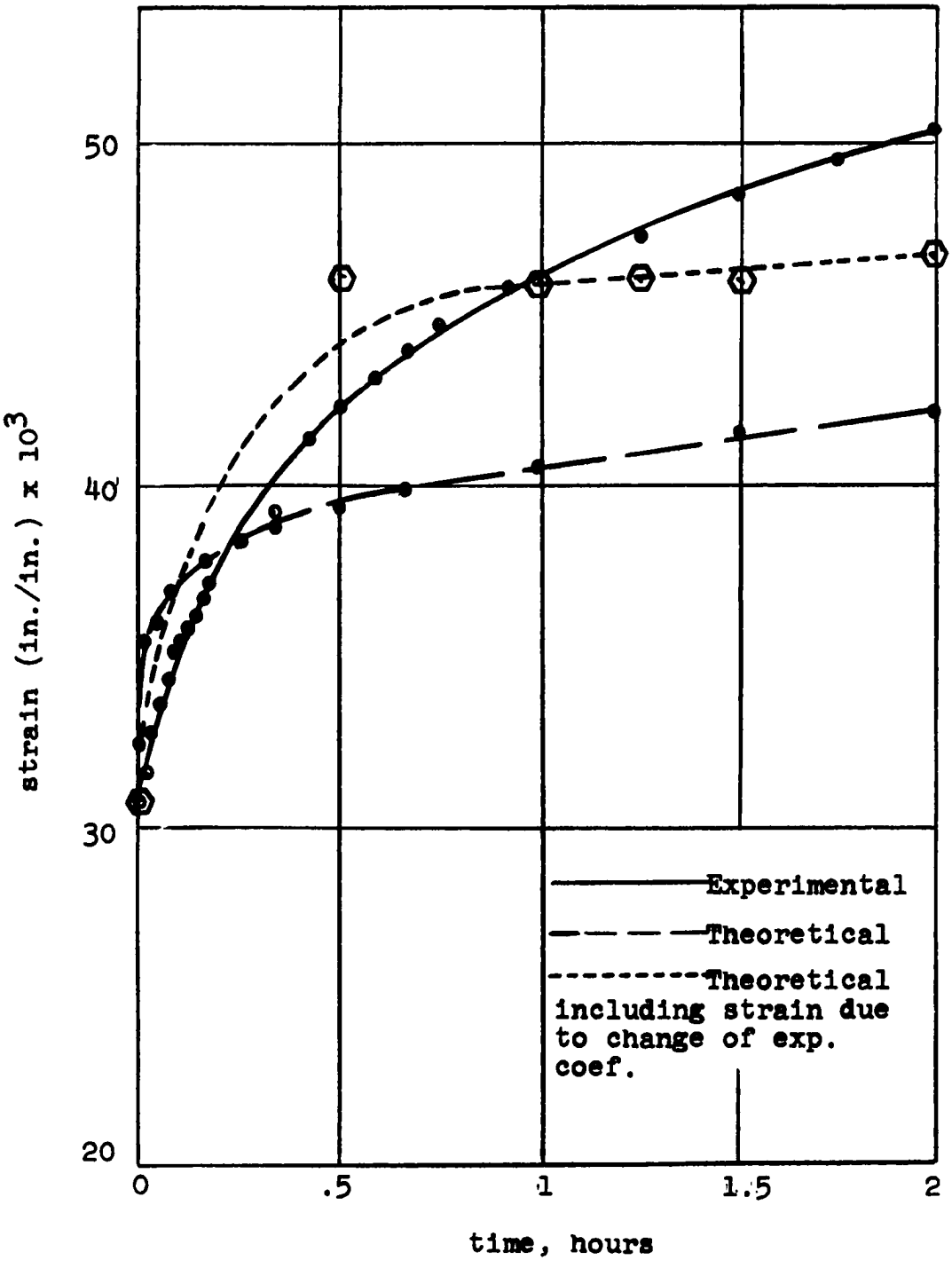

Figure 36. Creep curve at 160°F and 4000 psi.

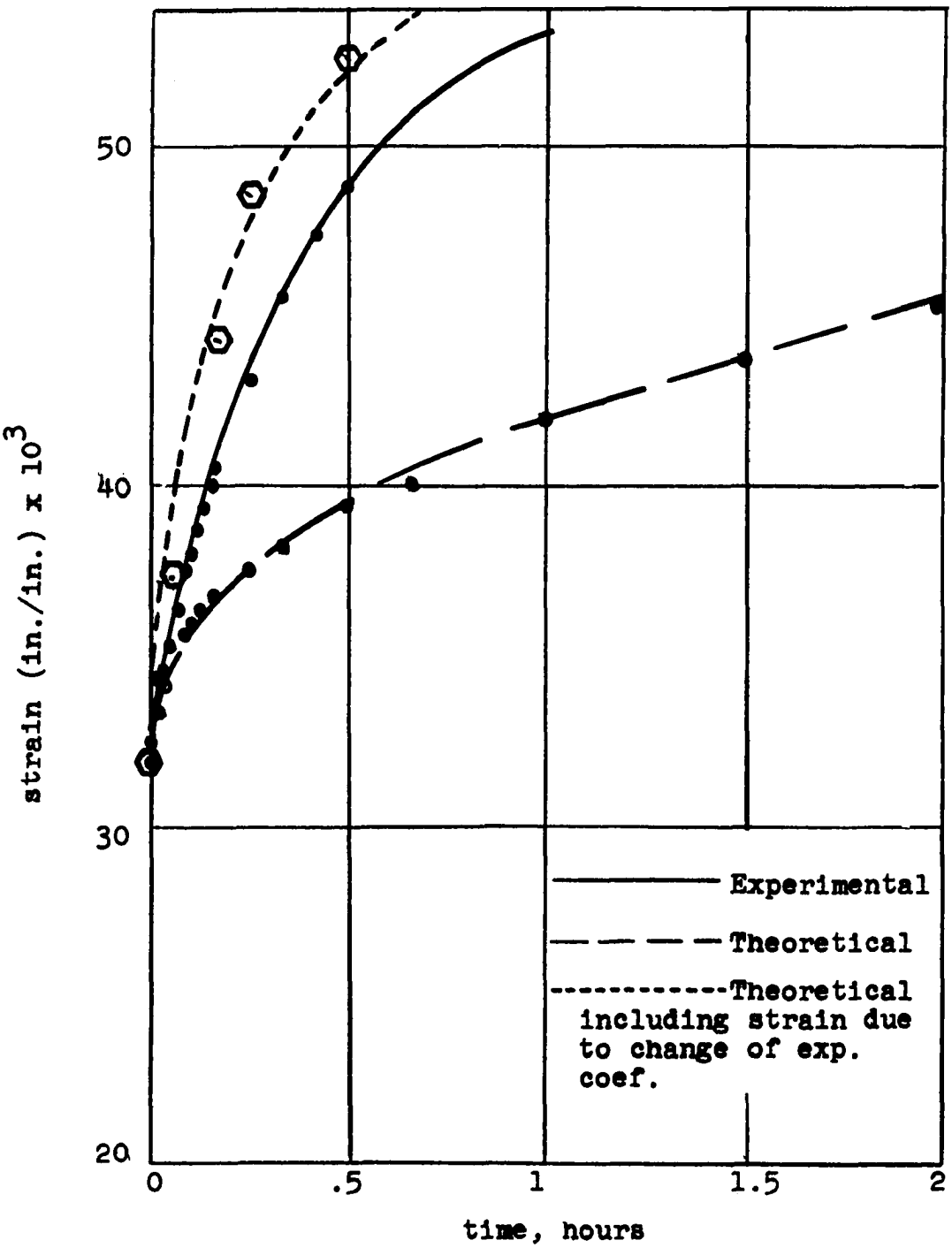

Figure 37. Creep curve at 190°F and 2600 psi

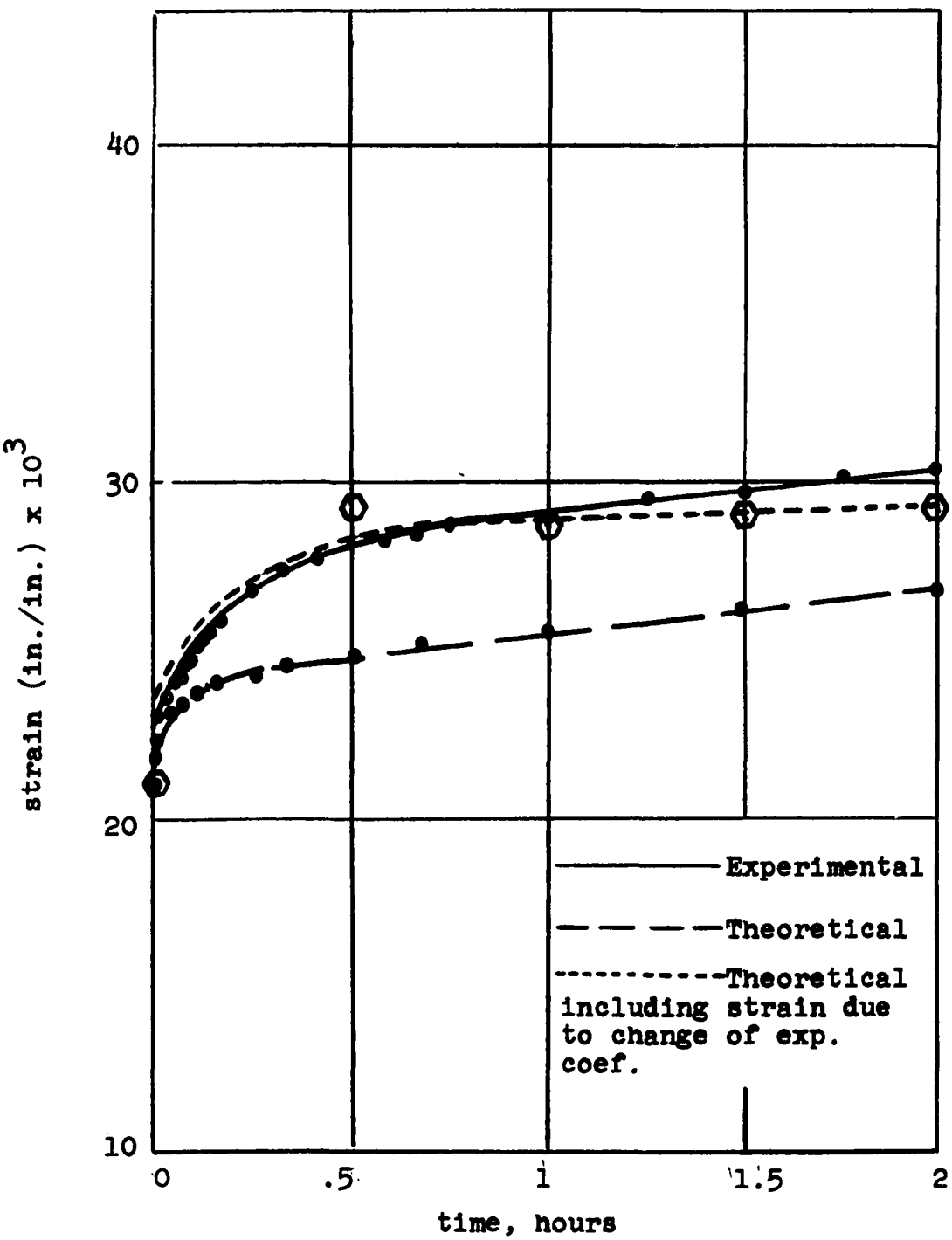

Figure 38. Creep curves at 160°F and 2600 psi

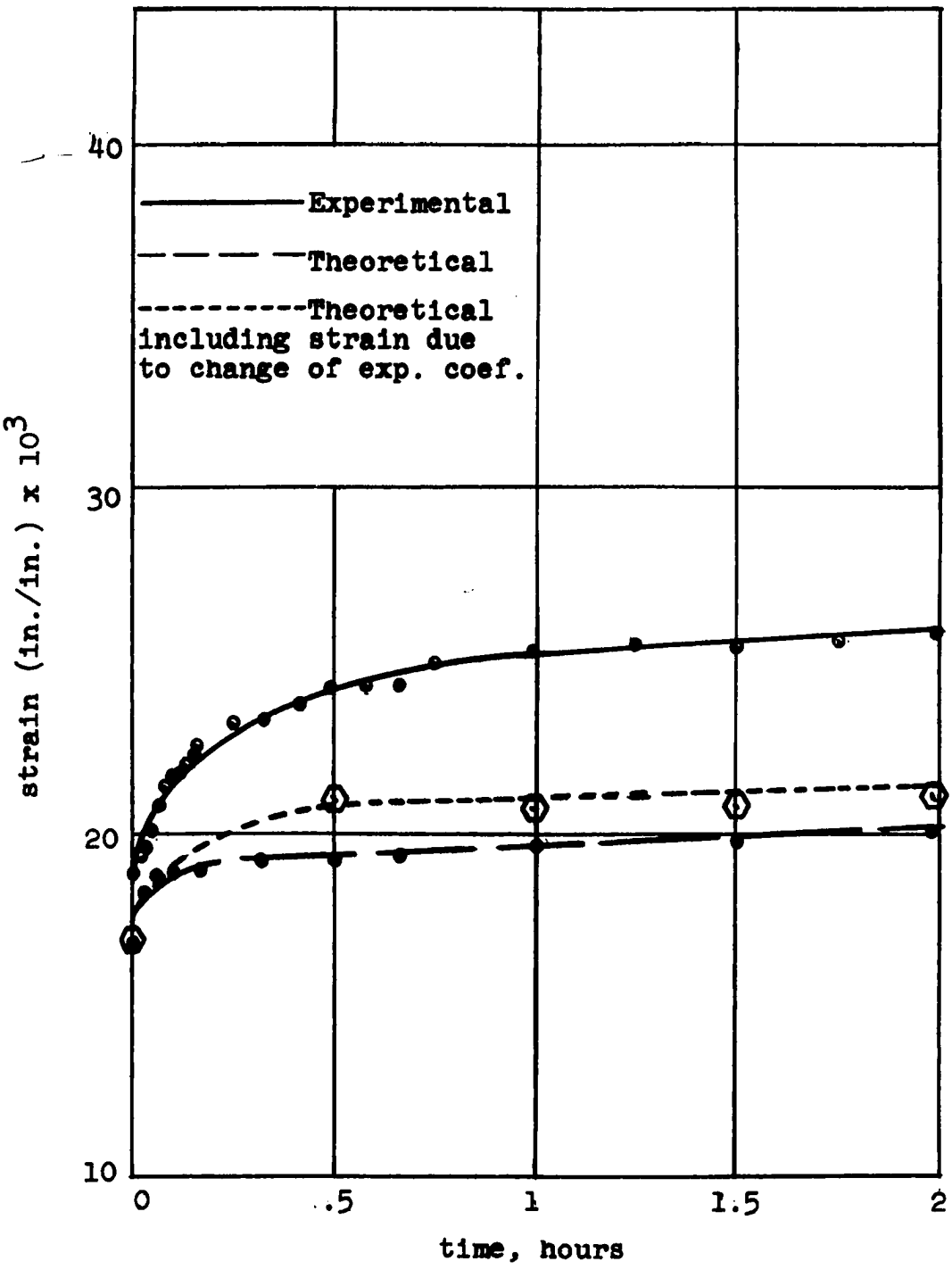

Figure 39. Creep curves at 140° F and 2600 psi

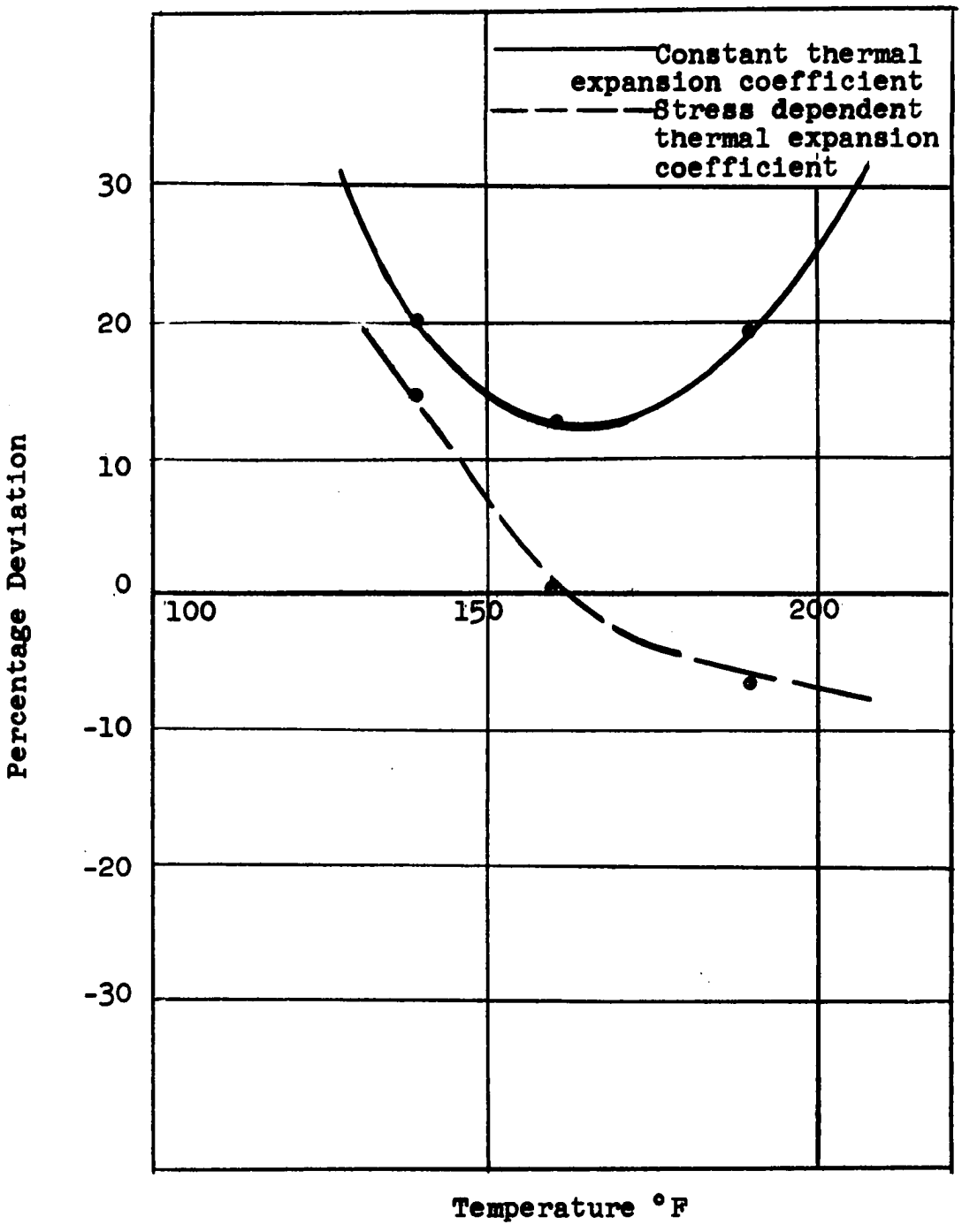

Figure 40. Percentage deviation from experimental data after thirty minutes at 2600 psi versus temperature.

under no stress with the thermal expansion factor α_0 before the experiment starts, the first term of equation (2-72)

$$\alpha = \alpha_0 + \int Z \, d\sigma \ ,$$

is already compensated and it only remains to calculate the strain corresponding to the second term. To do this, equation (5-8) is employed to obtain the creep function $J(t,\sigma_0)$

$$J(t,\sigma_0) = \frac{a}{\sigma_0} \sinh \frac{\sigma_0}{b} + \frac{c}{\sigma_0} t^n \sinh \frac{\sigma_0}{d} \ . \qquad (6\text{-}1)$$

To apply J in equation (2-71) and get Z in equation (2-72), equation (6-1) is differentiated with respect to time and stress,

$$\frac{\partial J(t,\sigma_0)}{\partial t} = \frac{cn}{\sigma_0} t^{n-1} \sinh \frac{\sigma_0}{d} \qquad (6\text{-}2)$$

$$\frac{\partial J(t,\sigma_0)}{\partial \sigma_0} = \frac{-a}{\sigma_0^2} \sinh \frac{\sigma_0}{} + \frac{a}{b\sigma_0} \cosh \frac{\sigma_0}{b} - \frac{ct^n}{\sigma_0^2} \sinh \frac{\sigma_0}{d}$$

$$+ \frac{c}{d\sigma_0} t^n \cosh \frac{\sigma_0}{d} \qquad (6\text{-}3)$$

Substitution of equations (6-2) and (6-3) into equation (2-71) results in

$$Z = \frac{\partial \alpha}{\partial \sigma_0} = \frac{d}{dt} \left[\frac{cn}{\sigma_0} t^{n-1} \sinh \frac{\sigma_0}{d} - \frac{a}{\sigma_0} \sinh \frac{\sigma_0}{b} + \frac{a}{b} \cosh \frac{\sigma_0}{b} \right.$$

$$- \frac{ct^n}{\sigma_0} \sinh \frac{\sigma_0}{d} + \frac{ct^n}{d} \cosh \frac{\sigma_0}{d} \Big] \tag{6-4}$$

or

$$Z = \frac{\partial \alpha}{\partial \sigma_0} = \frac{d}{dT} [\xi] \tag{6-5}$$

where

$$\xi = \frac{cn}{\sigma_0} t^{n-1} \sinh \frac{\sigma_0}{d} - \frac{a}{\sigma_0} \sinh \frac{\sigma_0}{b} + \frac{a}{b} \cosh \frac{\sigma_0}{b} - \frac{ct^n}{\sigma_0} \sinh \frac{\sigma_0}{d}$$

$$+ \frac{ct^n}{d} \cosh \frac{\sigma_0}{d} \tag{6-6}$$

and

$$\frac{d\xi}{dT} = \frac{\partial \xi}{\partial n} \frac{dn}{dT} + \frac{\partial \xi}{\partial a} \frac{da}{dT} + \frac{\partial \xi}{\partial c} \frac{dc}{dT} \tag{6-7}$$

But from equations (5-14), (5-15), and (5-16)

$$\frac{dn}{dT} = .0179 \, e^{(.0179T - 4.14)} \tag{6-8}$$

$$\frac{da}{dT} = .0141 \, e^{(.0141T - 3.4)} \tag{6-9}$$

$$\frac{dc}{dT} = \frac{.024}{100} \, e^{(.024T - 4.45)} \tag{6-10}$$

To differentiate t^n and t^{n-1} with respect to n the following approach is used

$$t^n = P$$

then

$$\log_e P = n \log_e t$$

and

$$P = e^{n \log_e t}$$

Thus

$$\frac{dP}{dn} = \frac{d}{dn} t^n = e^{n \log_e t} \log_e t = t^n \log_e t \qquad (6\text{-}11)$$

Therefore:

$$\frac{\partial \xi}{\partial n} = \frac{c}{\sigma_0} t^{n-1} \sinh \frac{\sigma_0}{d} + \frac{cn}{\sigma_0} t^{n-1} \log_e t \sinh \frac{\sigma_0}{d}$$

$$- \frac{ct^n}{\sigma_0} \log_e t \sinh \frac{\sigma_0}{d} + \frac{ct^n}{d} \log_e t \cosh \frac{\sigma_0}{d}$$

$$\frac{\partial \xi}{\partial n} = \left[t^{n-1} + nt^{n-1} \log_e t - t^n \log_e t \right] \frac{c}{\sigma_0} \sinh \frac{\sigma_0}{d}$$

$$+ \frac{ct^n}{d} \log_e t \cosh \frac{\sigma_0}{d} \qquad (6\text{-}12)$$

$$\frac{\partial \xi}{\partial a} = - \frac{1}{\sigma_0} \sinh \frac{\sigma_0}{b} + \frac{1}{b} \cosh \frac{\sigma_0}{b} \qquad (6\text{-}13)$$

$$\frac{\partial \xi}{\partial c} = \frac{n}{\sigma_0} t^{n-1} \sinh \frac{\sigma_0}{d} - \frac{t^n}{\sigma_0} \sinh \frac{\sigma_0}{d} + \frac{t^n}{d} \cosh \frac{\sigma_0}{d} \qquad (6\text{-}14)$$

Substitution of equations (6-8), (6-9), (6-10), (6-12), (6-13) and (6-14) in equation (6-7) and (6-5) results in:

$$Z = \frac{\partial \alpha}{\partial \sigma_0} = \left\{ \left[t^{n-1} + nt^{n-1} \log_e t - t^n \log_e t \right] \frac{c}{\sigma_0} \sinh \frac{\sigma_0}{d} \right.$$

$$+ \frac{ct^n}{d} \log_e t \cosh \frac{\sigma_0}{d} \Big\} \Big[.0179\, e^{(.0179T - 4.14)} \Big]$$

$$+ \Big\{ - \frac{1}{b} \sinh \frac{\sigma_0}{b} + \frac{1}{b} \cosh \frac{\sigma_0}{b} \Big\} \Big[.0141\, e^{(.0141T - 3.4)} \Big]$$

$$+ \Big\{ \frac{n}{\sigma_0} t^{n-1} \sinh \frac{\sigma_0}{d} - \frac{t^n}{\sigma_0} \sinh \frac{\sigma_0}{d}$$

$$+ \frac{t^n}{d} \cosh \frac{\sigma_0}{d} \Big\} \Big[\frac{.024}{100} e^{(.024T - 4.45)} \Big] \qquad (6\text{-}15)$$

Now equation (6-15) can be substituted into equation (2-72) and integrated to obtain:

$$\Delta\alpha = \alpha - \alpha_0 = \int Z \, d\sigma_0$$

$$\Delta\alpha = c \Big[.0179\, e^{(.0179T - 4.14)} \Big] \Big\{ (t^{n-1} + nt^{n-1} \log_e t$$

$$- t^n \log_e t) \int \frac{\sinh \frac{\sigma_0}{d}}{\sigma_0} d\sigma_0 + \frac{t^n}{d} \log_e t \int \cosh \frac{\sigma_0}{d} d\sigma_0 \Big\}$$

$$+ \Big[.0141\, e^{(.0141T - 3.4)} \Big] \Big\{ \frac{1}{b} \int \cosh \frac{\sigma_0}{b} d\sigma_0$$

$$- \int \frac{\sinh \frac{\sigma_0}{b}}{\sigma_0} d\sigma_0 \Big\} + \Big[\frac{.024}{100} e^{(.024T - 4.45)} \Big] \Big\{ (nt^{n-1}$$

$$- t^n) \int \frac{\sinh \frac{\sigma_0}{d}}{\sigma_0} d\sigma_0 + \frac{t^n}{d} \int \cosh \frac{\sigma_0}{d} d\sigma_0 \Big\} \qquad (6\text{-}16)$$

To integrate $\dfrac{\sinh \frac{\sigma_0}{d}}{\sigma_0}$ the following procedure has been applied:

$$\int \frac{\sinh \frac{\sigma_0}{d}}{\sigma_0} d\sigma_0 \quad \int \frac{e^{(\sigma_0/d)} - e^{(-\sigma_0/d)}}{2\sigma_0} d\sigma_0 \quad - \int \frac{e^{(\sigma_0/d)}}{\sigma_0}$$

$$\frac{1}{2} \int \frac{e^{(-\sigma_0/d)}}{\sigma_0} d\sigma_0 \cdot$$

But

$$\int \frac{e^{(\sigma_0/d)}}{} d\sigma_0 = \log_e \sigma_0 + \frac{\sigma_0}{d} + \frac{\sigma_0^2}{2 \cdot 2! d^2} + \frac{\sigma_0^3}{3 \cdot 3! d^3} + \frac{\sigma_0^4}{4 \cdot 4! d^4} + \frac{\sigma_0^5}{5 \cdot 5! d^5}$$

$$+ \ . \ . \ . \qquad (6\text{-}17)$$

$$\int \frac{e^{(-\sigma_0/d)}}{\sigma_0} d\sigma_0 = \log \sigma_0 - \frac{\sigma_0}{d} + \frac{\sigma_0^2}{2 \cdot 2! d^2} - \frac{\sigma_0^3}{3 \cdot 3! d^3} + \frac{\sigma_0^4}{4 \cdot 4! d^4}$$

$$- \frac{\sigma_0^5}{5 \cdot 5! d^5} \ . \ . \ . \qquad (6\text{-}18)$$

In equations (6-17) and (6-18) the terms after the sixth term are neglected because in comparison with other terms they are small enough that their effects are negligible. Subtraction of equation (6-18) from (6-17) gives

$$\int \frac{\sinh \frac{\sigma_0}{d}}{\sigma_0} d\sigma_0 = \frac{1}{2} \int \frac{e^{(\sigma_0/d)}}{\sigma_0} d\sigma_0 - \frac{1}{2} \int \frac{e^{(-\sigma_0/d)}}{\sigma_0}$$

$$= \frac{\sigma_0}{d} + \frac{\sigma_0^3}{3 \cdot 3! d^3} + \frac{\sigma_0^5}{5 \cdot 5! d^5} \qquad (6\text{-}19)$$

Now with equation (6-19) equation (6-16) becomes

$$\Delta\alpha = c\left[.0179\, e^{(.0179T - 4.14)}\right]\left\{(t^{n-1} + nt^{n-1}\log_e t + t^n\log_e t)\left(\frac{\sigma_0}{d} + \frac{\sigma_0^3}{3\cdot 3!d^3} + \frac{\sigma_0^5}{5\cdot 5!d^5}\right) + t^n\log_e t \sinh\frac{\sigma_0}{d}\right\}$$

$$+\left[.0141\, e^{(.0141T - 3.4)}\right]\left\{\sinh\frac{\sigma_0}{b} - \left(\frac{\sigma_0}{b} + \frac{\sigma_0^3}{3\cdot 3!b^3} + \frac{\sigma_0^5}{5\cdot 5!b^5}\right)\right\} + \left[\frac{.024}{100}\, e^{(.024\% - 4.45)}\right]\left\{nt^{n-1} - t^n\right)\left(\frac{\sigma_0}{d} + \frac{\sigma_0^3}{3\cdot 3!d^3} + \frac{\sigma_0^5}{5\cdot 5!d^5}\right) + t^n \sinh\frac{\sigma_0}{d}\right\} \qquad (6\text{-}20)$$

Equation (6-20) describes $\Delta\alpha$ in terms of temperature and stress for the material used. The following equations are the same equation particularized to the specific temperatures and stresses in which the high-stress level experiments were carried out.

For 140°F:

$$\Delta\alpha = 975 \times 10^{-8}\left[(t^{-.83} + .17t^{-.83}\log_e t - t^{.17}\log_e t)\left(\frac{\sigma_0}{d} + \frac{\sigma_0^3}{18d^3} + \frac{\sigma_0^5}{600d^5}\right) + t^{.17}\log_e t \sinh\frac{\sigma_0}{d}\right] + 366 \times 10^{-5}\left[\sinh\frac{\sigma_0}{b} - \left(\frac{\sigma_0}{b} + \frac{\sigma_0^3}{18b^3} + \frac{\sigma_0^5}{600b^5}\right)\right] + 77 \times 10^{-8}\left[(.17t^{-.83}\right.$$

$$- t^{.17}\Big)\Big(\frac{\sigma_0}{d} + \frac{\sigma_0^3}{18d^3} + \frac{\sigma_0^5}{600d^5}\Big) + t^{.17}\sinh\frac{\sigma_0}{d}\Big] \qquad (6.21)$$

For 160° F:

$$\Delta\alpha = 228 \times 10^{-7}\Big[(t^{-.76} + .24t^{-.76}\log_e t - t^{.24}\log_e t)\Big(\frac{\sigma_0}{d} + \frac{\sigma_0^3}{18d^3} + \frac{\sigma_0^5}{600d^5}\Big) + t^{.24}\log_e t \sinh\frac{\sigma_0}{d}\Big] + 456 \times 10^{-5}\Big[\sinh\frac{\sigma_0}{b} - \Big(\frac{\sigma_0}{b} + \frac{\sigma_0^3}{18d^3} + \frac{\sigma_0^5}{600b^5}\Big)\Big] + 127 \times 10^{-8}\Big[(.24t^{-.76} - t^{.24})\Big(\frac{\sigma_0}{d} + \frac{\sigma_0^3}{18d^3} + \frac{\sigma_0^5}{600d^5}\Big) + t^{.24}\sinh\frac{\sigma_0}{d}\Big] \qquad (6\text{-}22)$$

For 190° F:

$$\Delta\alpha = 85 \times 10^{-6}\Big[(t^{-.56} + .44t^{-.56}\log_e t - t^{.44}\log_e t)\Big(\frac{\sigma_0}{d} + \frac{\sigma_0^3}{18d^3} + \frac{\sigma_0^5}{600d^5}\Big) + t^{.44}\log_e t \sinh\frac{\sigma_0}{d}\Big] + 705 \times 10^{-5}\Big[\sinh\frac{\sigma_0}{b} - \Big(\frac{\sigma_0}{b} + \frac{\sigma_0^3}{18b^3} + \frac{\sigma_0^5}{600b^5}\Big)\Big] + 259 \times 10^{-8}\Big[(.44t^{-.56} - t^{.44})\Big(\frac{\sigma_0}{d} + \frac{\sigma_0^3}{18d^3} + \frac{\sigma_0^5}{600d^5}\Big) + t^{.44}\sinh\frac{\sigma_0}{d}\Big] \qquad (6\text{-}23)$$

From equations (6-21), (6-22), and (6-23), the additional strain can be calculated from the elementary equation

$$\Delta\varepsilon = (\Delta\alpha)(\Delta T) \qquad (6\text{-}24)$$

where ΔT is measured from the reference temperature $T = 0$. The additional strains have been calculated and added to the strains obtained from equation (5-8) in Figures 35 through 39.

Comparison can be made between the experimental data and the additional strains just obtained plus the strains previously calculated from equation (5-8).

In Figure 40 the percentage deviation from experimental data after thirty minutes is plotted for the same stress level versus temperature.

In the next chapter will be shown the percentage of error expected if the additional strain term is not added.

CHAPTER VIII

CONCLUSIONS AND SUGGESTIONS FOR FURTHER RESEARCH

1. Conclusions

Based on the theoretical derivations of Chapter II and the experimental information presented in Chapters V and VI, the following conclusions can be reached.

a. The thermal expansion coefficient of viscoelastic materials is not a constant or a function of temperature alone, but it is a function of stress and time as well. For the materials in which the relaxation function decreases with the temperature, the expansion coefficient will increase with the stress. The elastic solution can be reached as a particular case simply by substitution of

$$\eta_m = \infty \quad \text{and} \quad \eta_k = 0 \ .$$

For the elastic case Brock (49) has mentioned that the results of analysis would be identical, using the expansion coefficient corresponding to zero stress and the value of elastic modulus at the final temperature, instead of using the expansion coefficient as a function of stress. This can be proved by taking a partial integral; however, this will not hold for viscoelastic materials, since the relaxation

modulus at any temperature varies also with time.

To show how much error would enter in analyzing a thermal-stress problem in viscoelasticity, α_0, the thermal expansion coefficient at zero stress is measured and tabulated for polymethyl methacrylate. The experimental values and variations of expansion coefficients with time for different stresses are plotted in Figure 41. As it can be seen in Figure 41, after two hours the percentage error considering the thermal-expansion coefficient constant would be between 13.2 to 26 percent.

b. The nonlinear relation for the creep of plastics suggested by Findley in the form of

$$\epsilon = a \sinh \frac{\sigma}{b} + ct^n \sinh \frac{\sigma}{d}$$

is developed for polymethyl methacrylate at a variety of temperature levels. Results indicate that the coefficients b and d remain constant with temperature variations, but a, c and n vary exponentially with temperature as follows.

$$a = e^{(.0141T - 3.4)}$$

$$c = \frac{1}{100} e^{(.024T - 4.45)}$$

$$n = e^{(.0179T - 4.14)}$$

2. Some Suggestions for Future Research

Viscoelasticity being a relatively new field of research, there are still many aspects to be studied and

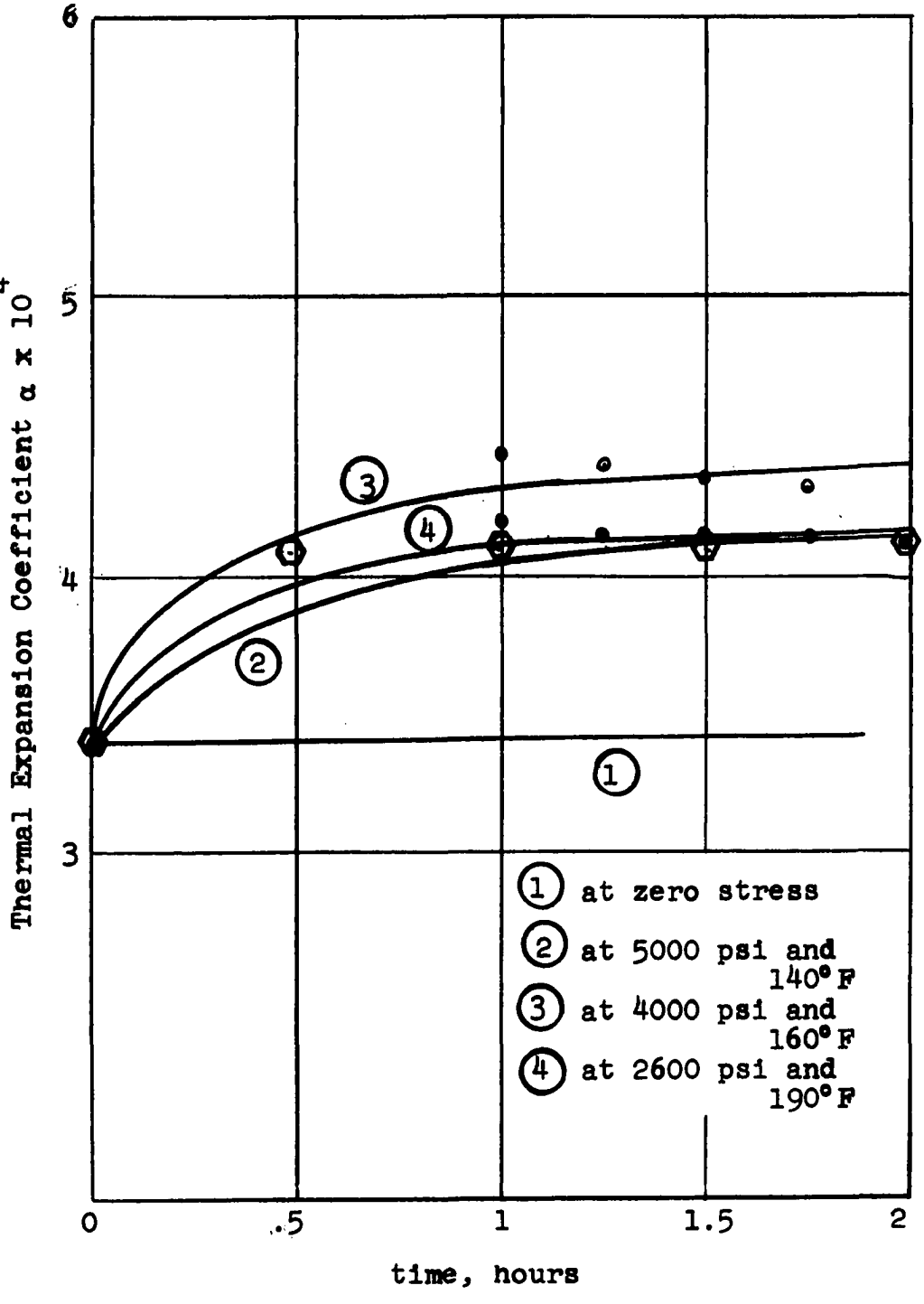

Figure 41. Variation of thermal expansion coefficients with and without stress.

theoretical and experimental methods to be developed. For further development of this field, it is important to investigate the following points as well as the other phases:

a. Possibilities of using strain gages to get more accurate readings of any kind of deformation without any influence due to the strain-gage mounting which has been a subject of discussion for a long time among the investigators.

b. Often in practical problems the load is not constant, therefore, experimental methods should be extended to cover this situation and the results correlated with theoretical results. There are possibilities of using a step loading as is explained by Felgar (50).

c. The experimental work in the present investigation was carried out at constant temperature levels; however, this is not always the case in practical problems. Therefore, it is necessary to develop the theory for obtaining the change of expansion coefficient of a viscoelastic material at transient temperatures.

d. Although some viscoelastic materials have less tendency to absorb moisture than others, in general they are affected by moisture content. It would be worthwhile to know how their behaviors change with the moisture content of the environment.

e. In the case of total or partial removal of the load, does the thermal-expansion coefficient return to the values which have been predicted theoretically for the case

of increasing stress and if so, how rapidly does this occur after removal of the load?

f. Development of experimental techniques for three-dimensional stress analysis of viscoelastic materials.

g. Stress dependency of other thermal coefficients such as thermal conductivity.

LIST OF SYMBOLS

a,b,c,d,A,B,C,D	Viscoelastic material constants
D	Differential operator
e_{ij}	Deviatoric strain
E	Elastic modulus
E_m	Elastic modulus for Maxwell type material
E_k	Elastic modulus for Kelvin type material
F	Free energy of solids
G	Elastic shear modulus
G_1	Volumetric relaxation function
G_2	Deviatoric relaxation function
G'	Storage relaxation function
G''	Loss relaxation function
J	Creep compliance
J_1	Volumetric creep function
J_2	Deviatoric creep function
J'	Storage creep function
J''	Loss creep function
K	Elastic bulk modulus
n	Material constant
p	Laplace operator
P_1,P_2	Operator notations

Q_1, Q_2	Operator notations
S_{ij}	Deviatoric stress
t	Time
T	Temperature
T_o	Reference temperature
ϵ	Strain
$\dot{\epsilon}$	Strain rate
$\bar{\epsilon}$	Laplace transform of strain
ϵ_{ii}	Volumetric strain
η	Viscous coefficient
η_m	Viscous coefficient for Maxwell type material
η_k	Viscous coefficient for Kelvin type material
ν	Poisson's ratio
σ	Stress
σ_{ii}	Volumetric stress
$\dot{\sigma}$	Stress rate
$\bar{\sigma}$	Laplace transform of stress
α	Thermal expansion coefficient
α_o	Thermal expansion coefficient at zero stress

REFERENCES

1. Alfrey, T. "Non Homogeneous Stresses in Viscoelastic Media," Quarterly of Applied Mathematics 2 (1944), pp. 113-119.

2. Tobolsky, A. V. and Andrews, R. D. "Systems Manifesting Superposed Elastic and Viscous Behavior," Journal of Chemical Physics. 13 (1945), pp. 3-27.

3. Gross, B. "On Creep and Relaxation," Journal of Applied Physics. 18 (1947), pp. 212-221.

4. Mindlin, R. D. "A Mathematical Theory of Photoviscoelasticity," Journal of Applied Physics. 20 (1949), pp. 206-216.

5. Read, W. T. Jr. "Stress Analysis for Compressible Viscoelastic Materials," Journal of Applied Mechanics. 21 (1950), pp. 671-674.

6. Tsien, H. S. "A Generalization of Alfrey's Theorem for Viscoelastic Media," Quarterly of Applied Mathematics. 8 (1950), pp. 104-106.

7. Schwarzl, F. and Staverman, A. J. "Time-Temperature Dependence of Linear Viscoelastic Behavior," Journal of Applied Physics. 23 (1952), pp. 838-843.

8. Freudenthal, A. M. "Effect of Rheological Behavior on Thermal Stresses," Journal of Applied Physics. 25 (1954), pp. 1110-1117.

9. Hilton, H. H. "Thermal Stresses in Thick-Walled Cylinder Exhibiting Temperature Dependent Viscoelastic Properties of the Kelvin Type," Proceedings of the Second U.S. National Congress of Applied Mechanics. (1954), pp. 547-553.

10. Lee, E. H. "Stress Analysis in Viscoelastic Bodies," Quarterly of Applied Mathematics. 13 (1955), pp. 183-190.

11. Radok, J. R. M. "Viscoelastic Stress Analysis," Quarterly of Applied Mathematics. 15 (1957), pp. 198-202.

12. Olszak, W. and Perzyna, P. "Variational Theorem in General Viscoelasticity," Ing. Arch. 28 (1959), pp. 246-250.

13. Yamamoto, M. "Phenomenological Theory of Viscoelasticity of Three Dimensional Body," Journal of Physical Science of Japan. 14 (1959), pp. 313-330.

14. Morland, L. W. and Lee, E. H. "Stress Analysis for Linear Viscoelastic Materials with Temperature Variation," Transactions of the Society of Rheology. 4 (1960), pp. 233-263.

15. Segawa, W. "Maxwell's Formula for Three-Dimensional and Large Deformation," Journal of Physical Science of Japan. 15 (1960), pp. 339-344.

16. Tschoegl, N. W. "The Characterization of Linear Viscoelastic Behavior by Respondance Functions. Stress Circuit Theory," Kolloid Zeitschrift. 174 (1960), pp. 113-133.

17. Hilton, H. H. and Russell, H. G. "An Extension of Alfrey's Analogy to Thermal Stress Problems in Temperature Dependent Linear Viscoelastic Media," Journal of Mechanics and Physics of Solids. 9 (1961), pp. 152-164.

18. Muki, R. and Sternberg, E. "On Transient Thermal Stresses in Viscoelastic Materials with Temperature Dependent Properties," Journal of Applied Mechanics. 28 (1961) pp. 193-207.

19. Tokuoka, T. "General Stress-Strain Relations in Non-Linear Theory of Viscoelasticity for Large Deformations," Ing. Arch. 30 (1961), pp. 385-393.

20. Novozhilov, V. V. Foundations of the Non-Linear Theory of Elasticity. Moscow: Gosteknizdat, 1948.

21. Tokuoka, T. "Three Dimensional Maxwell Stress-Strain Relations in Viscoelasticity," Ing. Arch. 31 (1961), pp. 187-193.

22. Pister, K. S. "Viscoelastic Plate on a Viscoelastic Foundation," Journal of Engineering Mechanics Div., Proc. of American Society of Civil Eng. 84 (1961), pp. 43-54.

23. Lee, E. H. and Rogers, T. G. "Solution of Viscoelastic Stress Analysis Problems Using Measured Creep or Relaxation Function," Journal of Applied Mechanics. 30 (1963), pp. 127-133.

24. Shinozuka, M. "Stress in a Linear Incompressible Viscoelastic Cylinder with Moving Inner Boundary," Journal of Applied Mechanics. 30 (1963), pp. 335-341.

25. Breuer, S. and Onat, E. T. "On the Determination of Free Energy in Linear Viscoelastic Solids," Office of Naval Research Cont. Nonr. 562(10) NR-064-406, Tech. Report No. 87, 1963.

26. Sternberg, E. "On Transient Thermal Stresses in Linear Viscoelasticity," Proceedings of the Third U.S. National Congress of Applied Mechanics. (1958), pp. 673-683.

27. Rosenfield, A. R. and Averbach, B. L. "Effect of Stress on the Expansion Coefficient," Journal of Applied Physics. 27 (1956), pp. 154-156.

28. Ungar, E. W., Bert, C. W. and Niedenfuhr, F. W. "Thermostructural Modeling for Design," ASME Paper No. 64-MD-5, 1964.

29. Boley, B. A. and Weiner, J. H. Theory of Thermal Stresses, Second Edition. New York: John Wiley and Sons, Inc., 1962.

30. Lee, E. H. "Viscoelasticity," Handbook of Engineering Mechanics. Edited by Flugge, W., New York: McGraw-Hill Book Co., 1962.

31. Ferry, J. D. Viscoelastic Properties of Polymers. New York: John Wiley and Sons, Inc., 1961.

32. Bieniek, M. D., Henry, L. H. and Freudenthal, A. M. "One Dimensional Response of Linear Viscoelastic Media," International Journal of Mechanical Sciences. 4 (1962), pp. 211-230.

33. Carslaw, H. S. and Jaeger, J. C. Operational Methods in Applied Mathematics, Second Edition. New York: Dover Publications, Inc., 1963.

34. Findley, W. N. "Creep Characteristics of Plastics," Symposium on Plastics, American Society of Testing Materials. (1944).

35. Findley, W. N. "Derivation of a Stress-Strain Equation from Creep Data for Plastics," Proceedings of First U.S. National Congress of Applied Mechanics. (1952), pp. 595-602.

36. Findley, W. N. and Poczatek, J. J. "Prediction of Creep Deflection and Stress Distribution in Beams from Creep in Tension," Journal of Applied Mechanics. 22 (1955), pp. 165-171.

37. Findley, W. N. "Prediction of Stress Relaxation from Creep Tests of Plastics," Proceedings of Third U.S. National Congress of Applied Mechanics. (1958), pp. 521-526.

38. Onoran, K. and Findley, W. N. "Combined Stress Creep Experiments on Viscoelastic Materials with Abrupt Changes in State of Stress," Division of Engineering, Brown University, Report No. ARPA/E5, EMRL-22. 1962.

39. Bergen, J. T. "Stress Relaxation of Polymeric Materials in Combined Torsion and Tension," Viscoelasticity Phenomenological Aspects, Edited by Bergen, J. T. New York: Academic Press, 1960.

40. Weissman, G. F., Pao, Y.-H. and Marin, J. "Prediction of Creep under Fluctuating Stress and Damping from Creep under Constant Stress," Proceedings of the Second U.S. National Congress of Applied Mechanics. (1954), pp. 577-583.

41. Marin, J. "Creep Relaxation Relations for Styrene and Acrylic Plastics," Proceedings of American Society for Testing Materials. 51 (1951), pp. 1277-1293.

42. Marin, J. and Pao, Y.-H. "The Theory of Combined Creep Strain-Stress Relations for Materials with Different Properties in Tension and Compression," Proceedings of the First U.S. National Congress of Applied Mechanics. (1951), pp. 585-593.

43. Modern Plastics Encyclopedia. New York: Plastics Catalogue Corp., 1964.

44. Sherby, O. D. and Dorn, J. E. "Anelastic Creep of Polymethyl Methacrylate," Journal of the Mechanics and Physics of Solids. 6 (1957), pp. 145-162.

45. Leaderman, H. "Creep Elastic Hysteresis and Damping in Bakelite under Torsion," Trans. of A.S.M.E. 61 (1939), pp. A79-A85.

46. Cottrell, A. H. and Aytekin, V. "Andrade's Creep Law and the Flow of Zinc Crystals," Nature. (1947), p. 328.

47. Pao, Y. and Marin, J. "Deflections and Stresses in Beams Subjected to Bending and Creep," Journal of Applied Mechanics. 19 (1952), pp. 478-484.

48. Findley, W. N. and Khosla, G. "An Equation for Tension Creep of Three Unfilled Thermoplastics," Journal of Society of Plastic Engineers. 12 (1956), pp. 20-25.

49. Brock, J. E. "Some Secondary Effects in a Simple Piping Structure under Heating," Journal of Applied Mechanics. 31 (1964), pp. 88-90.

50. Felgar, R. P. "Relation Between Analytical and Experimental Mechanics of Solid Propellants." Paper No. 6121-8247-KU000 presented at Society for Experimental Stress Analysis Spring Meeting. (1964).

APPENDIX A

TABLES

Table 1

Creep Data at 90° F and 400 psi

Original Length 8 inches

Time		Elongation	Strain	$\epsilon - \epsilon_0$
Hours	Minutes	1/10000 in.	(in./in.) x 10^3	(in./in.) x 10^3
0	0	74.0	0.925	.000
0	2	79.0	0.987	.062
0	3	79.4	0.992	.067
0	4	80.5	1.006	.081
0	6	80.8	1.010	.085
0	7	80.8	1.010	.085
0	8	80.9	1.011	.086
0	9	80.9	1.011	.086
0	10	81.5	1.013	.088
0	15	82.2	1.027	.102
0	20	82.7	1.033	.108
0	25	83.2	1.040	.115
0	30	84.0	1.050	.125
0	35	85.3	1.066	.141
0	40	87.4	1.092	.167
0	45	88.4	1.105	.180
2	0	88.8	1.110	.185
3	0	91.5	1.143	.218
4	0	92.0	1.150	.225
21	0	100.0	1.250	.325
23	0	102.0	1.275	.350
24	0	102.1	1.276	.351
25	0	102.1	1.276	.351
26	0	102.8	1.285	.360
27	0	105.5	1.318	.393
44	0	107.5	1.337	.412
45	0	109.4	1.367	.442
49	0	109.5	1.368	.443

Table 2

Creep Data at 90° F and 266 psi

Original Length 8 Inches

Time		Elongation	Strain	$\epsilon - \epsilon_o$
Hours	Minutes	1/10000 in.	(in./in.) x 10^3	(in./in.) x 10^3
0	0	48.0	.600	0
0	2	50.2	.627	.027
0	3	50.4	.630	.030
0	4	50.8	.635	.035
0	6	50.9	.636	.036
0	7	50.9	.636	.036
0	8	50.9	.637	.037
0	9	50.9	.637	.037
0	10	51.3	.641	.041
0	15	51.6	.645	.045
0	20	52.0	.650	.050
0	25	52.9	.661	.061
0	30	53.1	.663	.063
0	35	53.2	.664	.064
0	40	53.4	.667	.067
0	45	54.2	.667	.067
2	0	54.9	.686	.086
3	0	56.0	.700	.100
4	0	57.0	.712	.112
21	0	65.5	.820	.220
23	0	67.2	.840	.240
24	0	67.3	.841	.241
25	0	68.3	.853	.253
26	0	70.2	.877	.277
27	0	70.2	.877	.277
44	0	72.3	.903	.303
45	0	73.1	.913	.313
49	0	73.1	.913	.313

Table 3

Creep Data at 90° F and 213 psi

Original Length 8 Inches

Time Hours	Time Minutes	Elongation 1/10000 in.	Strain (in./in.) x 10^3	$\epsilon - \epsilon_0$ (in./in.) x 10^3
0	0	40.0	.500	0
0	2	40.1	.501	.001
0	3	40.2	.502	.002
0	4	40.3	.503	.003
0	6	40.4	.505	.005
0	7	40.5	.506	.006
0	8	40.6	.507	.007
0	9	40.6	.508	.008
0	10	40.8	.510	.010
0	15	40.8	.510	.010
0	20	40.9	.511	.011
0	25	41.0	.512	.012
0	30	41.8	.522	.022
0	35	42.9	.536	.036
0	40	44.0	.550	.050
0	45	44.6	.557	.057
2	0	45.4	.567	.067
3	0	46.3	.577	.077
4	0	47.5	.593	.093
21	0	50.2	.627	.127
23	0	50.4	.630	.130
24	0	50.5	.631	.131
25	0	50.5	.631	.131
26	0	50.5	.631	.131
27	0	50.6	.632	.132
44	0	50.6	.632	.132
45	0	50.6	.632	.132
49	0	50.6	.632	.132

Table 4

Creep Data at 105° F and 480 psi

Original Length 8 Inches

Time Hours	Time Minutes	Elongation 1/10000 in.	Strain (in./in.) x 10^3	$\epsilon - \epsilon_0$ (in./in.) x 10^3
0	0	116.0	1.450	0
0	1	-----	-----	----
0	2	-----	-----	----
0	3	125.0	1.562	.112
0	4	130.0	1.625	.175
0	5	130.5	1.631	.181
0	6	132.8	1.660	.210
0	7	132.8	1.660	.210
0	8	132.8	1.660	.210
0	9	133.0	1.662	.212
0	10	133.6	1.670	.220
0	15	135.6	1.695	.245
0	20	136.1	1.701	.251
0	25	136.1	1.701	.251
0	30	136.2	1.702	.252
0	35	136.2	1.702	.252
0	40	136.2	1.702	.252
0	45	136.3	1.703	.253
1	0	138.0	1.725	.275
2	0	146.0	1.825	.375
4	0	174.6	2.812	.732

Received without page(s) 114.

Filmed as received.

University Microfilms, Inc.

Table 6

Creep Data at 105° F and 320 psi

Original Length 8 Inches

Time Hours	Time Minutes	Elongation 1/10000 in.	Strain (in./in.) x 10^3	$\epsilon - \epsilon_0$ (in./in.) x 10^3
0	0	72.0	0.900	0
0	1	85.0	1.062	.162
0	2	87.0	1.087	.187
0	3	87.0	1.087	.187
0	4	88.0	1.100	.200
0	5	89.0	1.112	.212
0	6	90.0	1.125	.225
0	7	90.0	1.125	.225
0	8	91.0	1.137	.237
0	9	91.0	1.137	.237
0	10	92.0	1.150	.250
0	15	92.6	1.158	.258
0	20	93.0	1.162	.262
0	25	95.0	1.187	.287
0	30	96.0	1.200	.300
0	35	96.0	1.200	.300
0	40	97.0	1.212	.312
0	45	98.0	1.225	.325
1	0	99.0	1.237	.337
2	0	100.0	1.250	.350
4	0	104.0	1.300	.400

Table 7

Creep Data at 105° F and 280 psi

Original Length 8 Inches

Time Hours	Time Minutes	Elongation 1/10000 in.	Strain (in./in.) x 10^3	$\epsilon - \epsilon_0$ (in./in.) x 10^3
0	0	70.0	0.875	0
0	1	----	----	----
0	2	----	----	----
0	3	71.0	0.887	.012
0	4	72.0	0.900	.025
0	5	74.0	0.925	.050
0	6	75.0	0.937	.062
0	7	76.0	0.950	.075
0	8	76.2	0.953	.078
0	9	76.3	0.953	.078
0	10	76.7	0.956	.081
0	15	77.7	0.956	.081
0	20	80.0	1.000	.125
0	25	81.1	1.014	.139
0	30	82.0	1.025	.150
0	35	82.0	1.025	.150
0	40	82.2	1.028	.153
0	45	82.4	1.030	.155
1	0	83.0	1.037	.162
2	0	88.0	1.100	.225
4	0	100.0	1.250	.375

Table 8

Creep Data at 120° F and 400 psi

Original Length 8 Inches

Time Hours	Time Minutes	Elongation 1/10000 in.	Strain (in./in.) x 10^3	$\epsilon - \epsilon_0$ (in./in.) x 10^3
0	0	174.0	2.175	0
0	1	178.2	2.227	.052
0	2	179.0	2.237	.062
0	3	183.0	2.287	.112
0	4	185.0	2.312	.137
0	5	186.1	2.326	.141
0	6	186.2	2.327	.152
0	7	186.2	2.327	.152
0	8	186.2	2.327	.152
0	9	186.5	2.331	.156
0	10	187.0	2.337	.162
0	15	189.6	2.370	.195
0	20	189.7	2.371	.196
0	25	189.7	2.371	.196
0	30	189.7	2.371	.196
0	35	191.0	2.387	.212
0	40	191.1	2.389	.214
0	45	191.2	2.390	.216
1	0	193.3	2.416	.241
1	15	196.1	2.451	.376
1	30	196.1	2.451	.376
1	45	196.2	2.452	.377
2	0	196.2	2.452	.377

Table 9

Creep Data at 120° F and 320 psi

Original Length 8 Inches

Time Hours	Time Minutes	Elongation 1/10000 in.	Strain (in./in.) x 10^3	$\epsilon - \epsilon_0$ (in./in.) x 10^3
0	0	140.0	1.750	0
0	1	142.4	1.780	.030
0	2	143.1	1.788	.038
0	3	143.1	1.788	.038
0	4	143.1	1.788	.038
0	5	143.4	1.792	.042
0	6	143.4	1.792	.042
0	7	143.5	1.793	.043
0	8	150.6	1.882	.132
0	9	150.7	1.883	.133
0	10	150.8	1.885	.135
0	15	152.7	1.908	.158
0	20	156.7	1.958	.208
0	25	161.0	2.012	.262
0	30	161.5	2.018	.268
0	35	162.3	2.028	.278
0	40	163.1	2.038	.288
0	45	163.1	2.038	.288
2	0	170.0	2.125	.375

Table 10

Creep Data at 120° F and 280 psi

Original Length 8 Inches

Time Hours	Time Minutes	Elongation 1/10000 in.	Strain (in./in.) x 10^3	$\epsilon - \epsilon_0$ (in./in.) x 10^3
0	0	117.0	1.462	0
0	1	119.0	1.487	.025
0	2	119.1	1.488	.026
0	3	119.5	1.492	.030
0	4	119.5	1.492	.030
0	5	119.8	1.496	.034
0	6	119.9	1.497	.035
0	7	119.9	1.497	.035
0	8	120.0	1.500	.038
0	9	120.0	1.500	.038
0	10	120.4	1.505	.043
0	15	122.0	1.525	.043
0	20	122.1	1.526	.064
0	25	122.3	1.528	.066
0	30	122.4	1.530	.068
0	35	122.4	1.530	.068
0	40	122.4	1.530	.068
0	45	-----	-----	----
1	0	-----	-----	-----
1	15	140.2	1.752	.290
1	30	140.2	1.752	.290
1	45	140.2	1.752	.290
2	0	140.2	1.752	.290

Table 11

Creep Data at 135° F and 525 psi

Original Length 8 Inches

Time Hours	Time Minutes	Elongation 1/10000 in.	Strain (in./in.) x 10^3	$\epsilon - \epsilon_0$ (in./in.) x 10^3
0	0	263.0	3.287	0
0	1	273.0	3.412	.125
0	2	275.3	3.441	.154
0	3	275.3	3.441	.154
0	4	280.0	3.500	.213
0	5	280.0	3.500	.213
0	6	280.0	3.500	.213
0	7	285.1	3.563	.276
0	8	285.1	3.563	.276
0	9	289.0	3.612	.325
0	10	293.0	3.662	.375
0	15	293.4	3.667	.380
0	20	295.6	3.695	.408
0	25	303.0	3.787	.500
0	30	303.0	3.787	.500
0	35	303.0	3.787	.500
0	40	303.0	3.787	.500
0	45	303.0	3.787	.500
1	0	305.0	3.812	.525
1	15	305.0	3.812	.525
1	30	305.5	3.818	.531
1	45	313.5	3.918	.631
2	0	315.0	3.937	.650

Table 12

Creep Data at 135° F and 410 psi

Original Length 8 Inches

Time Hours	Time Minutes	Elongation 1/10000 in.	Strain (in./in.) x 10^3	$\epsilon - \epsilon_0$ (in./in.) x 10^3
0	0	213.0	2.662	0
0	1	220.5	2.756	.094
0	2	221.0	2.762	.100
0	3	222.5	2.781	.119
0	4	223.2	2.790	.128
0	5	224.0	2.800	.138
0	6	227.4	2.843	.181
0	7	233.4	2.893	.231
0	8	236.8	2.960	.292
0	9	240.6	3.008	.340
0	10	241.7	3.022	.354
0	15	246.8	3.086	.428
0	20	250.0	3.125	.463
0	25	254.0	3.175	.513
0	30	254.9	3.186	.524
0	35	256.0	3.200	.538
0	40	258.0	3.225	.563
0	45	258.0	3.225	.563
1	0	259.6	3.245	.583
1	15	259.6	3.245	.583
1	30	260.0	3.250	.588
1	45	260.0	3.250	.588
2	0	261.0	3.262	.600

Table 13

Creep Data at 135° F and 360 psi

Original Length 8 Inches

Time		Elongation	Strain	$\epsilon - \epsilon_0$
Hours	Minutes	1/10000 in.	(in./in.) x 10^3	(in./in.) x 10^3
0	0	170.0	2.125	0
0	1	176.0	2.200	.075
0	2	178.5	2.231	.106
0	3	180.0	2.250	.125
0	4	180.1	2.251	.126
0	5	180.9	2.261	.136
0	6	189.0	2.362	.237
0	7	189.6	2.370	.245
0	8	189.8	2.372	.247
0	9	189.8	2.372	.247
0	10	189.8	2.372	.247
0	15	190.5	2.381	.256
0	20	199.0	2.487	.362
0	25	199.5	2.493	.368
0	30	200.0	2.500	.375
0	35	200.1	2.501	.376
0	40	200.1	2.501	.376
0	45	200.2	2.502	.377
1	0	200.2	2.502	.377
1	15	200.2	2.502	.377
1	30	201.5	2.518	.393
1	45	208.5	2.606	.481
2	0	210.0	2.625	.500

Table 14

Creep Data at 135° F and 240 psi

Original Length 8 Inches

Time		Elongation	Strain	$\epsilon - \epsilon_0$
Hours	Minutes	1/10000 in.	(in./in.) x 10^3	(in./in.) x 10^3
0	0	110.0	1.375	0
0	1	112.0	1.400	.025
0	2	117.0	1.462	.088
0	3	119.0	1.487	.112
0	4	120.0	1.500	.125
0	5	121.0	1.512	.137
0	6	123.0	1.537	.162
0	7	123.0	1.537	.162
0	8	127.0	1.587	.212
0	9	128.0	1.600	.225
0	10	129.0	1.612	.237
0	15	130.0	1.625	.250
0	20	131.0	1.637	.262
0	25	131.0	1.637	.262
0	30	132.0	1.650	.275
0	35	133.0	1.662	.387
0	40	135.0	1.687	.412
0	45	136.0	1.700	.425
1	0	136.0	1.700	.425
1	15	137.0	1.712	.437
1	30	137.0	1.712	.437
1	45	138.0	1.725	.450
2	0	138.0	1.725	.450

Table 15

Creep Data at 150° F and 400 psi

Original Length 8 Inches

Time Hours	Time Minutes	Elongation 1/10000 in.	Strain (in./in.) x 10^3	$\epsilon - \epsilon_0$ (in./in.) x 10^3
0	0	242.0	3.025	0
0	1	254.0	3.174	.149
0	2	261.0	3.262	.237
0	3	264.0	3.300	.275
0	4	269.0	3.362	.337
0	5	274.0	3.425	.400
0	6	281.0	3.512	.487
0	7	281.0	3.512	.487
0	8	283.0	3.537	.512
0	9	284.0	3.550	.525
0	10	285.0	3.562	.537
0	15	291.0	3.637	.612
0	20	298.0	3.725	.700
0	25	301.0	3.762	.737
0	30	301.0	3.768	.743
0	35	301.5	3.768	.743
0	40	302.0	3.775	.750
0	45	302.0	3.775	.750
1	0	302.0	3.775	.750
1	15	302.0	3.775	.750
1	30	302.0	3.775	.750
1	45	302.0	3.775	.750
2	0	302.0	3.775	.750

Table 16

Creep Data at 150° F and 320 psi

Original Length 8 Inches

Time		Elongation	Strain	$\epsilon - \epsilon_0$
Hours	Minutes	1/10000 in.	(in./in.) x 10^3	(in./in.) x 10^3
0	0	180.0	2.250	0
0	1	186.0	2.325	.075
0	2	190.0	2.375	.125
0	3	195.0	2.437	.187
0	4	196.0	2.450	.200
0	5	201.0	2.512	.262
0	6	209.0	2.612	.362
0	7	210.0	2.625	.375
0	8	210.0	2.625	.375
0	9	211.0	2.637	.387
0	10	211.0	2.637	.387
0	15	213.0	2.662	.412
0	20	215.0	2.687	.437
0	25	218.0	2.725	.475
0	30	221.0	2.762	.512
0	35	242.0	2.775	.525
0	40	242.0	2.775	.525
0	45	243.0	2.787	.537
1	0	231.0	2.887	.637
1	15	231.0	2.887	.637
1	30	232.0	2.900	.650
1	45	233.0	2.912	.662
2	0	233.0	2.912	.662

Table 17

Creep Data at 150° F and 240 psi

Original Length 8 Inches

Time		Elongation	Strain	$\epsilon - \epsilon_0$
Hours	Minutes	1/10000 in.	(in./in.) x 10^3	(in./in.) x 10^3
0	0	135.0	1.687	0
0	1	140.0	1.750	.063
0	2	140.5	1.756	.069
0	3	140.5	1.756	.069
0	4	140.8	1.760	.073
0	5	140.8	1.760	.073
0	6	142.8	1.785	.098
0	7	143.0	1.787	.100
0	8	143.0	1.787	.100
0	9	143.5	1.793	.106
0	10	150.5	1.881	.194
0	15	152.0	1.900	.213
0	20	152.5	1.906	.319
0	25	162.5	2.031	.344
0	30	162.5	2.031	.344
0	35	162.5	2.031	.344
0	40	162.5	2.031	.344
0	45	162.5	2.031	.344
1	0	162.5	2.031	.344
1	15	162.5	2.031	.344
1	30	162.5	2.031	.344
1	45	163.0	2.037	.350
2	0	163.0	2.037	.350

Table 18

Creep Data at 150° F and 200 psi

Original Length 8 Inches

Time Hours	Time Minutes	Elongation 1/10000 in.	Strain (in./in.) x 10^3	$\epsilon - \epsilon_0$ (in./in.) x 10^3
0	0	128.0	1.600	0
0	1	132.0	1.650	.050
0	2	133.0	1.662	.062
0	3	134.0	1.675	.075
0	4	134.0	1.675	.075
0	5	135.0	1.687	.087
0	6	136.0	1.700	.100
0	7	137.0	1.712	.112
0	8	138.0	1.725	.125
0	9	139.0	1.737	.137
0	10	139.0	1.737	.137
0	15	142.0	1.775	.175
0	20	144.0	1.800	.200
0	25	146.0	1.825	.225
0	30	147.0	1.837	.237
0	35	148.0	1.850	.250
0	40	148.0	1.850	.250
0	45	149.0	1.862	.262
1	0	150.0	1.875	.275
1	15	151.0	1.887	.287
1	30	152.0	1.900	.300
1	45	152.0	1.900	.300
2	0	152.0	1.900	.300

Table 19

Creep Data at 165° F and 400 psi

Original Length 8 Inches

Time Hours	Time Minutes	Elongation 1/10000 in.	Strain (in./in.) x 10^3	$\epsilon - \epsilon_0$ (in./in.) x 10^3
0	0	300.0	3.750	0
0	1	309.0	3.862	0.112
0	2	313.0	3.912	0.162
0	3	319.0	3.987	0.237
0	4	322.0	4.025	0.275
0	5	328.0	4.100	0.350
0	6	330.0	4.125	0.375
0	7	332.0	4.150	0.400
0	8	333.0	4.162	0.412
0	9	340.0	4.250	0.500
0	10	343.0	4.287	0.537
0	15	355.0	4.437	0.687
0	20	366.0	4.575	0.825
0	25	373.0	4.662	0.912
0	30	376.0	4.700	0.950
0	35	380.0	4.750	1.000
0	40	380.0	4.750	1.000
0	45	380.0	4.750	1.000
1	0	380.0	4.750	1.000
1	15	381.0	4.762	1.012
1	30	382.0	4.775	1.025
1	45	382.0	4.775	1.025
2	0	382.0	4.775	1.025

Table 20

Creep Data at 165° F and 320 psi

Original Length 8 Inches

Time Hours	Time Minutes	Elongation 1/10000 in.	Strain (in./in.) x 10^3	$\epsilon - \epsilon_0$ (in./in.) x 10^3
0	0	230.0	2.875	0
0	1	242.0	3.025	.150
0	2	242.0	3.025	.150
0	3	250.0	3.125	.250
0	4	253.0	3.162	.287
0	5	260.0	3.250	.375
0	6	260.0	3.250	.375
0	7	262.0	3.275	.400
0	8	263.0	3.287	.412
0	9	269.0	3.362	.487
0	10	272.0	3.400	.525
0	15	281.0	3.512	.637
0	20	282.0	3.525	.650
0	25	285.0	3.562	.687
0	30	289.0	3.612	.737
0	35	290.0	3.625	.750
0	40	290.0	3.625	.750
0	45	290.0	3.625	.750
1	0	290.0	3.625	.750
1	15	290.0	3.625	.750
1	30	290.0	3.625	.750
1	45	290.0	3.625	.750
2	0	290.0	3.625	.750

Table 21

Creep Data at 165° F and 240 psi

Original Length 8 Inches

Time		Elongation	Strain	$\epsilon - \epsilon_o$
Hours	Minutes	1/10000 in.	(in./in.) x 10^3	(in./in.) x 10^3
0	0	160.0	2.000	0
0	1	167.0	2.087	.087
0	2	171.0	2.137	.137
0	3	173.0	2.162	.162
0	4	173.0	2.162	.162
0	5	174.0	2.175	.175
0	6	176.0	2.200	.200
0	7	177.0	2.212	.212
0	8	179.0	2.237	.237
0	9	180.0	2.250	.250
0	10	181.0	2.262	.262
0	15	190.0	2.375	.375
0	20	192.0	2.400	.400
0	25	192.0	2.400	.400
0	30	193.0	2.412	.412
0	35	197.0	2.462	.462
0	40	202.0	2.525	.525
0	45	203.0	2.537	.537
1	0	209.0	2.612	.612
1	15	211.0	2.637	.637
1	30	212.0	2.650	.650
1	45	212.0	2.650	.650
2	0	212.0	2.650	.650

Table 22

Creep Data at 165° F and 200 psi

Original Length 8 Inches

Time Hours	Time Minutes	Elongation 1/10000 in.	Strain (in./in.) x 10^3	$\epsilon - \epsilon_0$ (in./in.) x 10^3
0	0	143	1.787	0
0	1	149	1.862	.075
0	2	155	1.937	.150
0	3	157	1.962	.175
0	4	159	1.987	.200
0	5	159	1.987	.200
0	6	160	2.000	.212
0	7	160	2.000	.212
0	8	162	2.025	.237
0	9	163	2.037	.250
0	10	164	2.050	.262
0	15	167	2.087	.300
0	20	168	2.100	.312
0	25	168	2.100	.312
0	30	169	2.112	.325
0	35	169	2.112	.325
0	40	169	2.112	.325
0	45	170	2.125	.337
1	0	176	2.200	.413
1	15	177	2.212	.425
1	30	178	2.225	.437
1	45	179	2.237	.450
2	0	179	2.237	.450

Table 23

Creep Data at 180° F and 400 psi

Original Length 8 Inches

Time Hours	Time Minutes	Elongation 1/10000 in.	Strain (in./in.) x 10^3	$\epsilon - \epsilon_0$ (in./in.) x 10^3
0	0	360.0	4.500	0
0	1	383.0	4.785	0.285
0	2	391.0	4.887	0.387
0	3	393.0	4.912	0.412
0	4	401.0	5.012	0.512
0	5	403.0	5.037	0.537
0	6	413.0	5.162	0.662
0	7	420.0	5.250	0.750
0	8	423.0	5.287	0.787
0	9	430.0	5.375	0.875
0	10	431.0	5.387	0 887
0	15	442.0	5.525	1.025
0	20	451.0	5.637	1.137
0	25	460.0	5.750	1.250
0	30	462.0	5.775	1.275
0	35	463.0	5.787	1.287
0	40	463.0	5.787	1.287
0	45	463.0	5.787	1.287
1	0	473.0	5.912	1.412
1	15	481.0	6.012	1.512
1	30	481.0	6.012	1.512
1	45	483.0	6.037	1.537
2	0	483.0	6.037	1.537

Table 24

Creep Data at 180° F and 320 psi

Original Length 8 Inches

Time Hours	Time Minutes	Elongation 1/10000 in.	Strain (in./in.) x 10^3	$\epsilon - \epsilon_0$ (in./in.) x 10^3
0	0	300.0	3.750	0
0	1	311.0	3.887	0.137
0	2	316.0	3.950	0.200
0	3	322.0	4.025	0.275
0	4	330.0	4.125	0.375
0	5	336.0	4.200	0.450
0	6	342.0	4.275	0.525
0	7	348.0	4.350	0.600
0	8	354.0	4.425	0.675
0	9	357.0	4.462	0.712
0	10	370.0	4.625	0.875
0	15	372.0	4.650	0.900
0	20	374.0	4.675	0.925
0	25	380.0	4.750	1.000
0	30	381.0	4.762	1.012
0	35	382.0	4.775	1.025
0	40	382.0	4.775	1.025
0	45	383.0	4.787	1.037
1	0	386.0	4.825	1.075
1	15	388.0	4.850	1.100
1	30	390.0	4.875	1.125
1	45	391.0	4.887	1.137
2	0	391.0	4.887	1.137

Table 25

Creep Data at 180° F and 240 psi

Original Length 8 Inches

Time Hours	Time Minutes	Elongation 1/10000 in.	Strain (in./in.) x 10^3	$\epsilon - \epsilon_0$ (in./in.) x 10^3
0	0	230.0	2.875	0
0	1	240.0	3.000	.125
0	2	250.0	3.125	.250
0	3	253.0	3.162	.287
0	4	253.0	3.162	.287
0	5	255.0	3.187	.312
0	6	210.0	3.250	.375
0	7	264.0	3.300	.425
0	8	265.0	3.312	.437
0	9	272.0	3.400	.525
0	10	274.0	3.425	.550
0	15	278.0	3.475	.600
0	20	285.0	3.562	.687
0	25	286.0	3.575	.700
0	30	286.0	3.575	.700
0	35	287.0	3.587	.712
0	40	288.0	3.600	.725
0	45	289.0	3.612	.737
1	0	289.0	3.612	.737
1	15	289.0	3.612	.737
1	30	289.0	3.612	.737
1	45	289.0	3.612	.737
2	0	289.0	3.612	.737

Table 26

Creep Data at 180° F and 200 psi

Original Length 8 Inches

Time Hours	Time Minutes	Elongation 1/10000 in.	Strain (in./in.) x 10^3	$\epsilon - \epsilon_0$ (in./in.) x 10^3
0	0	190.0	2.375	0
0	1	202.0	2.525	.150
0	2	212.0	2.650	.275
0	3	213.0	2.662	.287
0	4	222.0	2.775	.400
0	5	223.0	2.787	.412
0	6	229.0	2.862	.487
0	7	234.0	2.925	.550
0	8	236.0	2.950	.575
0	9	236.0	2.950	.575
0	10	237.0	2.962	.587
0	15	242.0	3.025	.650
0	20	246.0	3.075	.700
0	25	247.0	3.087	.712
0	30	248.0	3.100	.725
0	35	248.0	3.100	.725
0	40	248.0	3.100	.725
0	45	249.0	3.112	.737
1	0	252.0	3.150	.775
1	15	254.0	3.175	.800
1	30	255.0	3.187	.812
1	45	256.0	3.200	.825
2	0	258.0	3.225	.850

Table 27

Creep Data at 195° F and 400 psi

Original Length 8 Inches

Time Hours	Time Minutes	Elongation 1/10000 in.	Strain (in./in.) x 10^3	$\epsilon - \epsilon_0$ (in./in.) x 10^3
0	0	400.0	5.000	0
0	1	421.0	5.262	0.262
0	2	427.0	5.337	0.337
0	3	429.0	5.362	0.362
0	4	437.0	5.462	0.462
0	5	447.0	5.587	0.587
0	6	450.0	5.625	0.625
0	7	455.0	5.687	0.687
0	8	459.0	5.837	0.837
0	9	470.0	5.875	0.875
0	10	479.0	5.987	0.987
0	15	486.0	6.075	1.075
0	20	496.0	6.200	1.200
0	25	500.0	6.250	1.250
0	30	511.0	6.387	1.387
0	35	518.0	6.475	1.475
0	40	522.0	6.525	1.525
0	45	529.0	6.612	1.612
1	0	538.0	6.725	1.725
1	15	547.0	6.837	1.837
1	30	560.0	7.000	2.000
1	45	567.0	7.087	2.087
2	0	577.0	7.212	2.212

Table 28

Creep Data at 195° F and 320 psi

Original Length 8 Inches

Time Hours	Time Minutes	Elongation 1/10000 in.	Strain (in./in.) x 10^3	$\epsilon - \epsilon_0$ (in./in.) x 10^3
0	0	300.0	3.750	0
0	1	320.0	4.000	0.250
0	2	323.0	4.037	0.287
0	3	332.0	4.150	0.400
0	4	332.0	4.150	0.400
0	5	341.0	4.262	0.512
0	6	350.0	4.375	0.625
0	7	352.0	4.400	0.650
0	8	352.0	4.400	0.650
0	9	362.0	4.525	0.775
0	10	372.0	4.650	0.900
0	15	383.0	4.787	1.037
0	20	393.0	4.912	1.162
0	25	410.0	5.125	1.375
0	30	412.0	5.150	1.400
0	35	420.0	5.250	1.500
0	40	420.0	5.250	1.500
0	45	421.0	5.262	1.512
1	0	422.0	5.275	1.525
1	15	424.0	5.300	1.550
1	30	426.0	5.325	1.575
1	45	426.0	5.325	1.575
2	0	428.0	5.350	1.600

Table 29

Creep Data at 195°F and 240 psi

Original Length 8 Inches

Time		Elongation	Strain	$\epsilon - \epsilon_o$
Hours	Minutes	1/10000 in.	(in./in.) x 10^3	(in./in.) x 10^3
0	0	236.0	2.950	0
0	1	248.0	3.100	.150
0	2	258.0	3.225	.275
0	3	262.0	3.275	.325
0	4	264.0	3.300	.350
0	5	265.0	3.312	.362
0	6	270.0	3.375	.425
0	7	273.0	3.412	.462
0	8	275.0	3.437	.487
0	9	276.0	3.450	.500
0	10	276.0	3.450	.500
0	15	283.0	3.537	.537
0	20	285.0	3.562	.612
0	25	286.0	3.575	.625
0	30	294.0	3.675	.725
0	35	296.0	3.700	.750
0	40	296.0	3.700	.750
0	45	296.0	3.700	.750
1	0	297.0	3.712	.762
1	15	298.0	3.725	.775
1	30	298.0	3.725	.775
1	45	300.0	3.750	.800
2	0	302.0	3.775	.825

Table 30

Creep Data at 195° F and 200 psi

Original Length 8 Inches

Time		Elongation	Strain	$\epsilon - \epsilon_0$
Hours	Minutes	1/10000 in.	(in./in.) x 10^3	(in./in.) x 10^3
0	0	200.0	2.500	0
0	1	206.0	2.575	.075
0	2	207.0	2.587	.087
0	3	210.0	2.625	.125
0	4	215.0	2.687	.187
0	5	218.0	2.725	.225
0	6	220.0	2.750	.250
0	7	220.0	2.750	.250
0	8	221.0	2.762	.262
0	9	221.0	2.762	.262
0	10	223.0	2.787	.287
0	15	229.0	2.862	.362
0	20	236.0	2.950	.450
0	25	240.0	3.000	.500
0	30	244.0	3.050	.550
0	35	250.0	3.125	.625
0	40	251.0	3.137	.637
0	45	251.0	3.137	.637
1	0	253.0	3.162	.662
1	15	260.0	3.250	.750
1	30	261.0	3.262	.762
1	45	262.0	3.275	.775
2	0	262.0	3.275	.775

Table 31

Creep Data at 210° F and 8 Inches

Original Length 8 Inches

Time Hours	Time Minutes	Elongation 1/10000 in.	Strain (in./in.) x 10^3	$\epsilon - \epsilon_0$ (in./in.) x 10^3
0	0	305.0	3.812	0
0	1	315.0	3.937	0.125
0	2	330.0	4.125	0.313
0	3	340.0	4.250	0.438
0	4	350.0	4.375	0.563
0	5	365.0	4.562	0.650
0	6	382.0	4.775	0.963
0	7	400.0	5.000	1.188
0	8	414.0	5.175	1.363
0	9	425.0	5.312	1.500
0	10	433.0	5.412	1.600
0	15	460.0	5.750	1.938
0	20	474.0	5.925	2.113
0	25	484.0	6.050	2.238
0	30	500.0	6.250	2.438
0	35	505.0	6.312	2.500
0	40	515.0	6.437	2.625
0	45	520.0	6.500	2.688
1	0	540.0	6.750	2.938
1	15	580.0	7.250	3.438
1	30	594.0	7.425	3.613
1	45	600.0	7.500	3.688
2	0	604.0	7.550	3.738

Table 32

Creep Data at 210° F and 200 psi

Original Length 8 Inches

Time		Elongation	Strain	$\epsilon - \epsilon_0$
Hours	Minutes	1/10000 in.	(in./in.) x 10^3	(in./in.) x 10^3
0	0	290.0	3.625	0
0	1	300.0	3.750	0.125
0	2	308.0	3.850	0.225
0	3	310.0	3.875	0.250
0	4	325.0	4.062	0.437
0	5	338.0	4.225	0.600
0	6	352.0	4.400	0.775
0	7	370.0	4.625	1.000
0	8	381.0	4.762	1.137
0	9	391.0	4.877	1.252
0	10	400.0	5.000	1.375
0	15	420.0	5.250	1.625
0	20	430.0	5.375	1.750
0	25	442.0	5.525	1.900
0	30	472.0	5.900	2.275
0	35	500.0	6.250	2.525
0	40	507.0	6.337	2.712
0	45	516.0	6.450	2.825
1	0	530.0	6.625	3.000
1	15	540.0	6.750	3.125
1	30	556.0	6.950	3.325
1	45	558.0	6.975	3.350
2	0	560.0	7.000	3.375

Table 33

Creep Data at 210° F and 160 psi

Original Length 8 Inches

Time		Elongation	Strain	$\epsilon - \epsilon_0$
Hours	Minutes	1/10000 in.	(in./in.) x 10^3	(in./in.) x 10^3
0	0	263.0	3.287	0
0	1	272.0	3.400	0.113
0	2	283.0	3.537	0.250
0	3	290.0	3.625	0.338
0	4	292.0	3.650	0.363
0	5	300.0	3.750	0.463
0	6	312.0	3.900	0.610
0	7	322.0	4.025	0.738
0	8	352.0	4.400	1.113
0	9	373.0	4.662	1.375
0	10	390.0	4.875	1.588
0	15	400.0	5.000	1.713
0	20	409.0	5.112	1.825
0	25	421.0	5.262	1.975
0	30	442.0	5.525	2.238
0	35	463.0	5.787	2.500
0	40	468.0	5.850	2.563
0	45	471.0	5.887	2.600
1	0	488.0	6.100	2.813
1	15	490.0	6.125	2.838
1	30	492.0	6.150	2.863
1	45	492.0	6.150	2.863
2	0	493.0	6.162	2.875

Table 34

Creep Data at 225° F and 200 psi

Original Length 8 Inches

Time Hours	Time Minutes	Elongation 1/10000 in.	Strain (in./in.) x 10^{-2}	$\epsilon - \epsilon_0$ (in./in.) x 10^{3}
0	0	400.0	5.000	0
0	1	412.0	5.275	0.275
0	2	430.0	5.375	0.375
0	3	443.0	5.537	0.537
0	4	463.0	5.787	0.787
0	5	492.0	6.150	1.150
0	6	502.0	6.275	1.275
0	7	510.0	6.375	1.375
0	8	533.0	6.662	1.662
0	9	542.0	6.775	1.775
0	10	580.0	7.250	2.250
0	15	603.0	7.537	2.537
0	20	673.0	8.412	3.412
0	25	713.0	8.912	3.912
0	30	730.0	9.125	4.125
0	35	812.0	10.150	5.150
0	40	862.0	10.775	5.775
0	45	910.0	11.375	6.375
1	0	950.0	11.875	6.375
1	15	983.0	12.287	7.287
1	30	1010.0	12.625	7.625
1	45	1050.0	13.125	8.125
2	0	1061.0	13.262	8.262

Table 35

Creep Data at 225° F and 160 psi

Original Length 8 Inches

Time Hours	Time Minutes	Elongation 1/10000 in.	Strain (in./in.) x 10^3	$\epsilon - \epsilon_0$ (in./in.) x 10^3
0	0	330.0	4.125	0
0	1	340.0	4.250	0.125
0	2	342.0	4.275	0.150
0	3	352.0	4.400	0.275
0	4	362.0	4.525	0.400
0	5	371.0	4.637	0.512
0	6	382.0	4.775	0.650
0	7	392.0	4.900	0.775
0	8	403.0	5.037	0.912
0	9	424.0	5.300	1.175
0	10	472.0	5.900	1.775
0	15	532.0	6.650	2.525
0	20	590.0	7.375	3.250
0	25	632.0	7.900	3.775
0	30	683.0	8.537	4.412
0	35	744.0	9.300	5.175
0	40	792.0	9.900	5.775
0	45	852.0	10.650	6.775
1	0	893.0	11.162	7.037
1	15	923.0	11.537	7.412
1	30	930.0	11.625	7.500
1	45	971.0	12.137	8.012
2	0	975.0	12.187	8.062

Table 36

Variation of Constants with Temperature

Temperature °F	n	a	b	c x 10^3	d
90	.065	.095	40000	1.20	3300
105	.080	.136	40000	1.50	3300
120	.125	.234	40000	2.00	3300
135	.160	.242	40000	3.00	3300
150	.200	.291	40000	3.00	3300
165	.280	.362	40000	6.50	3300
180	.350	.458	40000	9.00	3300
195	.490	.500	40000	11.00	3300
210	.600	.720	40000	50.00	3300
220	.970	1.020	40000	200.00	3300

Table 37

Creep Data at 140° F and 5000 psi

Original Length 8 Inches

Time		Elongation	Strain
Hours	Minutes	1/10000 in.	(in./in.) x 10^3
0	0	2503.0	31.287
0	1	2728.0	34.100
0	2	2848.0	35.600
0	3	2958.0	36.975
0	4	3038.0	37.975
0	5	3079.0	38.487
0	6	3121.0	39.012
0	7	3143.0	39.287
0	8	3160.0	39.500
0	9	3188.0	39.850
0	10	3219.0	40.237
0	15	3333.0	41.662
0	20	3440.0	43.000
0	25	3540.0	44.250
0	30	3620.0	45.250
0	35	3680.0	46.000
0	40	3750.0	46.875
0	45	3992.0	47.400
1	0	3890.0	48.375
1	15	3973.0	49.662
1	30	4043.0	50.353
1	45	4100.0	51.250
2	0	4132.0	51.650

Table 38

Creep Data at 160° F and 4000 psi

Original Length 8 Inches

Time		Elongation	Strain
Hours	Minutes	1/10000 in.	(in./in.) x 10^3
0	0	2463.0	30.787
0	1	2523.0	31.537
0	2	2618.0	32.725
0	3	2680.0	33.500
0	4	2749.0	34.362
0	5	2808.0	35.100
0	6	2843.0	35.537
0	7	2869.0	35.862
0	8	2899.0	36.237
0	9	2938.0	36.725
0	10	2963.0	37.037
0	15	3070.0	38.375
0	20	3135.0	39.187
0	25	3305.0	41.312
0	30	3391.0	42.387
0	35	3463.0	43.287
0	40	3514.0	43.925
0	45	3562.0	44.525
1	0	3681.0	46.012
1	15	3781.0	47.262
1	30	3870.0	48.375
1	45	3950.0	49.375
2	0	4028.0	50.350

Table 39

Creep Data at 190° F and 2600 psi

Original Length 8 Inches

Time		Elongation	Strain
Hours	Minutes	1/10000 in.	(in./in.) x 10^3
0	0	2564.0	32.050
0	1	2674.0	33.425
0	2	2739.0	34.237
0	3	2834.0	35.425
0	4	2914.0	36.425
0	5	3004.0	37.550
0	6	3039.0	37.987
0	7	3091.0	38.637
0	8	3149.0	39.362
0	9	3201.0	40.012
0	10	3241.0	40.512
0	15	3451.0	43.137
0	20	3639.0	45.487
0	25	3789.0	47.362
0	30	3910.0	48.875

Table 40

Free Thermal Expansion of Methyl Methacrylate

Original Length 10 Inches

Temperature °F	Extension in.	Strain in./in.	Expansion Coefficient in./in. °F
98	0	0	
102	.001	.0001	.0000333
105	.002	.0001	.0000333
108	.003	.0001	.0000333
111	.004	.0001	.0000333
114	.005	.0001	.0000333
117	.006	.0001	.0000333
120	.007	.0001	.0000333
123	.008	.0001	.0000333
126	.009	.0001	.0000333
129	.010	.0001	.0000333
142	.015	.0005	.0000380
154	.202	.0005	.0000416
182	.030	.0010	.0000343

Table 41

Creep Data at 160° F and 2600 psi

Original Length 8 Inches

Time		Elongation	Strain
Hours	Minutes	1/10000 in.	(in./in.) x 10^3
0	0	1792.0	22.400
0	1	1840.0	23.000
0	2	1884.0	23.550
0	3	1920.0	24.000
0	4	1940.0	24.250
0	5	1968.0	24.600
0	6	1984.0	24.800
0	7	2012.0	25.150
0	8	2032.0	25.400
0	9	2048.0	25.600
0	10	2076.0	25.950
0	15	2144.0	26.800
0	20	2180.0	27.250
0	25	2224.0	27.300
0	30	2252.0	28.150
0	35	2273.0	28.412
0	40	2276.0	28.450
0	45	2288.0	28.600
1	0	2312.0	28.900
1	15	2352.0	29.400
1	30	2368.0	29.600
1	45	2400.0	30.000
2	0	2424.0	30.300

Table 42

Creep Data at 140° F and 2600 psi

Original Length 8 Inches

Time		Elongation	Strain
Hours	Minutes	1/10000 in.	(in./in.) x 10^3
0	0	1520.0	19.000
0	1	1544.0	19.300
0	2	1568.0	19.600
0	3	1616.0	20.200
0	4	1664.0	20.800
0	5	1712.0	21.400
0	6	1744.0	21.800
0	7	1748.0	21.850
0	8	1760.0	22.000
0	9	1792.0	22.400
0	10	1808.0	22.600
0	15	1848.0	23.100
0	20	1868.0	23.350
0	25	1908.0	23.850
0	30	1937.0	24.212
0	35	1948.0	24.350
0	40	1952.0	24.400
0	45	2056.0	25.700
1	0	2016.0	25.200
1	15	2040.0	25.500
1	30	2044.0	25.550
1	45	2056.0	25.700
2	0	2064.0	25.800